

Growing excesses of new scalars at the Electro-weak scale at the LHC

Bruce Mellado

The Institute for Collider Particle Physics and iThemba LABS



THE UNIVERSITY
of LIVERPOOL

INSTITUTE FOR
COLLIDER
PARTICLE
PHYSICS



UNIVERSITY OF THE WITWATERSRAND



HEP seminar, University of Liverpool, 26/04/24

Outline

□ Introduction

□ The multilepton anomalies

□ Methodology

□ The anatomy

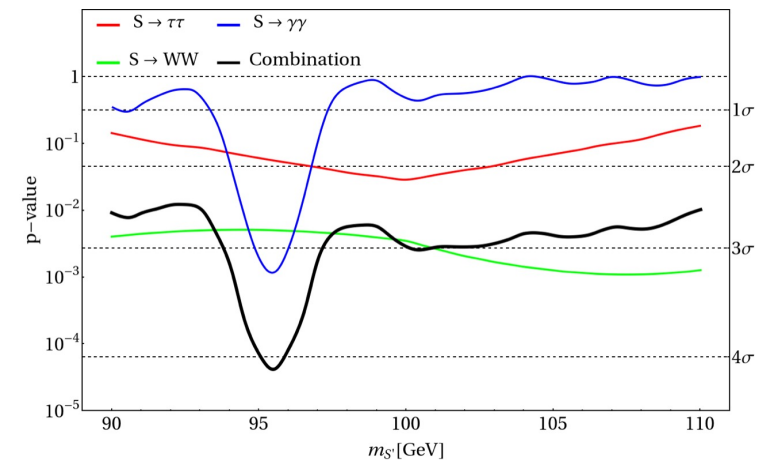
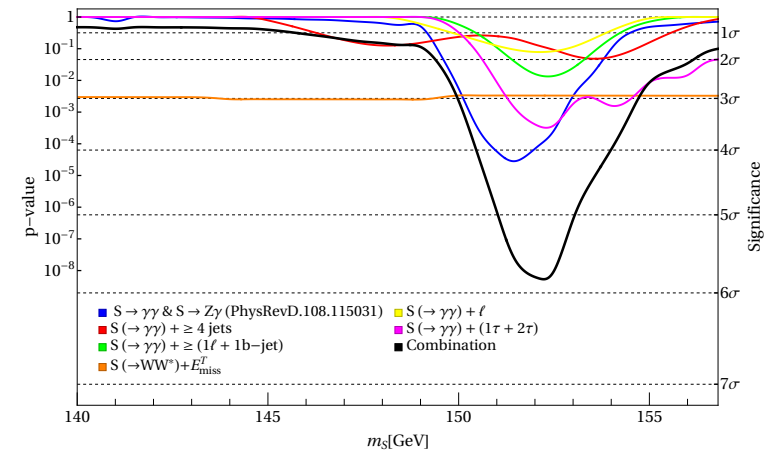
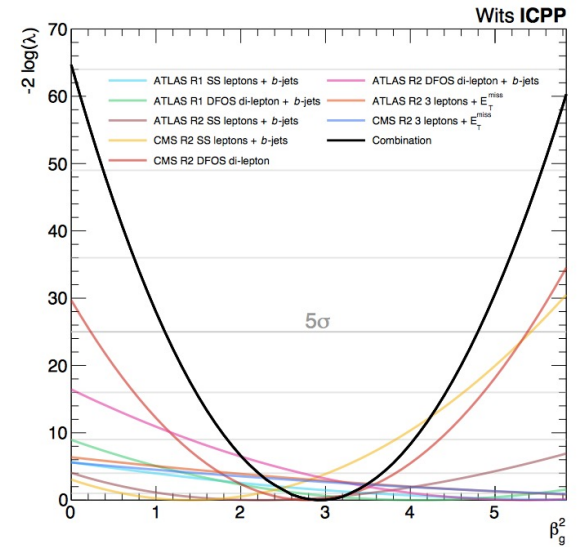
□ The S(152) candidate

□ First combination of $\gamma\gamma$, $Z\gamma$

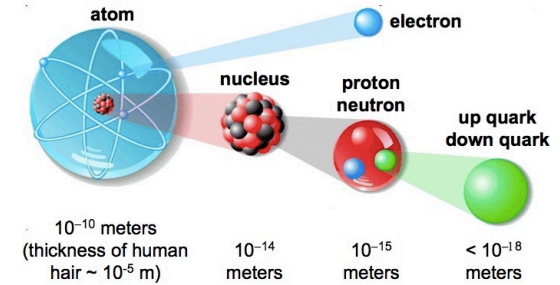
□ New results

□ The S(95) candidate

□ Impact on e^+e^- colliders



Building Blocks of Matter in the Standard Model



❑ **Quarks and leptons are organized in families or generations of matter**

❑ **So far we observe three generations (I, II, III)**

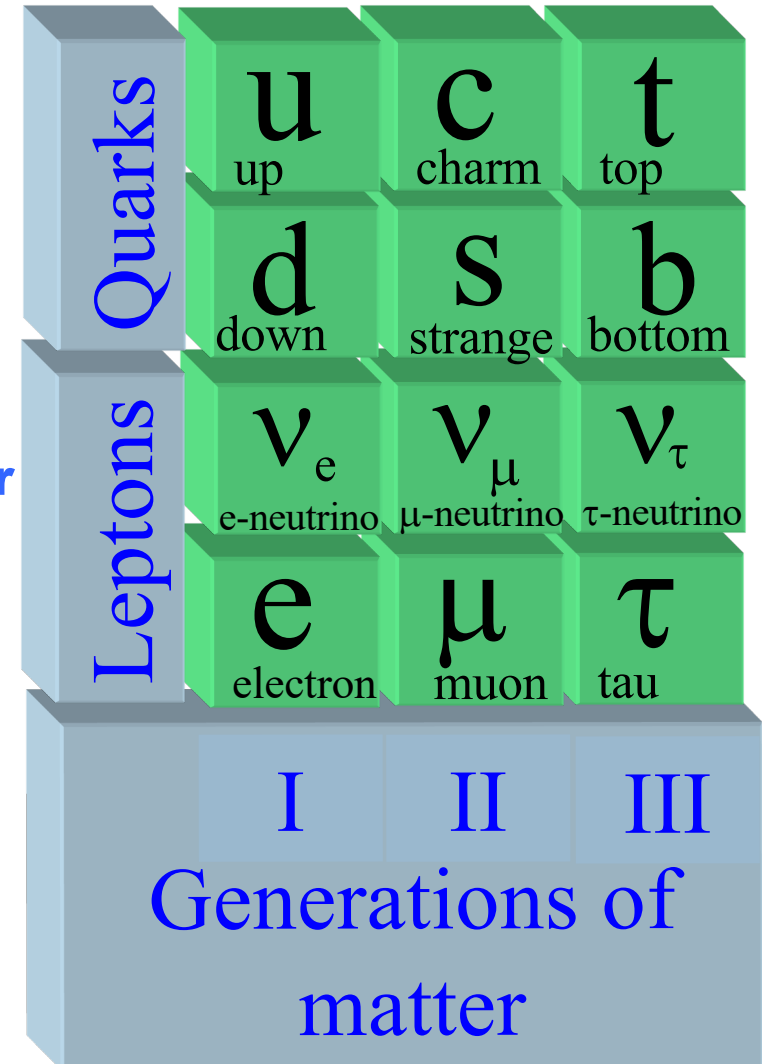
▪ **Second and third generations are copies of the first, only much heavier**

❑ **All have intrinsic angular momentum (spin) of $\frac{1}{2}$ (fermions)**

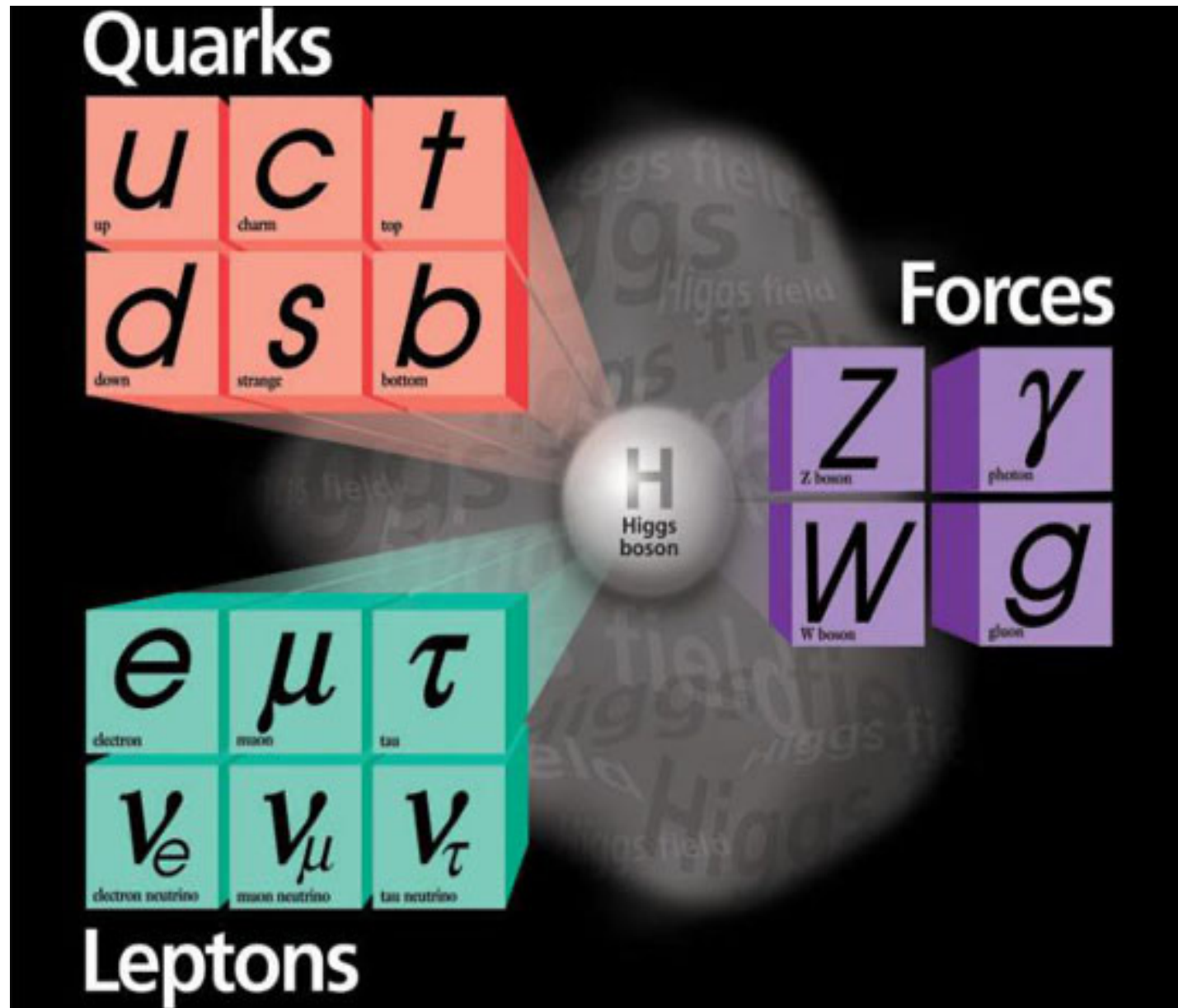
❑ **All particles have anti-particles**

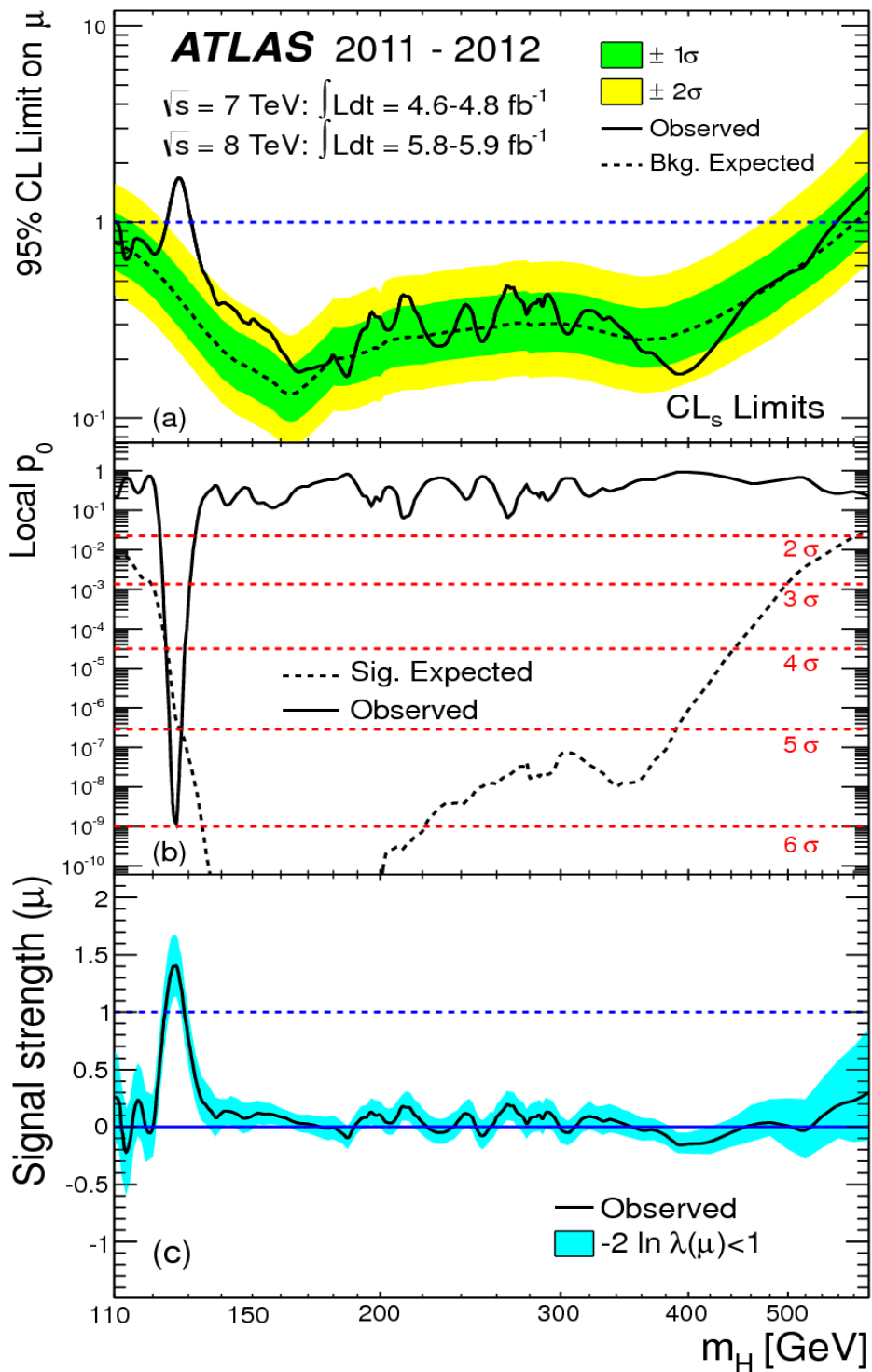
❑ **Display same mass and spin**

❑ **Opposite electric charge**



The Higgs boson provides for explanation for the mass of quarks, leptons and weak bosons. It is a cornerstone of the theory of fundamental interactions.



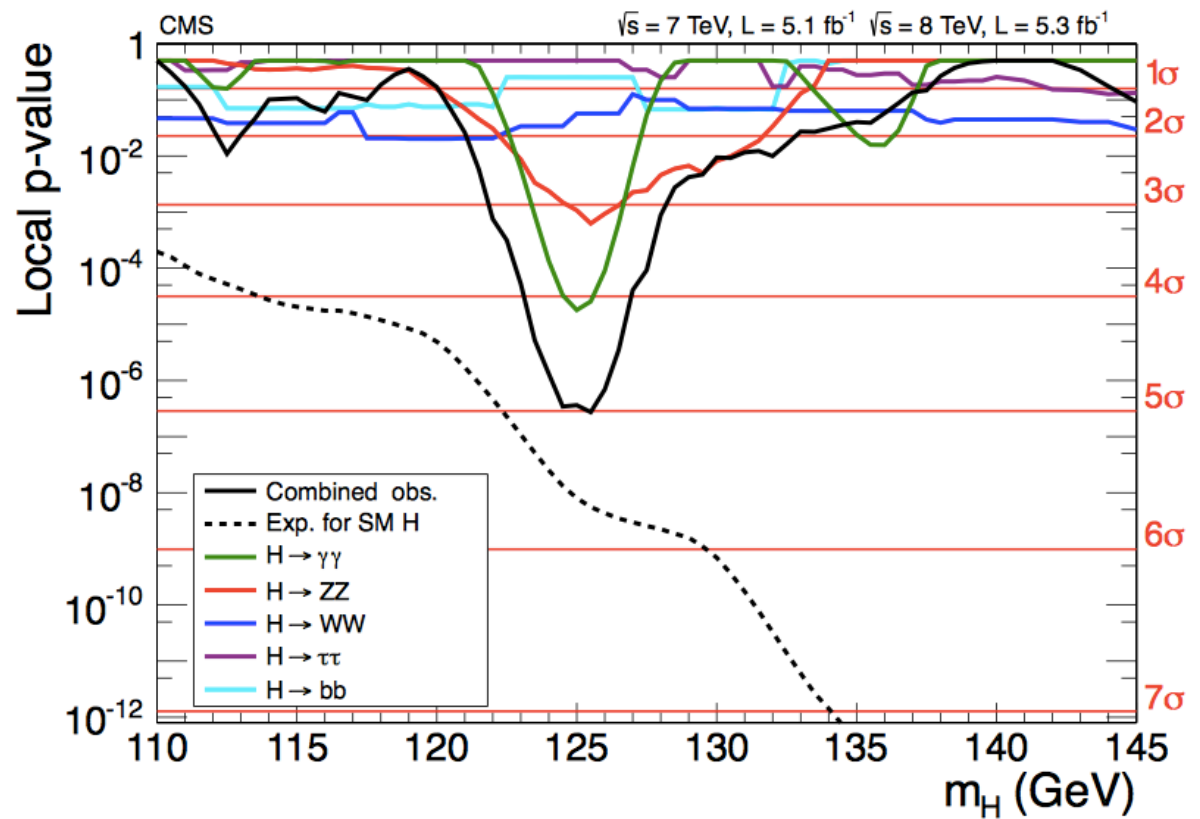


Habemus novum Boson

Phys.Lett. B716 (2012) 1-29

Phys.Lett. B716 (2012) 30-61

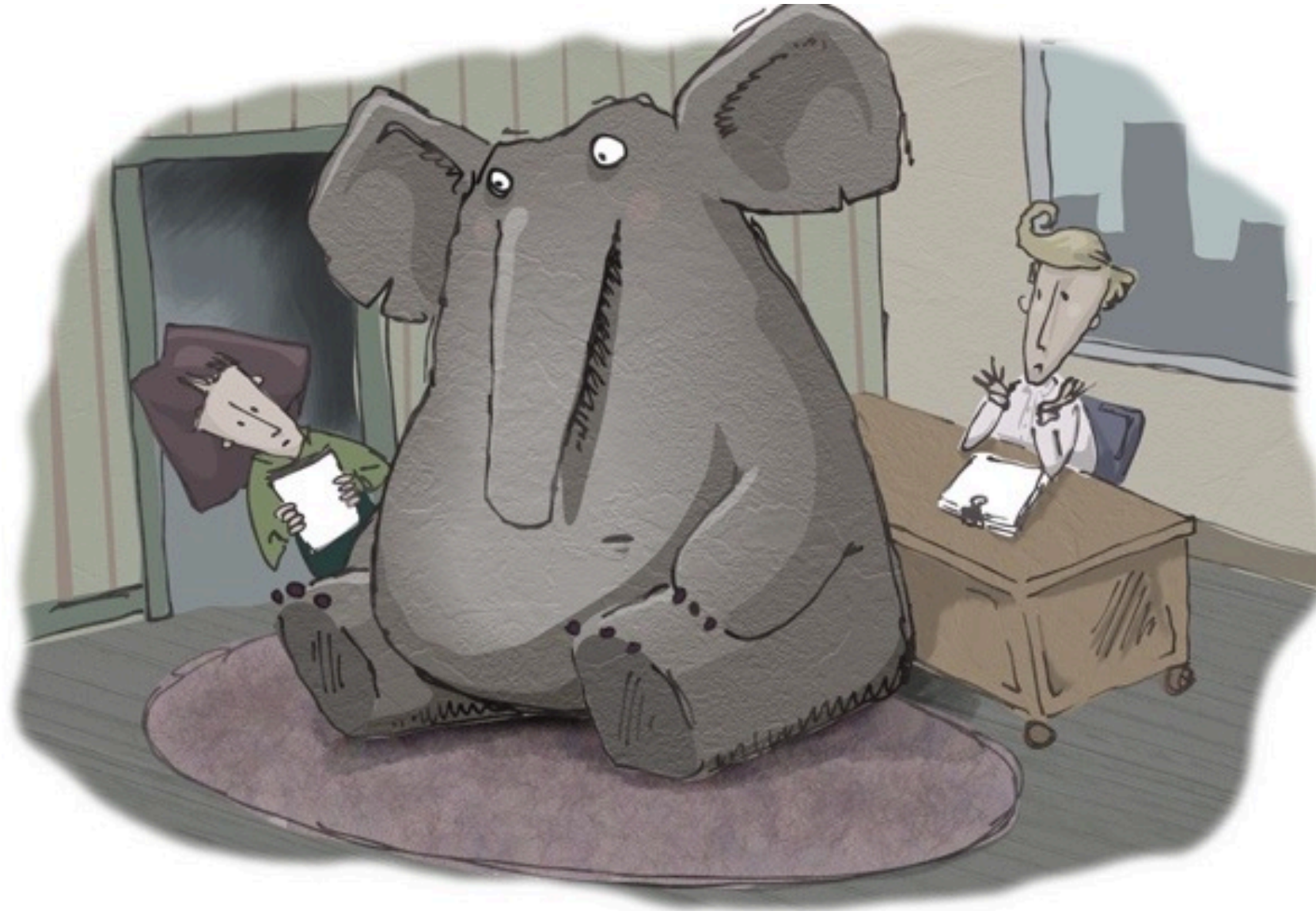
On July 4th 2012 reported both experiments reported $\sim 5\sigma$ effects

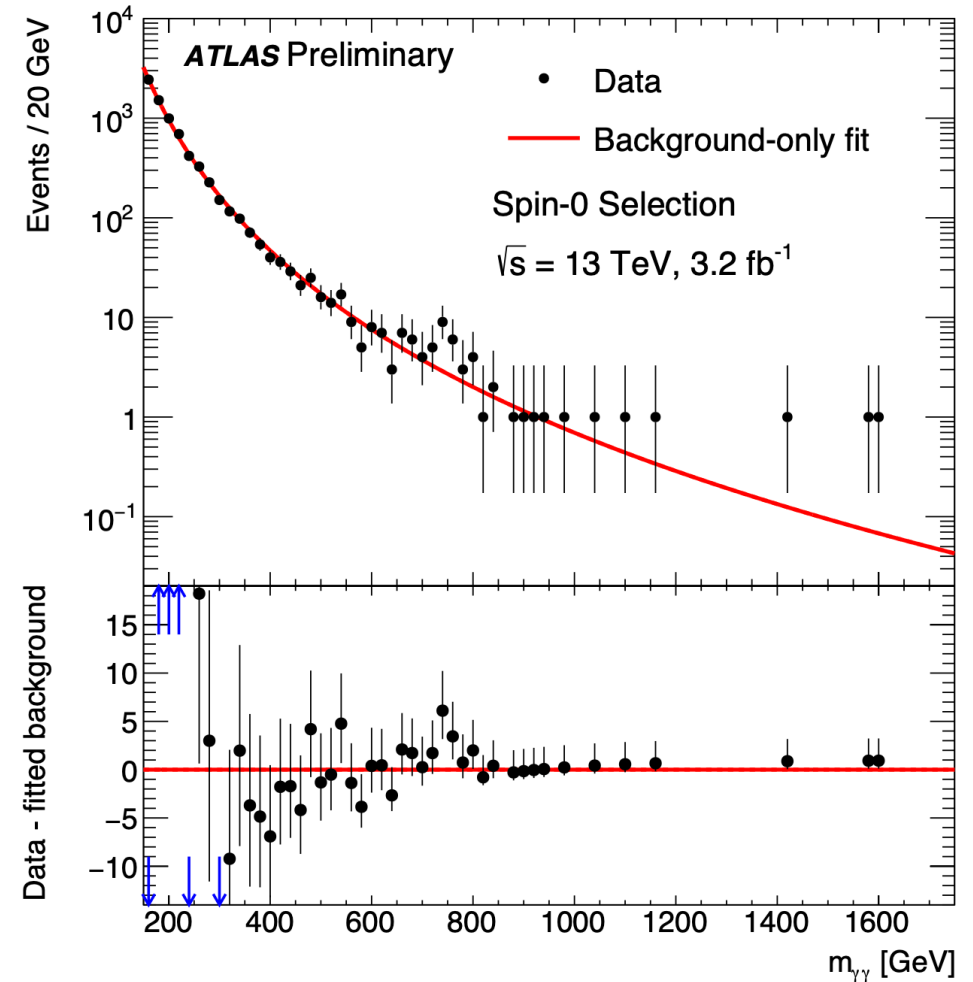
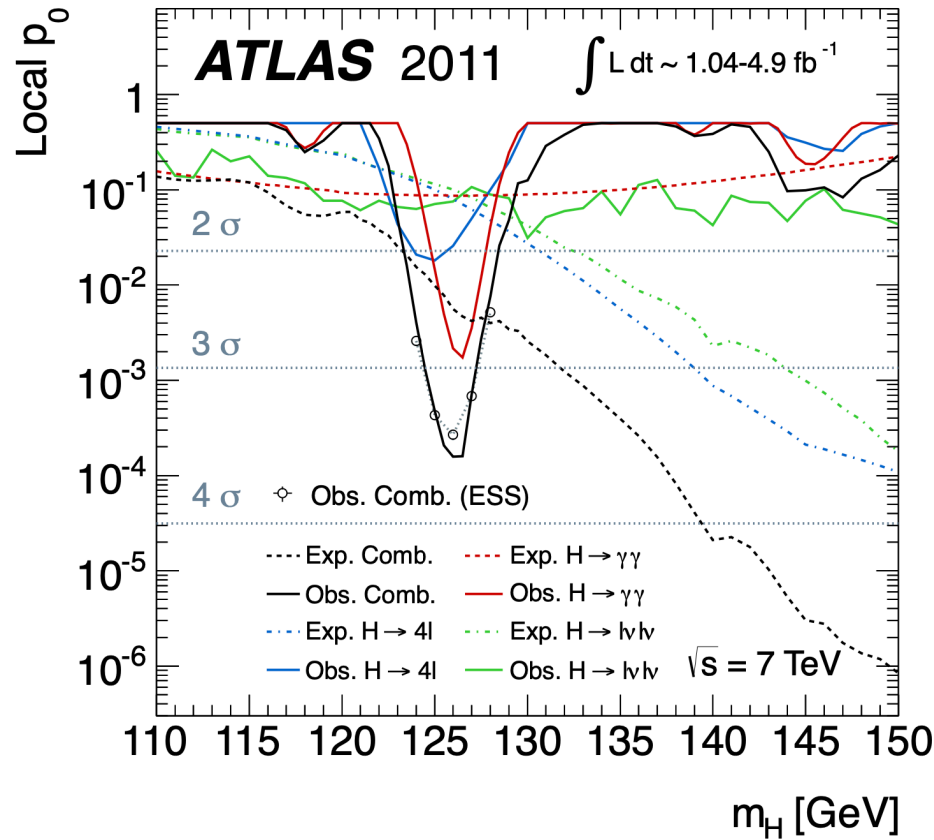


I wonder if there are others like me.



Let's address the Big Elephant in the room





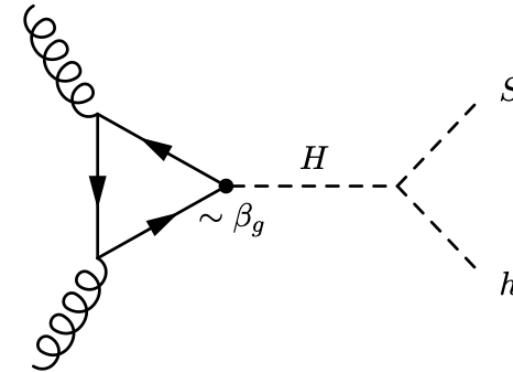
125 GeV	Criterion	750 GeV
YES	Multiple final states	NO
YES	Indirect evidence	NO
YES	Theoretical motivation and explanation	?

The 750 GeV excess had several red flags from inception

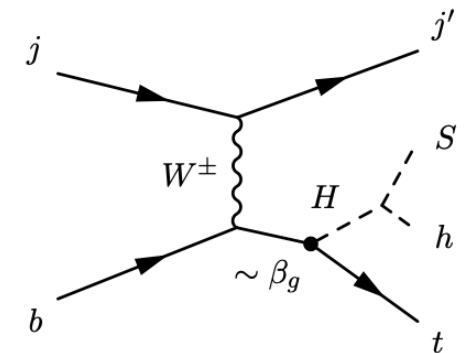
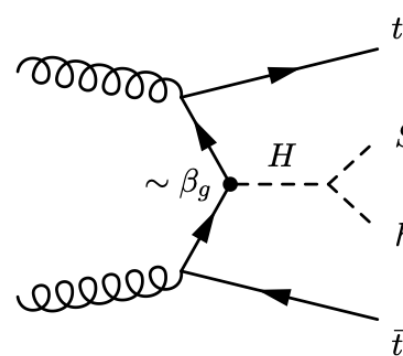
The Simplified Model

The simplified Model (from Run I)

- 1. The starting point of the hypothesis is the existence of a boson, H, that contains Higgs-like interactions, with a mass in the range 250-280 GeV**
- 2. In order to avoid large quartic couplings, incorporate a mediator scalar, S, that interacts with the SM and Dark Matter.**
- 3. Dominance of $H \rightarrow Sh, SS$ decay over other decays**



(a) Gluon fusion (ggF).



$$\mathcal{L}_{\text{int}} \supset -\beta_g \frac{m_t}{v} t\bar{t}H + \beta_V \frac{m_V^2}{v} g_{\mu\nu} V^\mu V^\nu H$$

$$\mathcal{L}_{HhS} = -\frac{1}{2} v \left[\lambda_{hhS} hhS + \lambda_{hSS} hSS + \lambda_{HHS} HHS + \lambda_{HSS} HSS + \lambda_{HhS} HhS \right],$$

The Decays of H

- In the general case, H can have couplings as those displayed by a Higgs boson in addition to decays involving the intermediate scalar and Dark Matter

$$H \rightarrow WW, ZZ, q\bar{q}, gg, Z\gamma, \gamma\gamma, \chi\chi$$
$$+ H \rightarrow SS, Sh, hh$$

Dominant decays

Diboson decay

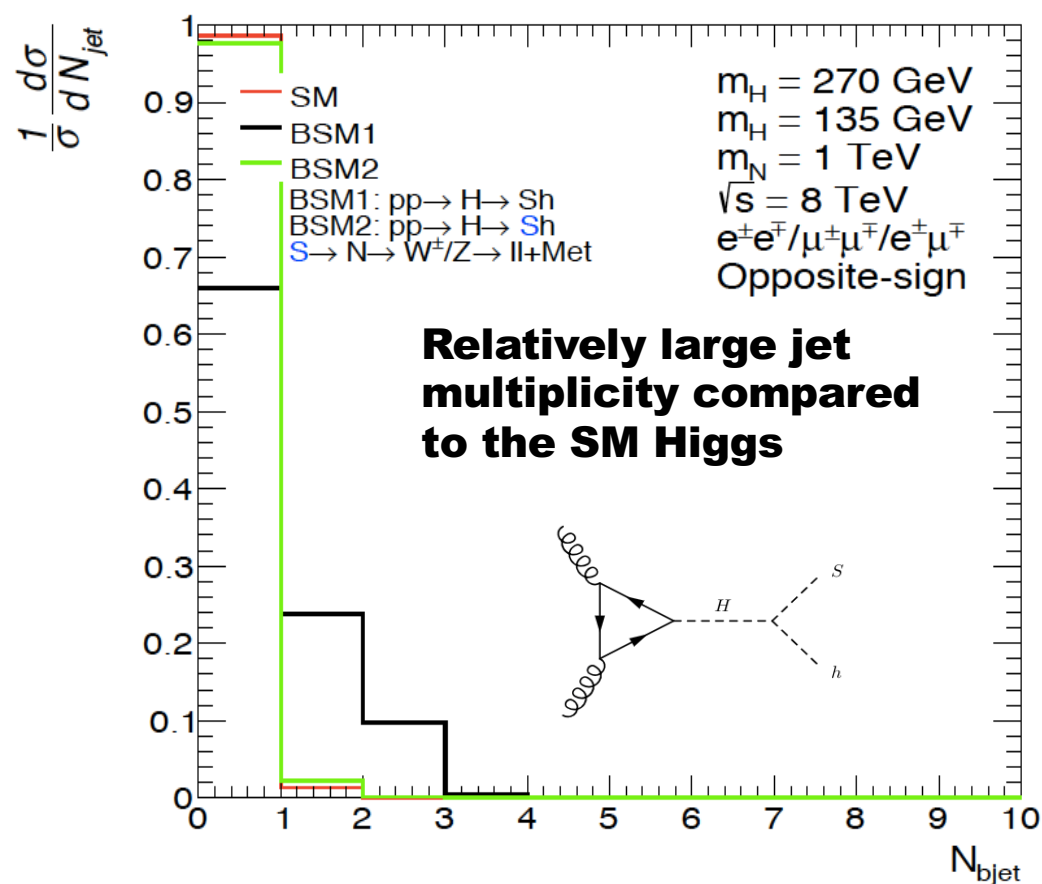
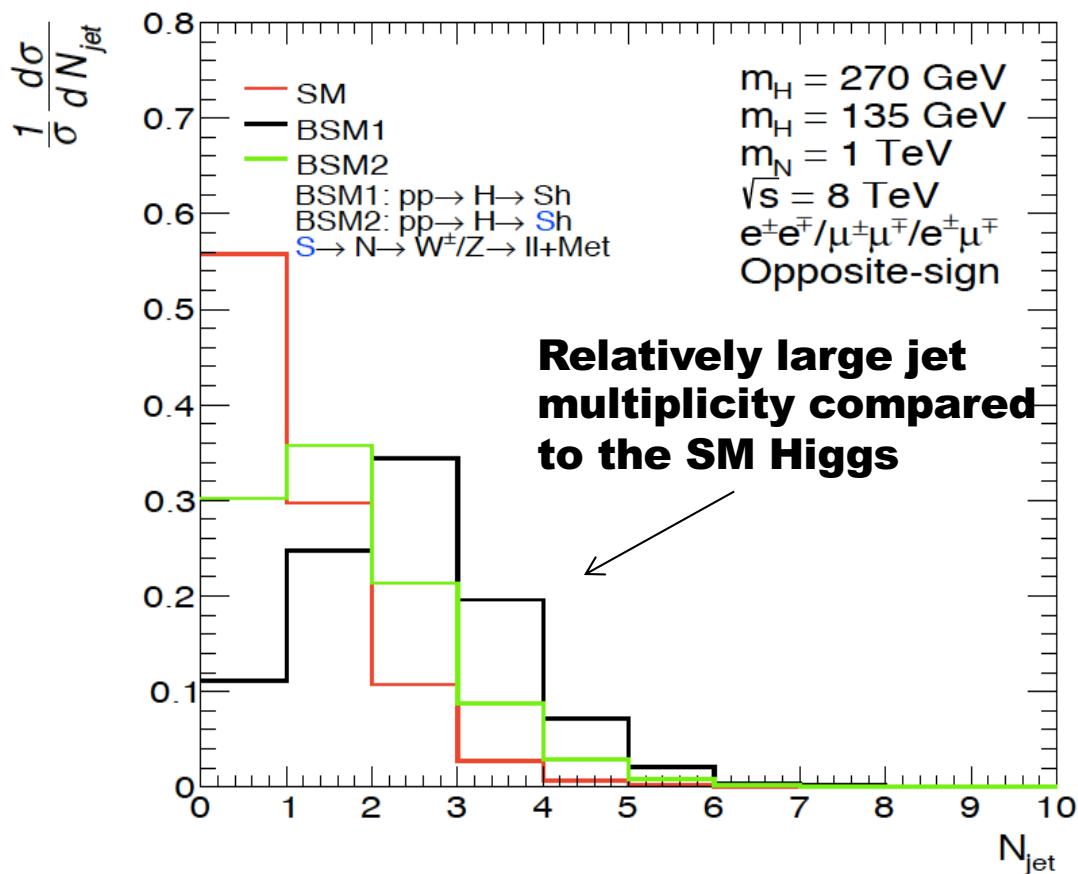
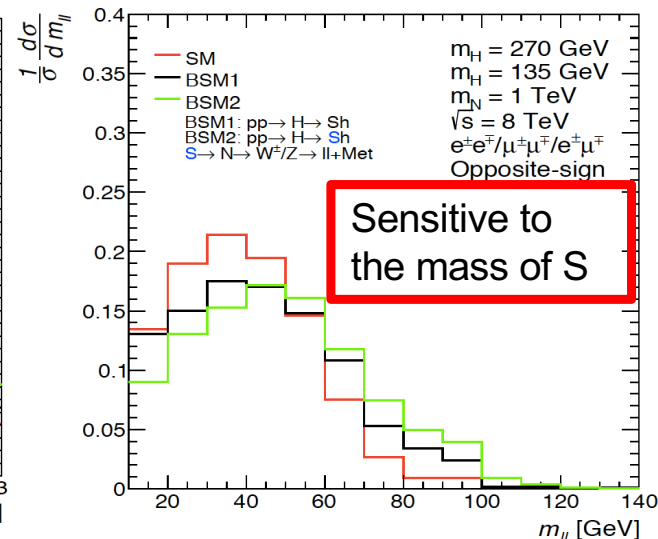
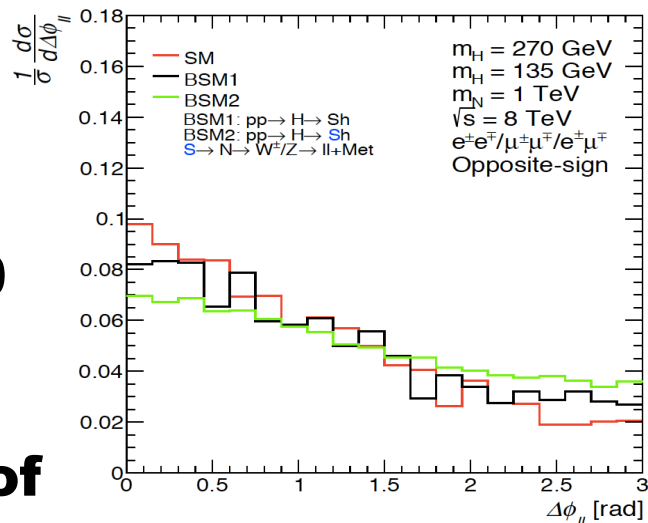
$$H \rightarrow h(+X), S(+X)$$

Multi-lepton final states

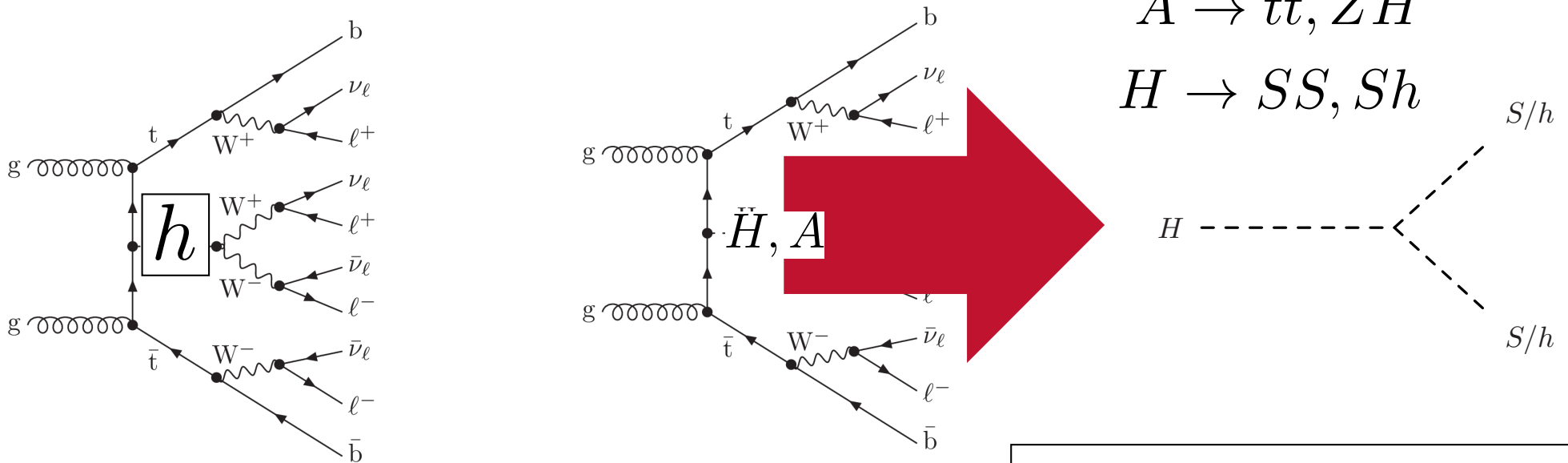
It is paramount to remark that the excesses are seen in final states that were predicted 2015/2016 on the basis of a simplified model and not the result of scan of the available phase-space. Additionally, the parameters of the model were fixed then leaving only one degree of freedom: normalization. Thus, no look-elsewhere effects in parameter or phase-space

$$pp \rightarrow H \rightarrow Sh, SS \rightarrow \ell^+ \ell^- + X$$

Expect di-leptons ($m_{ll} < 100$ GeV, due to $S \rightarrow WW \rightarrow l\nu l\nu$) with jets and b-jets with rates comparable to that of the SM Higgs boson



Top associated Higgs production (Multi-lepton final states)



Reduced cross-section of $t\bar{t}H+tH$ is compensated by di-boson, (SS, Sh) decay and large $\text{Br}(S \rightarrow WW)$. Production of same sign leptons, three leptons is enhanced. Enhanced tH cross-section

Produces SS 2l, 3l with b-jets, including 3 b-jets

Explains anomalously large $t\bar{t}W+t\bar{t}h+4t$ cross-sections seen by ATLAS and CMS

Methodology

(to avoid biases and look-else-where effects)

Based Higgs p_T , hh, tth, VV in Run 1
Eur. Phys. J. C (2016) 76:580

Model defined and predictions made for
multilepton excesses

Multi-lepton excesses in Run 1 and few
Run 2 results available in 2017

J.Phys.G 45 (2018) 11, 115003

Model parameters fixed in 2017 with
 $m_H=270$ GeV, $m_S=150$ GeV,
S treated as SM Higgs-like,
dominance of $H \rightarrow Sh, SS$

Fixed final states and phase-space
defined by fixed model parameters.
NO tuning, NO scanning

Update same final states with
more data in Run 2

Study new final states where
excesses predicted and data
available in Run 1 and Run 2
(e.g., SS0b, 3l0b, ZW0b)

J.Phys. G46 (2019) no.11, 115001

JHEP 1910 (2019) 157

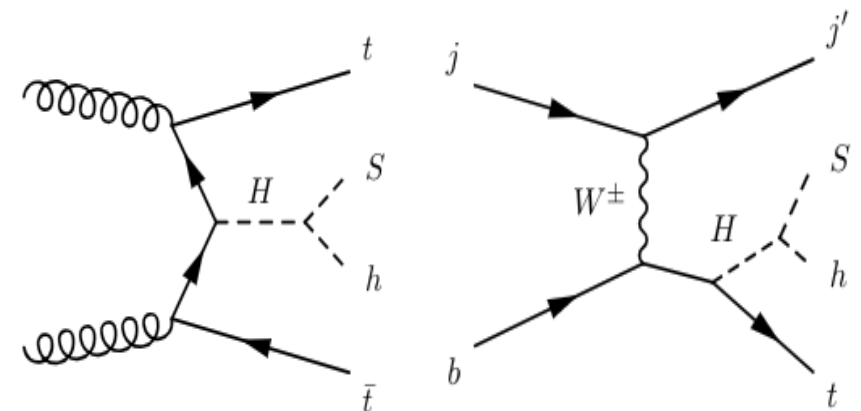
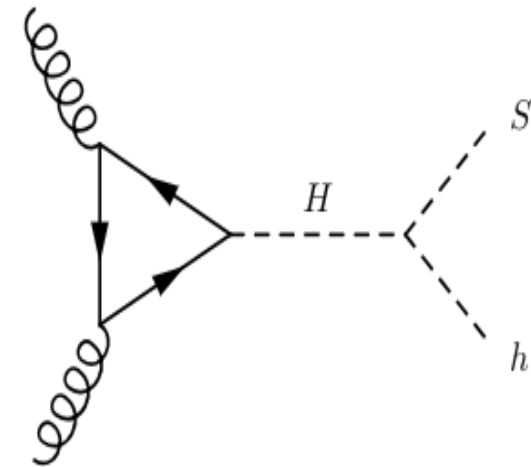
Chin.Phys.C 44 (2020) 6, 063103

Physics Letters B 811 (2020) 135964

Eur.Phys.J.C 81 (2021) 365

BSM inputs to the fit

- The following assumptions are made:
 - a. The masses of H and S are fixed to $m_H = 270$ GeV and $m_S = 150$ GeV
 - b. The only significant production mechanisms of H come from the t - t - H Yukawa coupling:
 - Gluon fusion
 - Top associated production
 - c. The Yukawa coupling is scaled away from the SM Higgs-like value by the free parameter β_g
 - d. The BR of $H \rightarrow Sh$ is fixed to 100%
 - e. The BRs of S are Higgs-like
- Therefore, the only free parameter in the fits is β_g^2



Combination of fit results (2019)

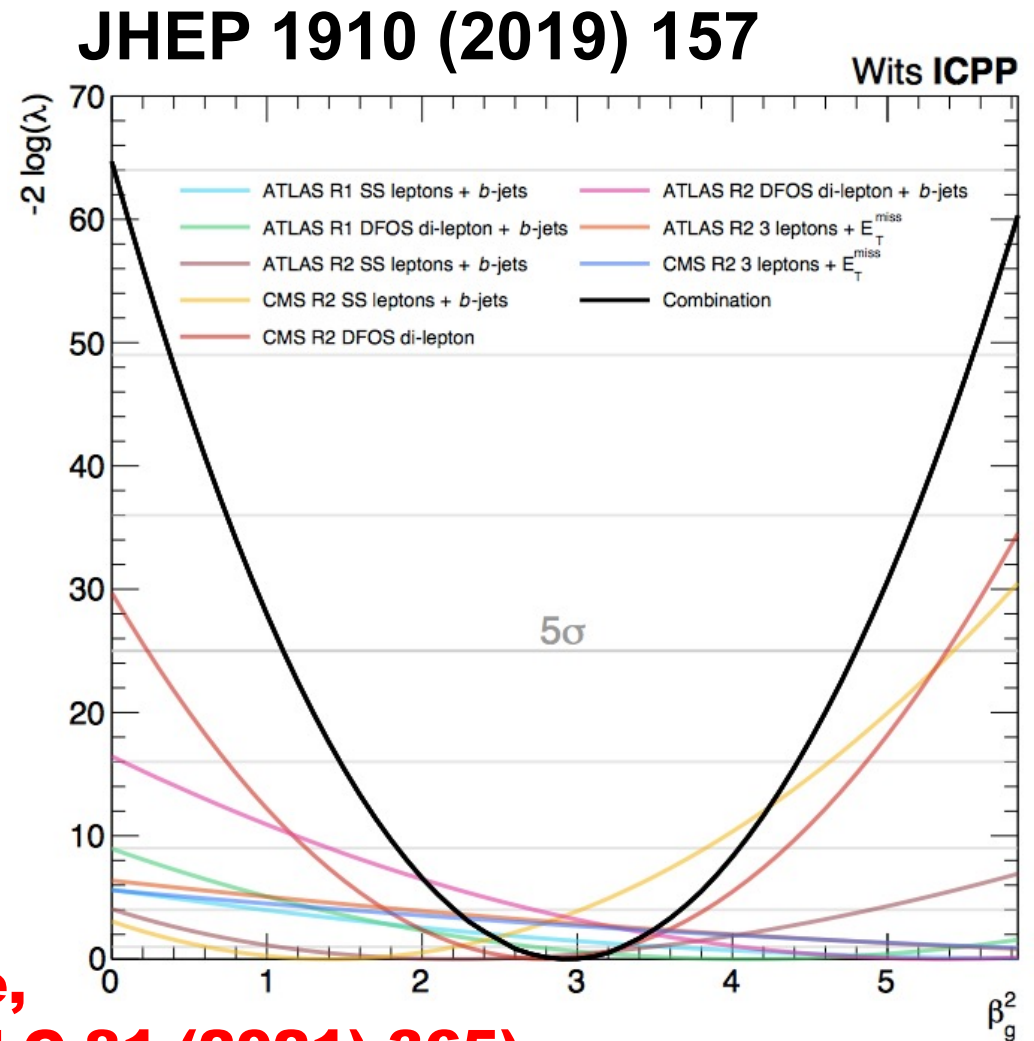
- **Simultaneous fit for all measurements:**
- **To the right: (-2 log) profile likelihood ratio for each individual result and the combination of them all**
- **The significance for each fit is calculated as**

$$\sqrt{-2 \log \lambda(0)}$$

- **Best-fit: $\beta_g^2 = 2.92 \pm 0.35$**
- **Corresponds to 8.04σ**

Excesses have been growing since, and new have emerged (Eur.Phys.J.C 81 (2021) 365)

Interpretation: Measure of the inability of current MC tools to describe multiple-lepton data and how a simplified model with $H \rightarrow Sh$ is able to capture the effect with one parameter

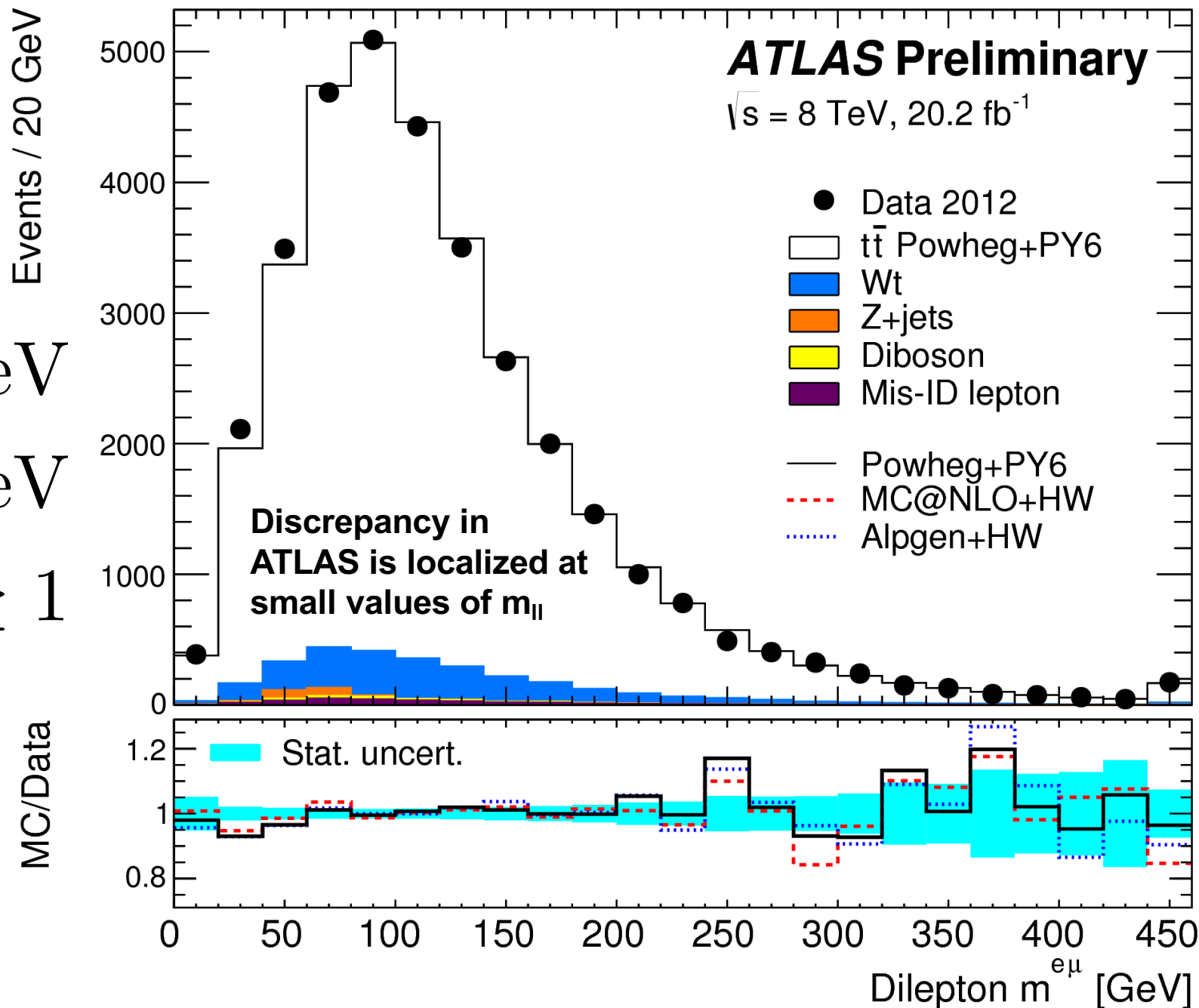


Is the discrepancy due to $t\bar{t}$ events?

$$p_{T\ell} > 25 \text{ GeV}$$

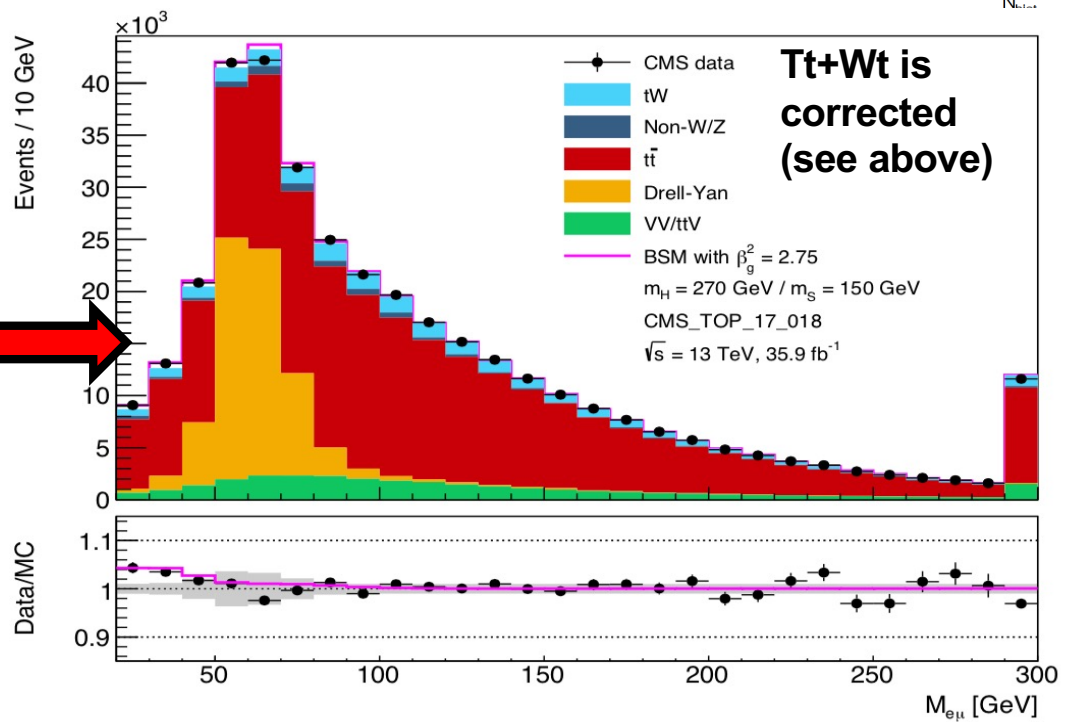
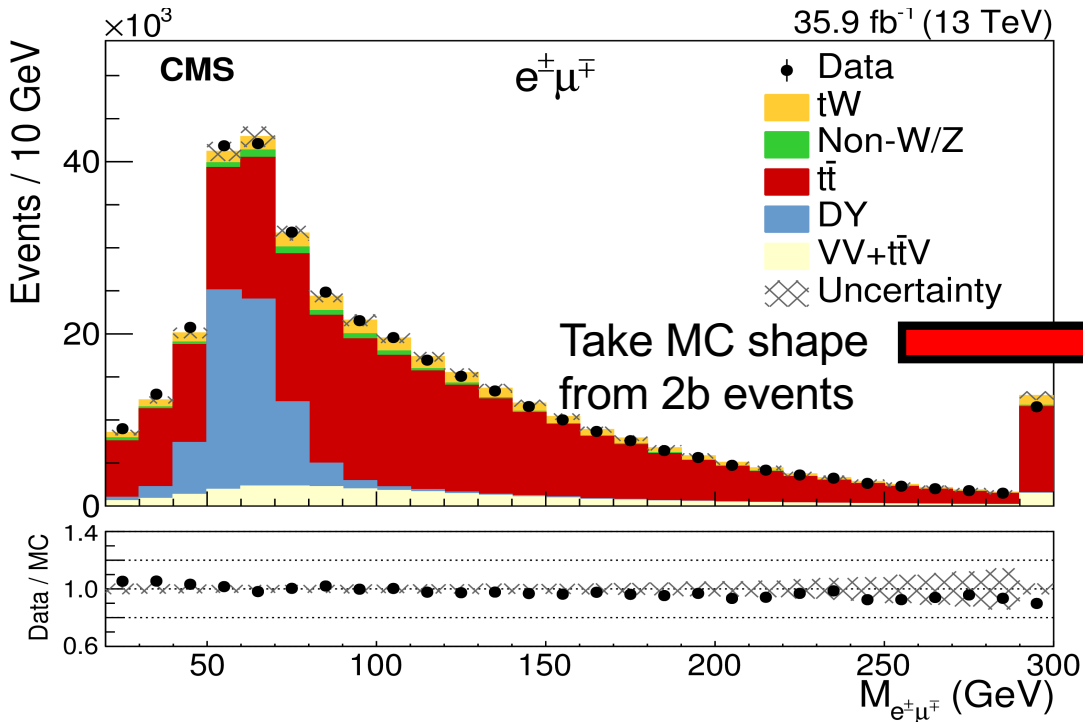
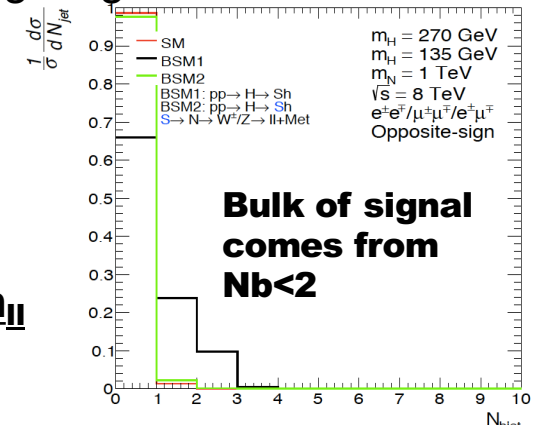
$$p_{Tb} > 25 \text{ GeV}$$

$$N_{bjet} \geq 1$$

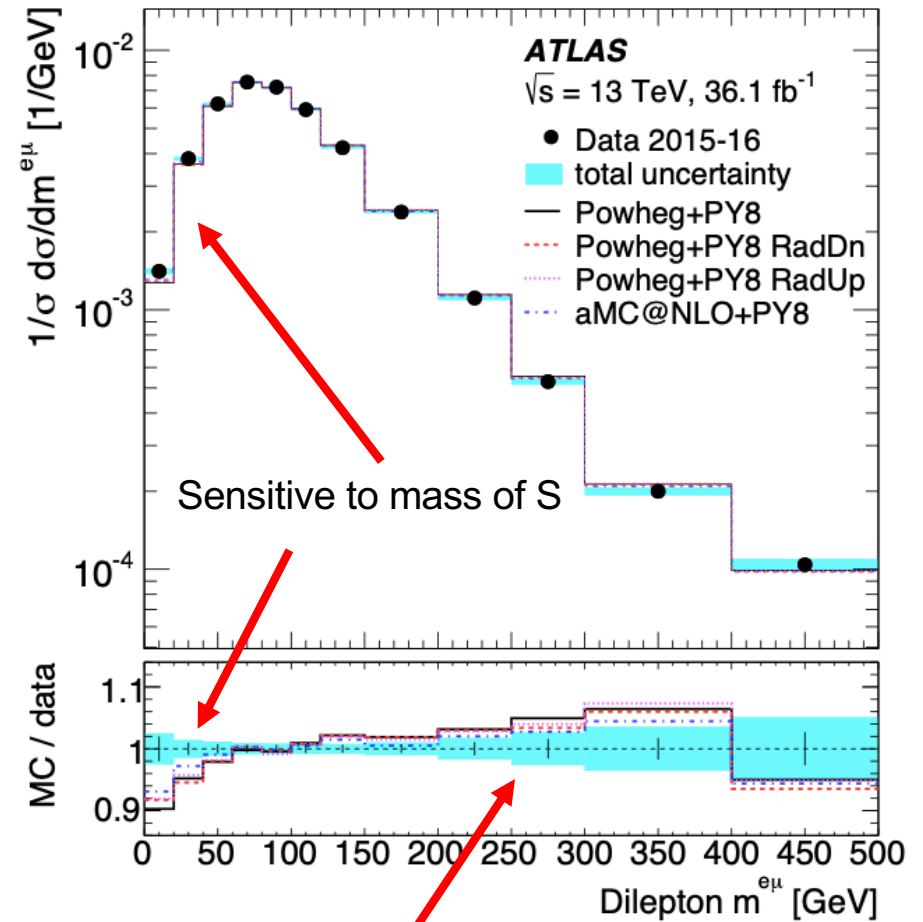
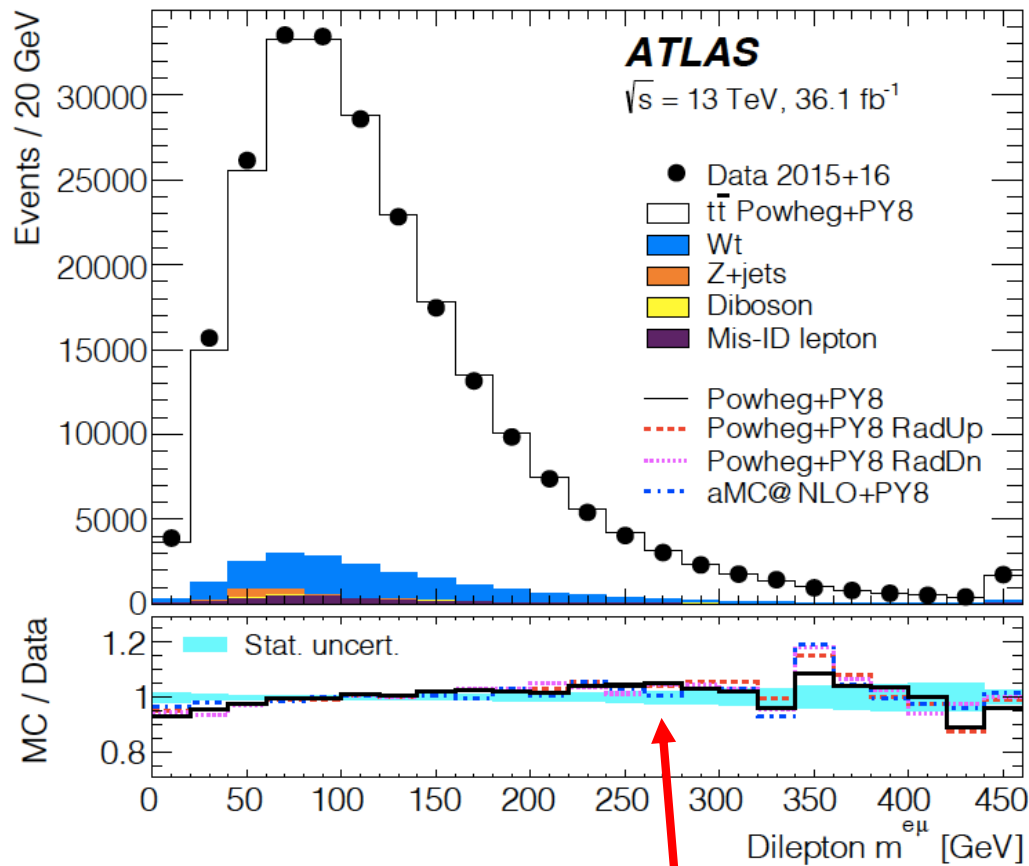


- Poor modeling of POWHEG + Pythia8 distribution is improved through reweighting
- We fix the normalisation of the SM by scaling it to the data in the region $m_{ll} > 110$ GeV
 - A normalisation systematic of 3% is applied to all but DY
 - DY systematic = 6.8%. 3% systematic on m_{ll} shape in top
 - The fit is done to the region below 110 GeV
- Fit results:
 - $\beta_g^2 = 2.79 \pm 0.52$
 - Fit is extremely well constrained

Very Small MC dependence, as m_{ll} shape comes from data

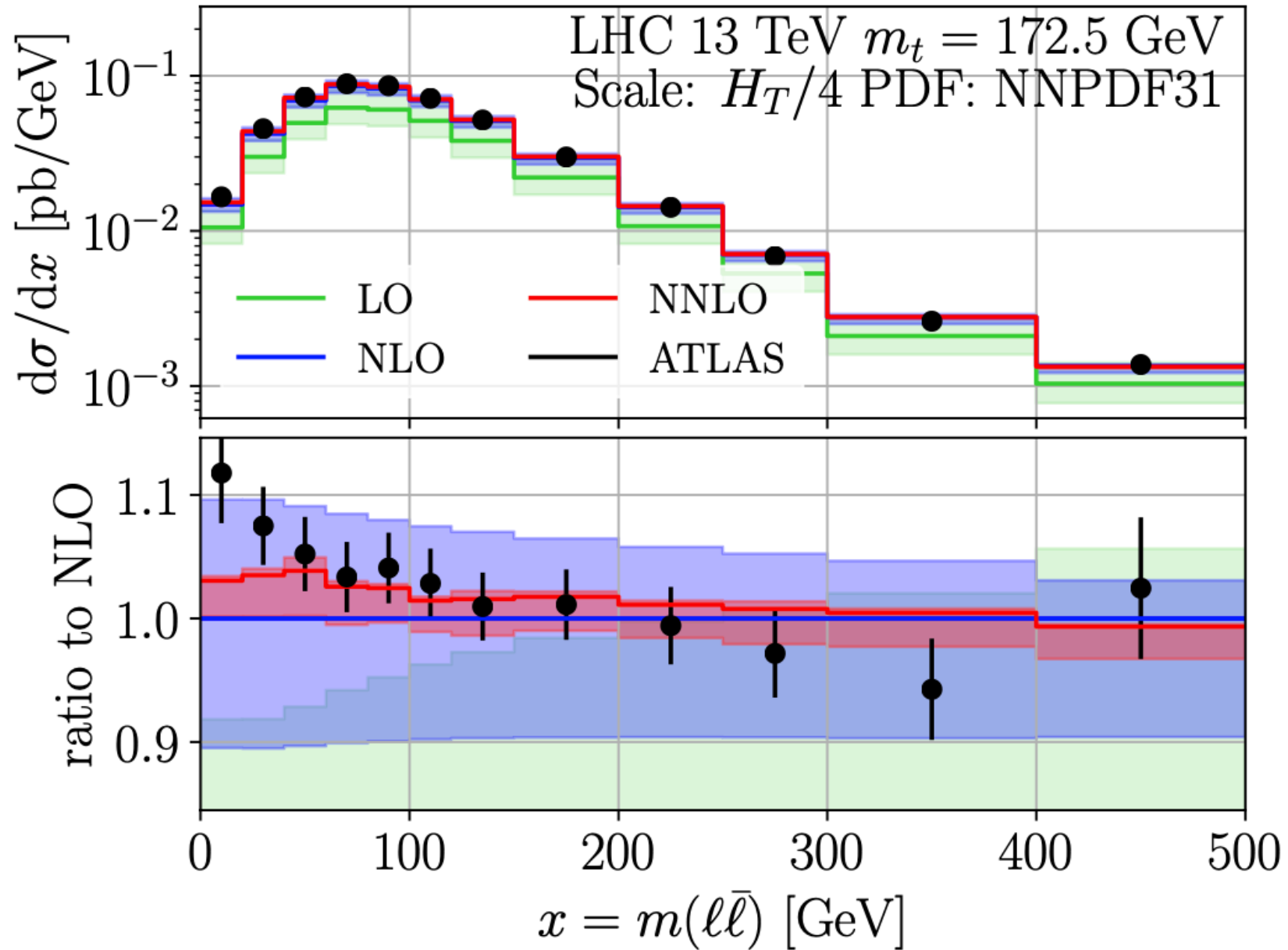


Used conservative assumption that l^+l^-+2b -jet final state is well described by the SM. The discrepancy comes from events with $N_b < 2$. Excess unlikely due to $t\bar{t}$



Residual discrepancies at high m_{ll} will be fixed with missing NNLO QCD and NLO EW corrections

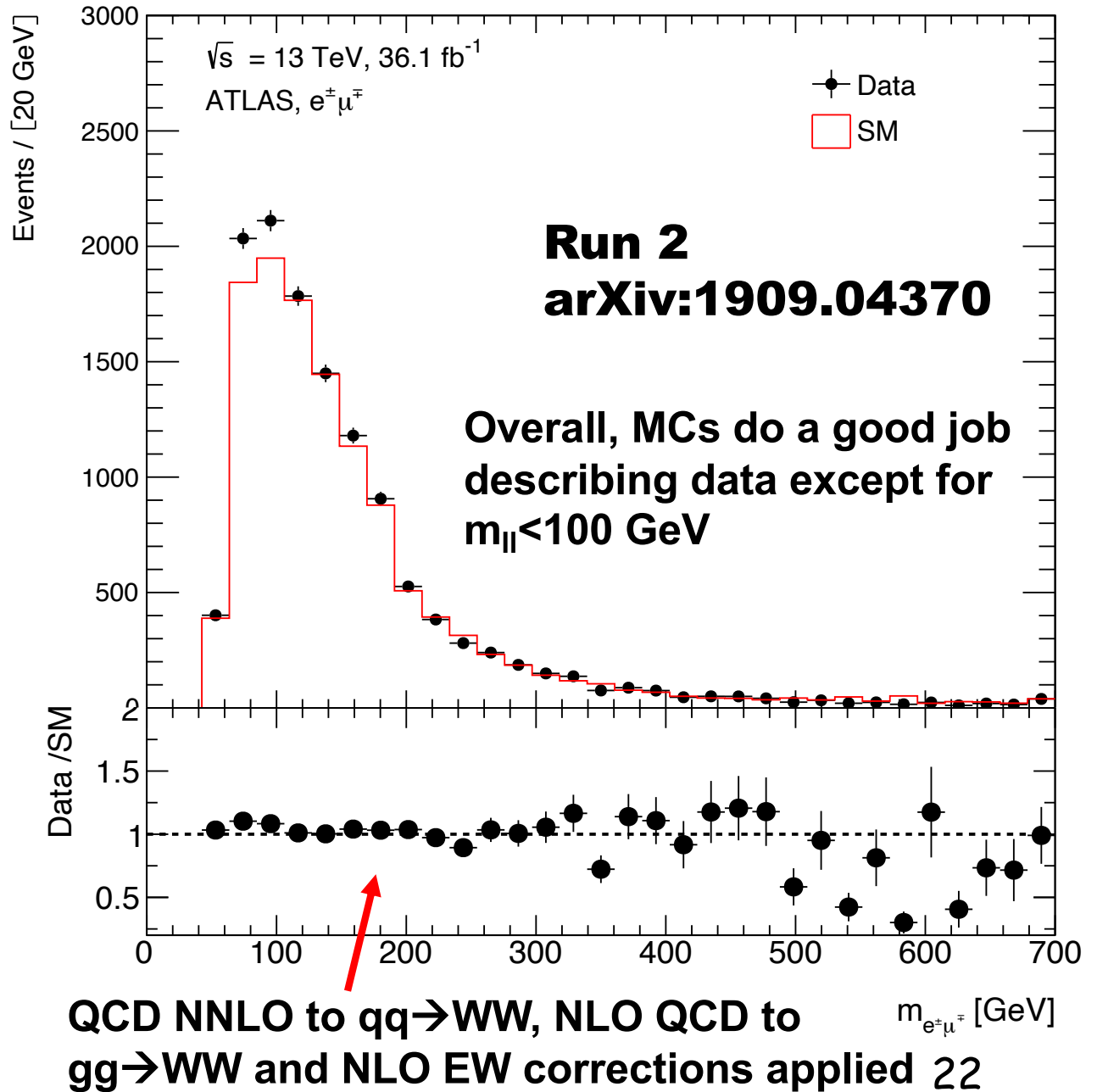
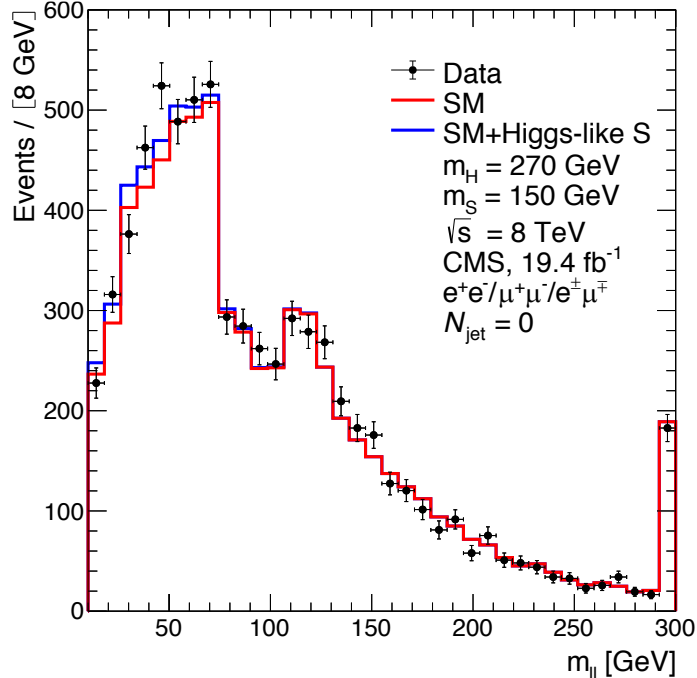
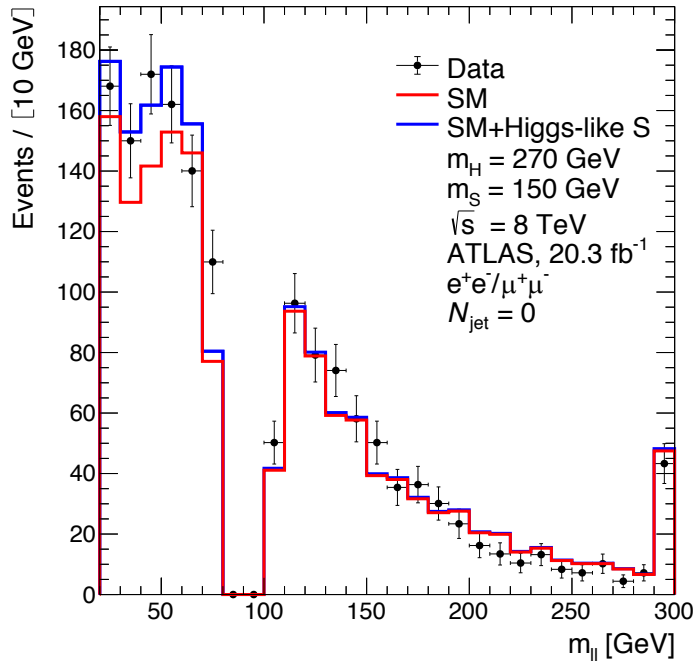
Excess at low m_{ll} remains prevalent, indicating that effects seen in Run 1 were not statistical fluctuations. NNLO QCD corrections do not fix the issue (see Mitov et al.)



Excesses in di-leptons with full-jet veto. Excludes tt as source.

From Run 1 multi-lepton excesses model-dependent prediction of $m_s = 150 \pm 5$ GeV

Run 1, J.Phys. G45 (2018) no.11, 115003



Anatomy of the multi-lepton anomalies (2024)

Final state	Characteristic	Dominant SM process	Significance
l^+l^- + jets, b-jets	$m_{ll} < 100$ GeV, dominated by 0b-jet and 1b-jet	tt+Wt	$>5\sigma$
l^+l^- + full-jet veto	$m_{ll} < 100$ GeV	WW	$\sim 3\sigma$
$l^\pm l^\pm$ & $l^\pm l^\pm$ + b-jets	Moderate H_T	ttW, 4t, ttZ/tWZ	$>3\sigma$
$l^\pm l^\pm$ & $l^\pm l^\pm$ et al., no b-jets	In association with h	Wh, WWW	4.2σ
Z($\rightarrow l^+l^-$)+l	$p_{TZ} < 100$ GeV	ZW	$>3\sigma$

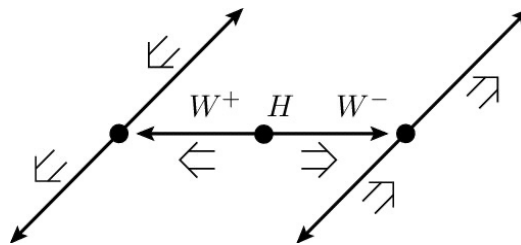
Di-lepton invariant mass in MLA predict a scalar with a mass **150 ± 5 GeV** (J.Phys. G45 (2018) no.11, 115003, see also Phys.Rev.D 108 (2023) 11, 115031 and arXiv:2306.17209) in association with leptons and jets.

Prediction from the multi-lepton anomalies.

The di-lepton invariant mass is sensitive to the mass of S .

Assuming $S \rightarrow WW \rightarrow ll\nu\nu$:

$$m_S = 150 \pm 5 \text{ GeV}$$

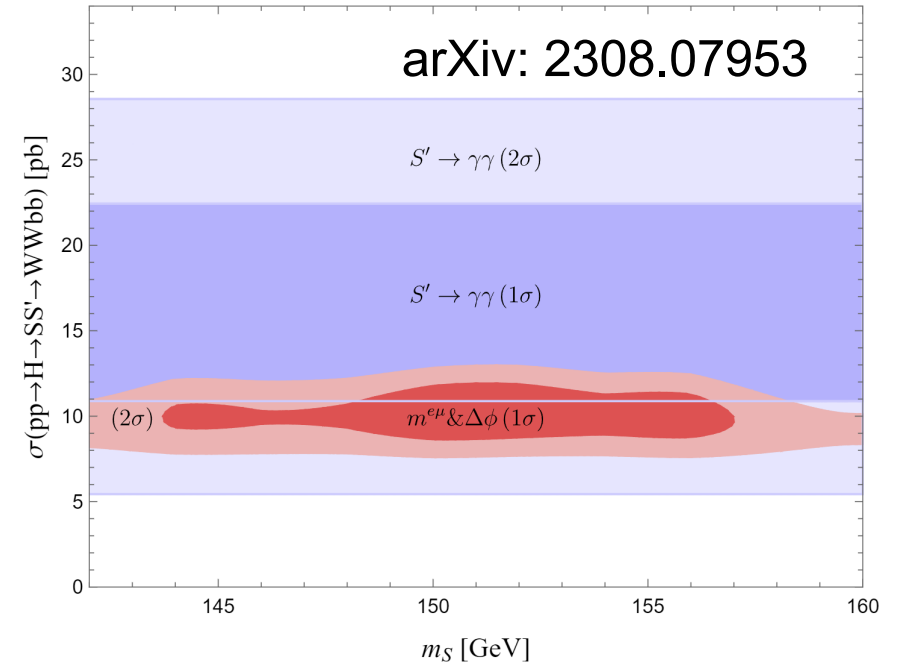
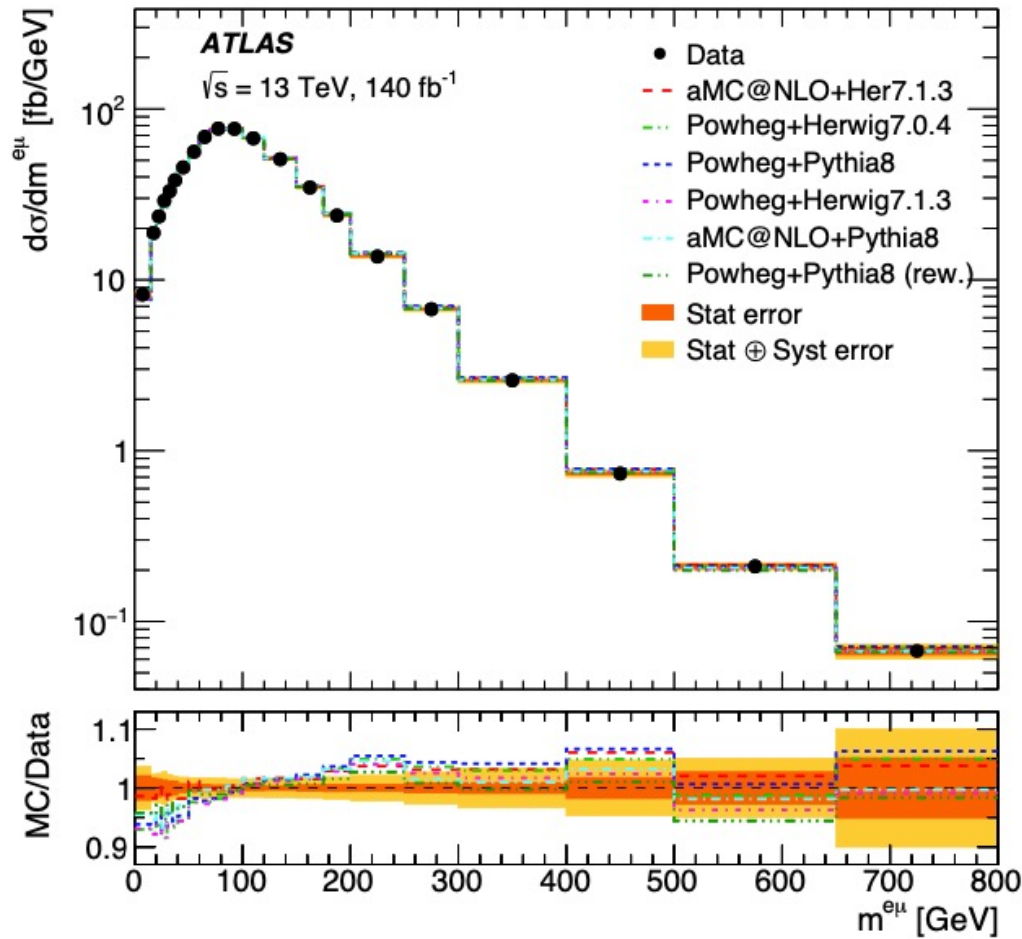


J.Phys. G45 (2018) no.11, 115003

**The 152 GeV
Candidate**

Confirmed with new measurement in arXiv:2308.07953

New determination of m_S with di-lepton events with ATLAS di-lepton $t\bar{t}$ measurement



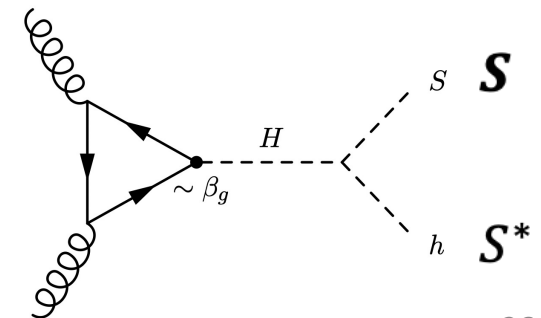
$m^{e\mu}$ bins [GeV]	$d\sigma/dm^{e\mu}$ [fb/GeV]	Data stat. [%]	MC stat. [%]	$t\bar{t}$ mod. [%]	Lep. [%]	Jets/ b -tag. [%]	Bkg. [%]	Lumi + E_{beam} [%]	Total unc. [%]
0.0–15.0	8.21	2.08	0.47	2.38	0.90	0.14	1.31	0.93	3.69
15.0–20.0	18.81	1.71	0.36	0.59	0.85	0.12	0.76	0.92	2.36
20.0–25.0	23.48	1.54	0.33	1.19	0.84	0.12	0.73	0.92	2.45
25.0–30.0	29.02	1.33	0.30	1.72	0.84	0.09	1.07	0.92	2.75
30.0–35.0	33.04	1.24	0.29	1.17	0.85	0.09	0.79	0.92	2.28
35.0–40.0	38.24	1.19	0.26	0.37	0.84	0.09	0.74	0.93	1.93
40.0–50.0	45.49	0.75	0.18	0.75	0.84	0.10	0.80	0.93	1.84
50.0–60.0	56.16	0.70	0.21	0.45	0.85	0.11	0.74	0.93	1.71
60.0–70.0	68.55	0.63	0.20	0.51	0.84	0.11	0.72	0.93	1.67
70.0–85.0	76.71	0.47	0.13	0.67	0.80	0.11	0.70	0.93	1.65
85.0–100.0	76.44	0.47	0.10	0.48	0.77	0.12	0.68	0.92	1.54
100.0–120.0	67.32	0.44	0.09	0.56	0.75	0.13	0.68	0.92	1.55

Confirmation of early determination of m_S with Run 2 data and using a different final state ($ll+b$ -jets)

Procedure

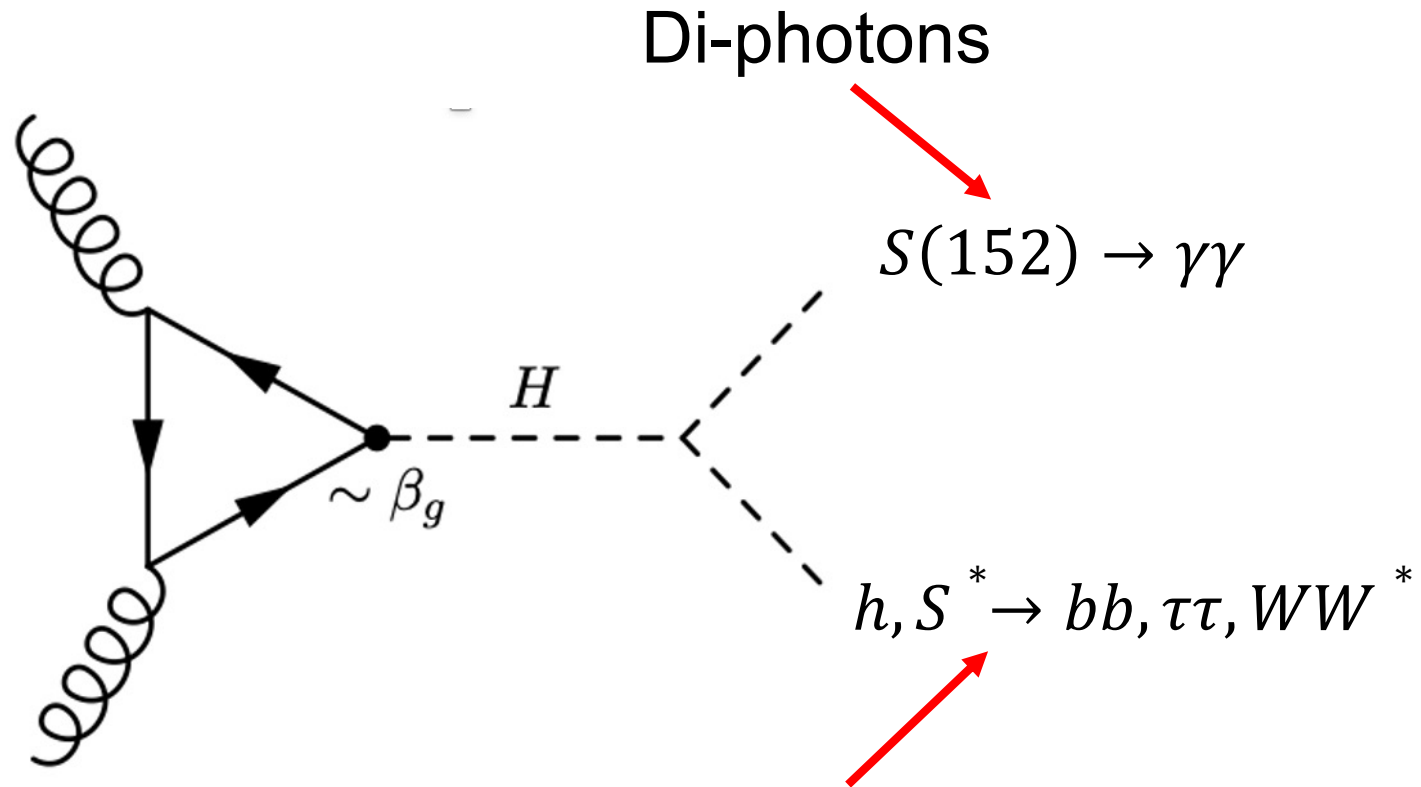
(avoiding “cherry picking”)

- ❑ **Setting a well-defined procedure is essential to the integrity of a search. Scanning nullifies significance**
- ❑ **From the di-lepton anomalies: $m_h < m_s < 170$ GeV**
 - ❑ **It is critical that search be localized and motivated**
- ❑ **Focus on $\gamma\gamma$ and $Z\gamma$ decays**
- ❑ **As per the model that described the multi-lepton anomalies, we select final state according to di-boson signatures. S is produced via the decay of something heavier and not directly**
 - ❑ **Re-use Higgs boson data**
 - ❑ **Remove VBF and boosted topologies**
 - **Related to direct production**



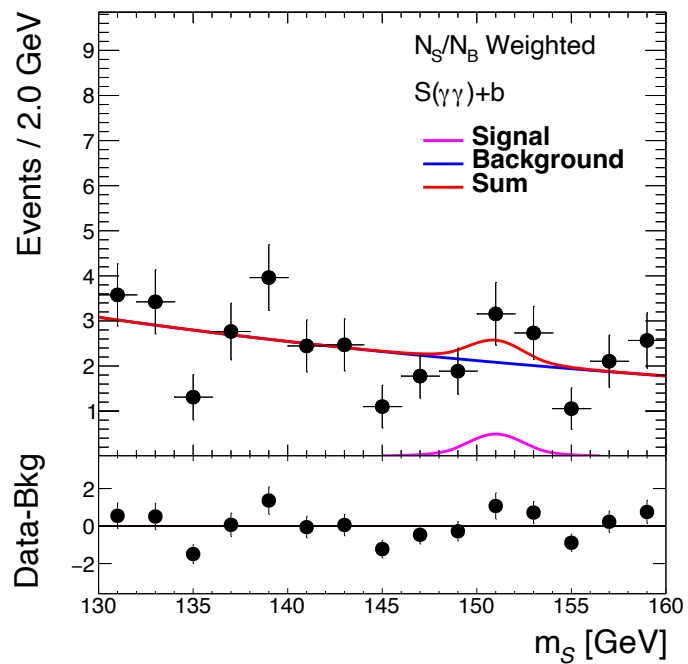
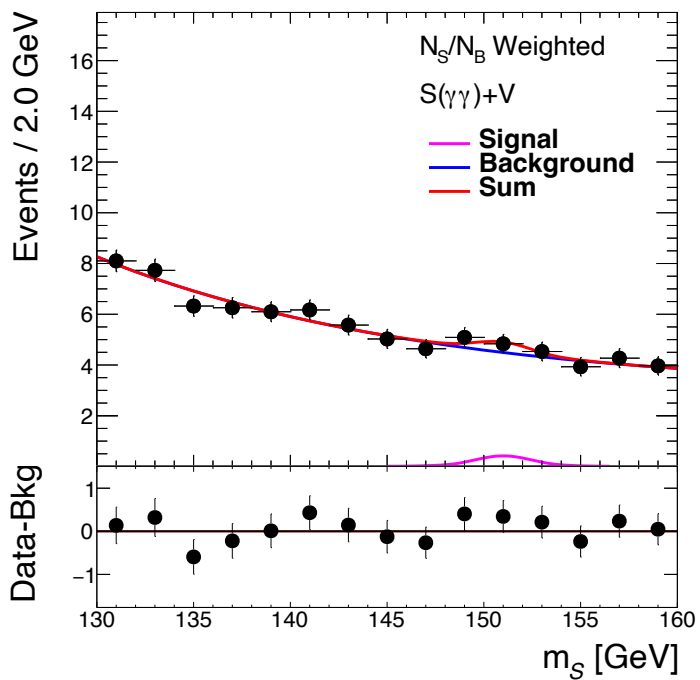
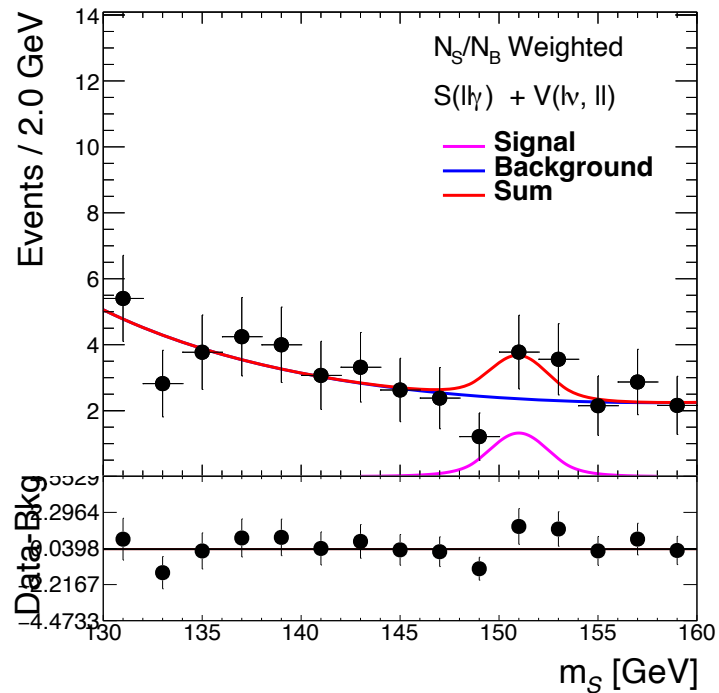
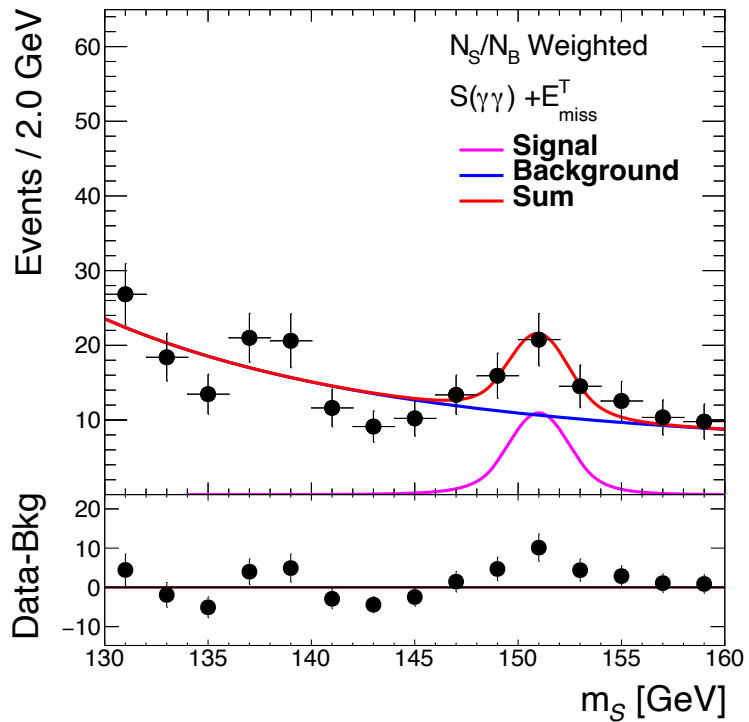
From Run 1 multi-lepton excesses model-dependent prediction of $m_s = 150 \pm 5$ GeV

Procedure to choose final state: di-photon in association with b-jets, τ -had, leptons (e/μ) and jets



Source of b-jet, τ -had, leptons, jets

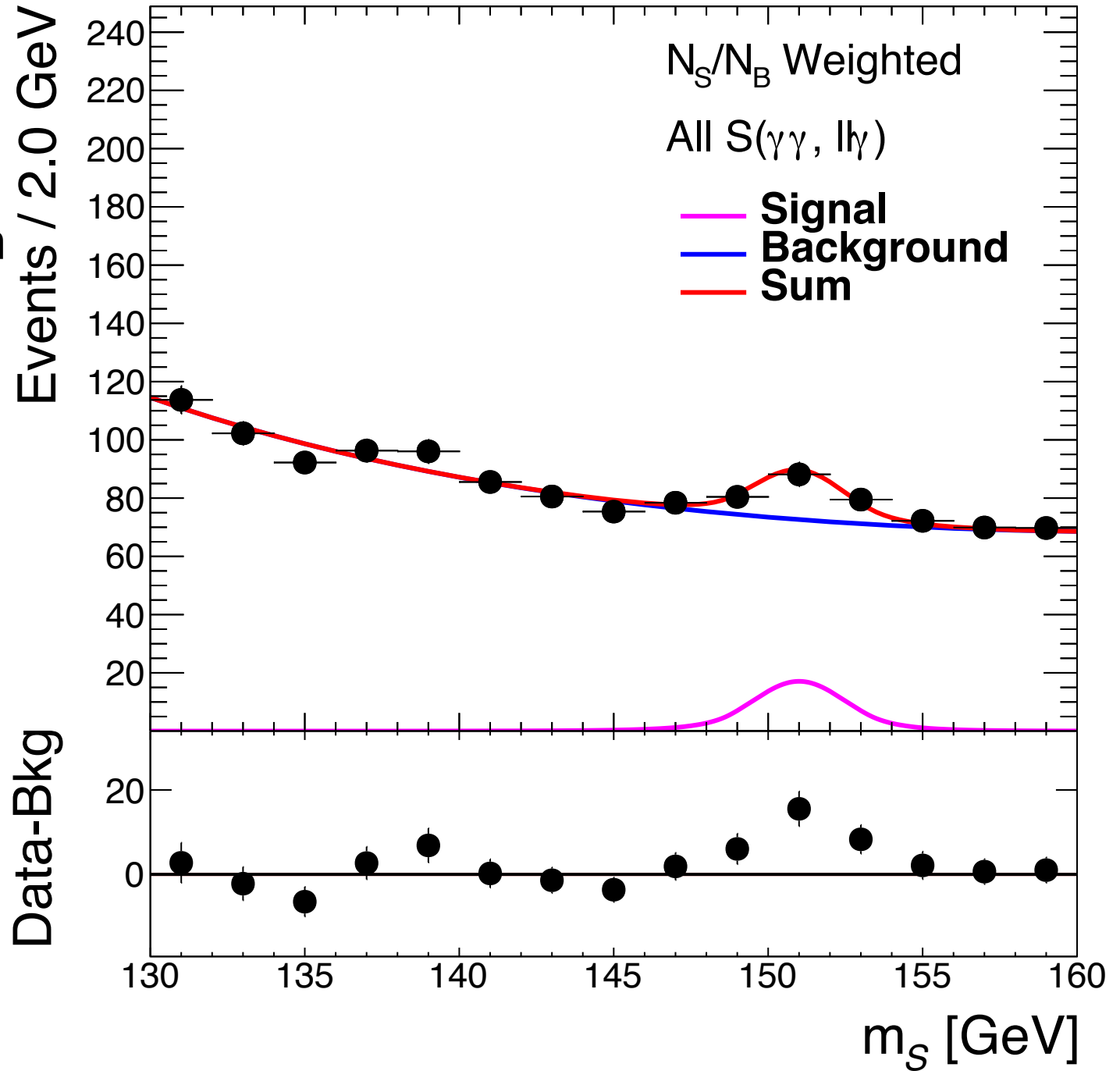
In *Eur.Phys.J.C* 76 (2016) 10, 580 also considered $S \rightarrow \text{MET}$



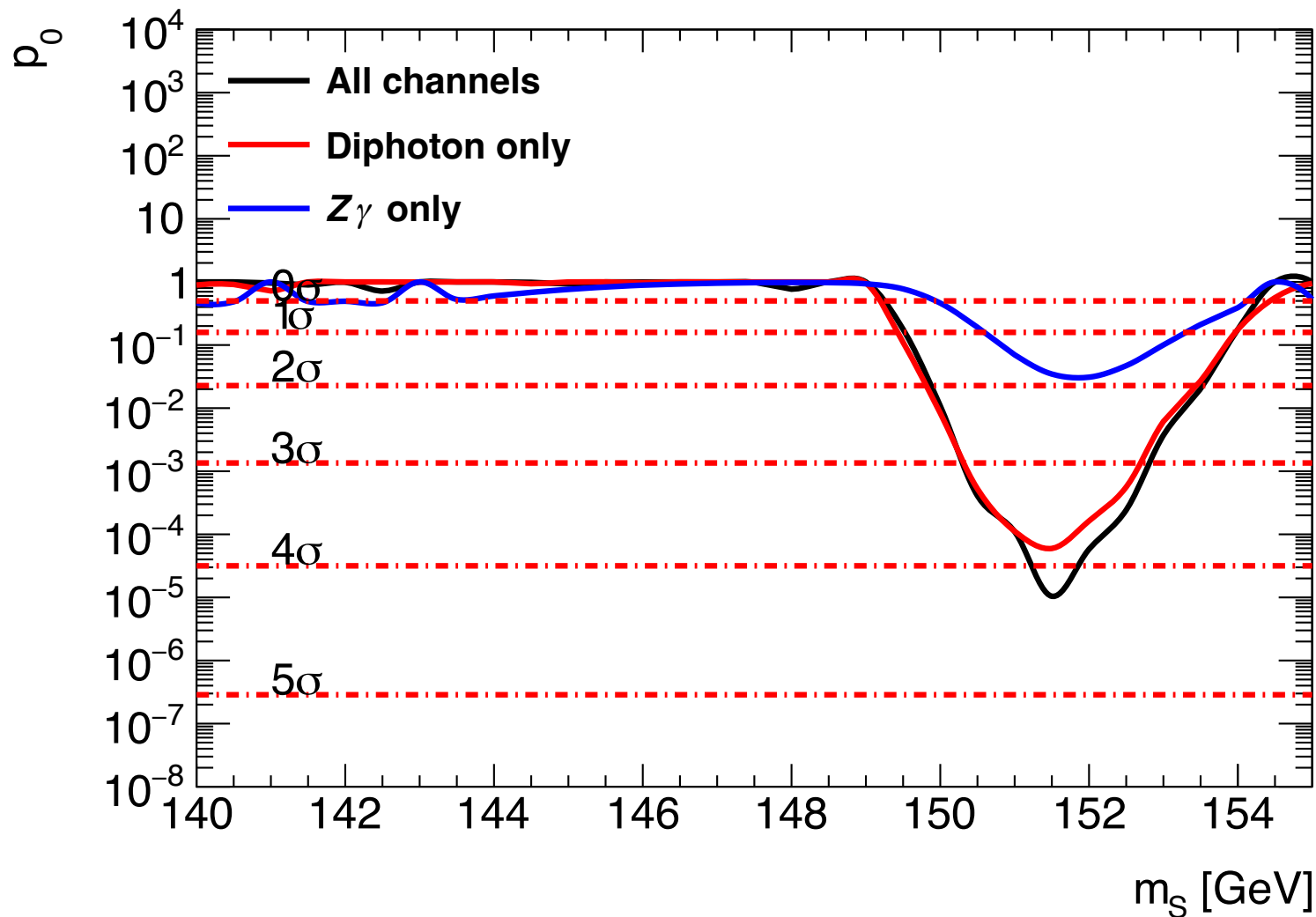
Analysis of publicly available $\gamma\gamma$, $Z\gamma$ spectra in associated production gives an excess at $m_S=151.5$ GeV.

Fiducial yields consistent with $H\rightarrow SS^*$ hypothesis with $m_H=270$ GeV, which is used for the extraction of significance.

Excess not seen in $S\rightarrow ZZ\rightarrow 4l$

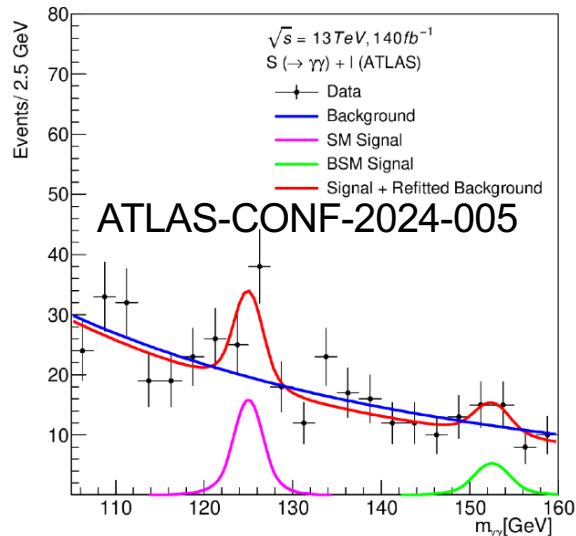


Result is obtained with public results from the LHC experiments. Using a simplified model and two degrees of freedom to include the decay of $S \rightarrow \text{MET}$ (as in Eur.Phys.J.C 76 (2016) 10, 580) and residual LEE, global significance goes to 3.9σ at 151.5 GeV.

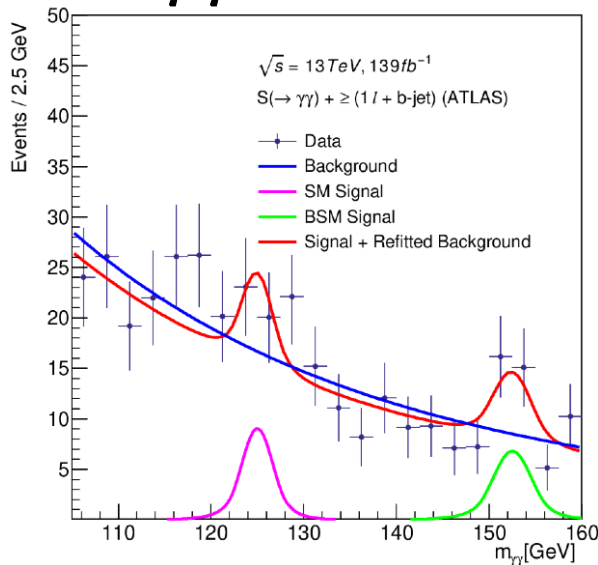


New excesses @151.5 GeV that appeared after the first combination (see above) in topologies consistent with associated production:

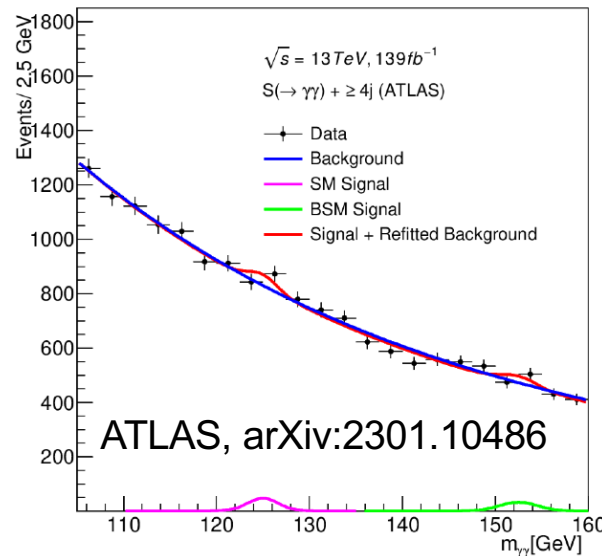
$\gamma\gamma + l (b - veto)$



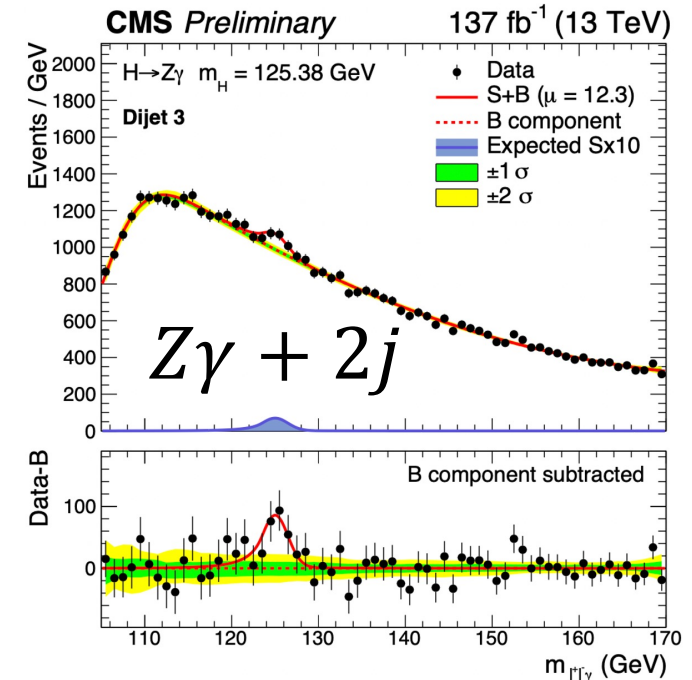
$\gamma\gamma + l + b$



$\gamma\gamma + 4j$



CMS-PAS-HIG-19-014

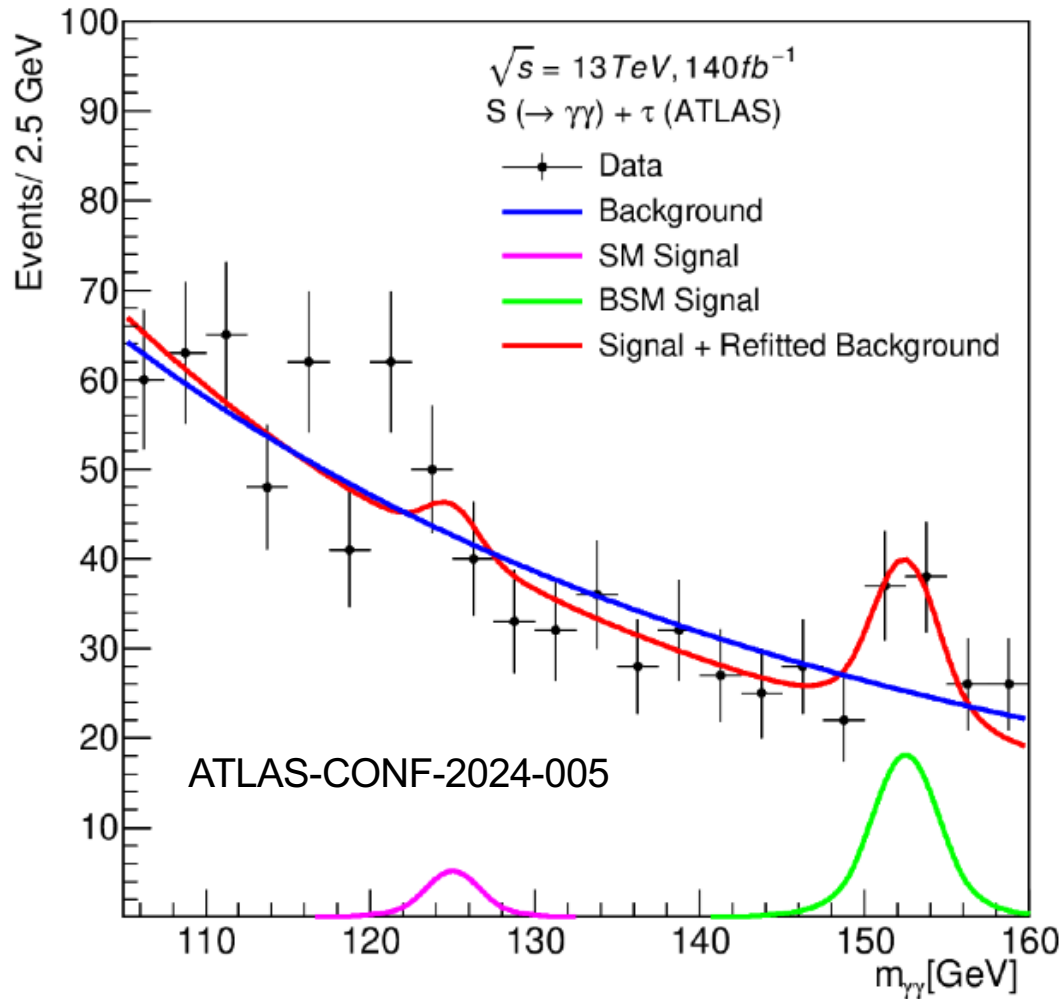


Excesses appear in corners of the phase-space predicted by the naive $H \rightarrow SS^*$ model with S being SM Higgs-like. In addition, seem to see S in association with MET and, possibly, with an extra photon

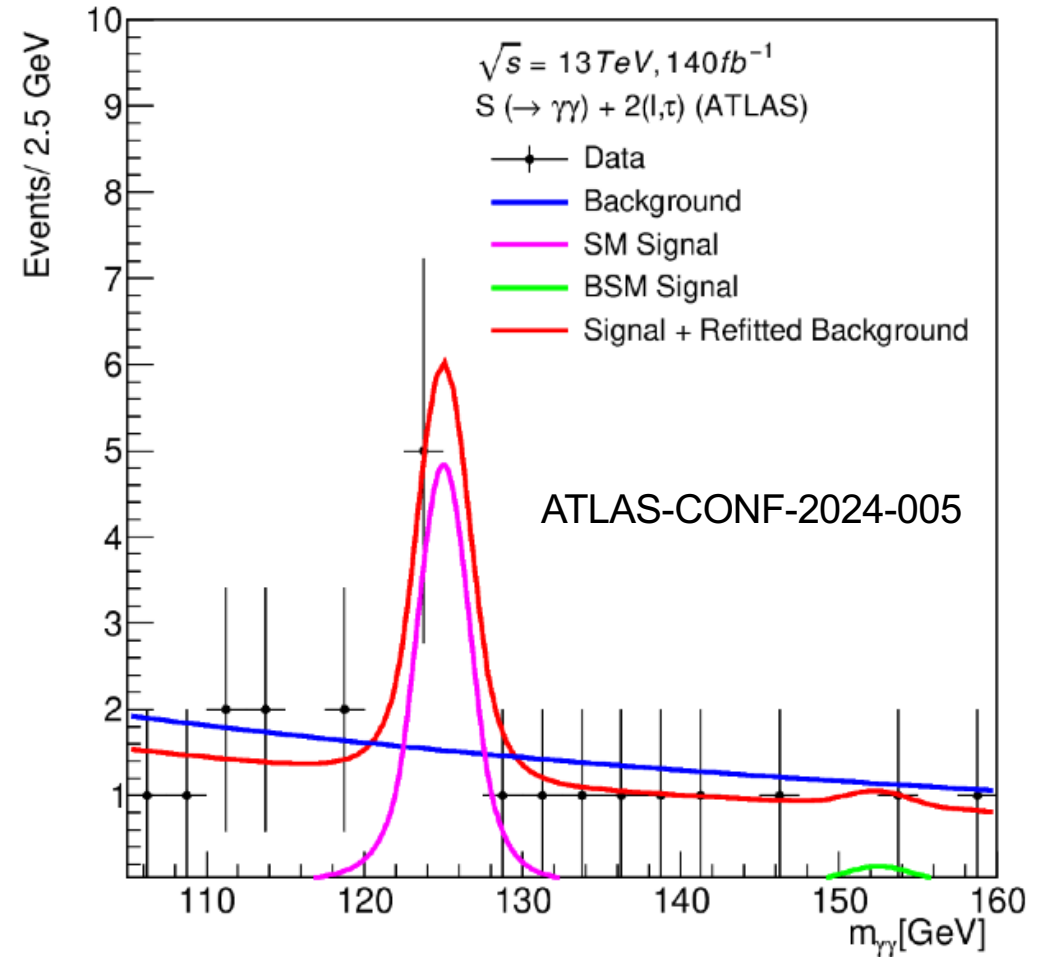
Bin for associated production VH, ttH , where excess is seen with di-photons.

ATLAS, arXiv:2301.10486

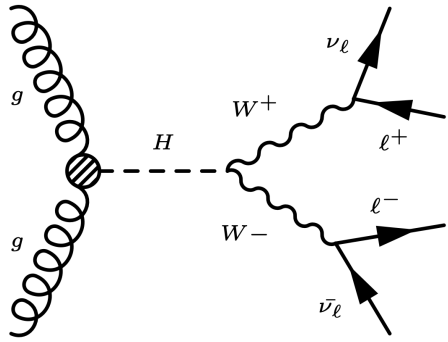
$\gamma\gamma + \tau$



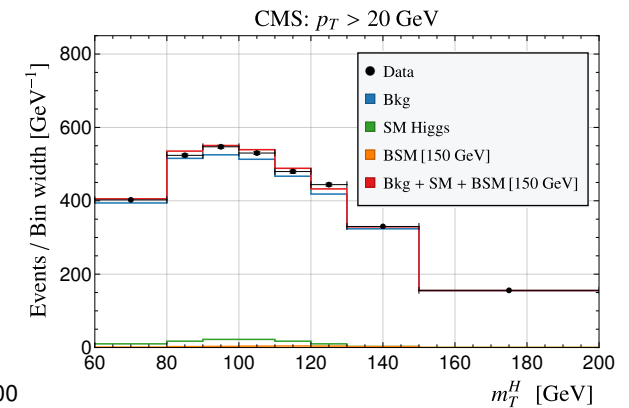
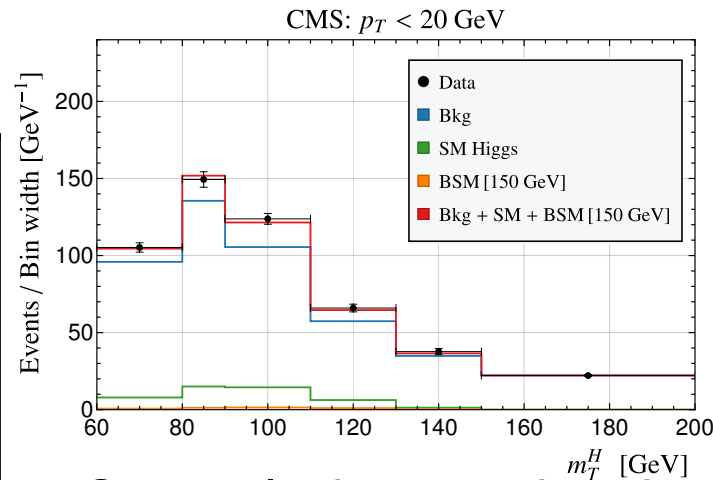
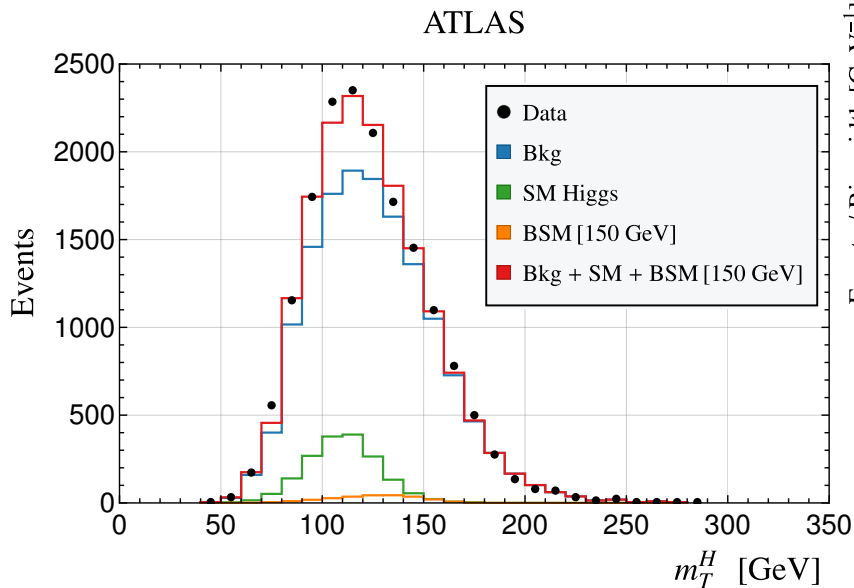
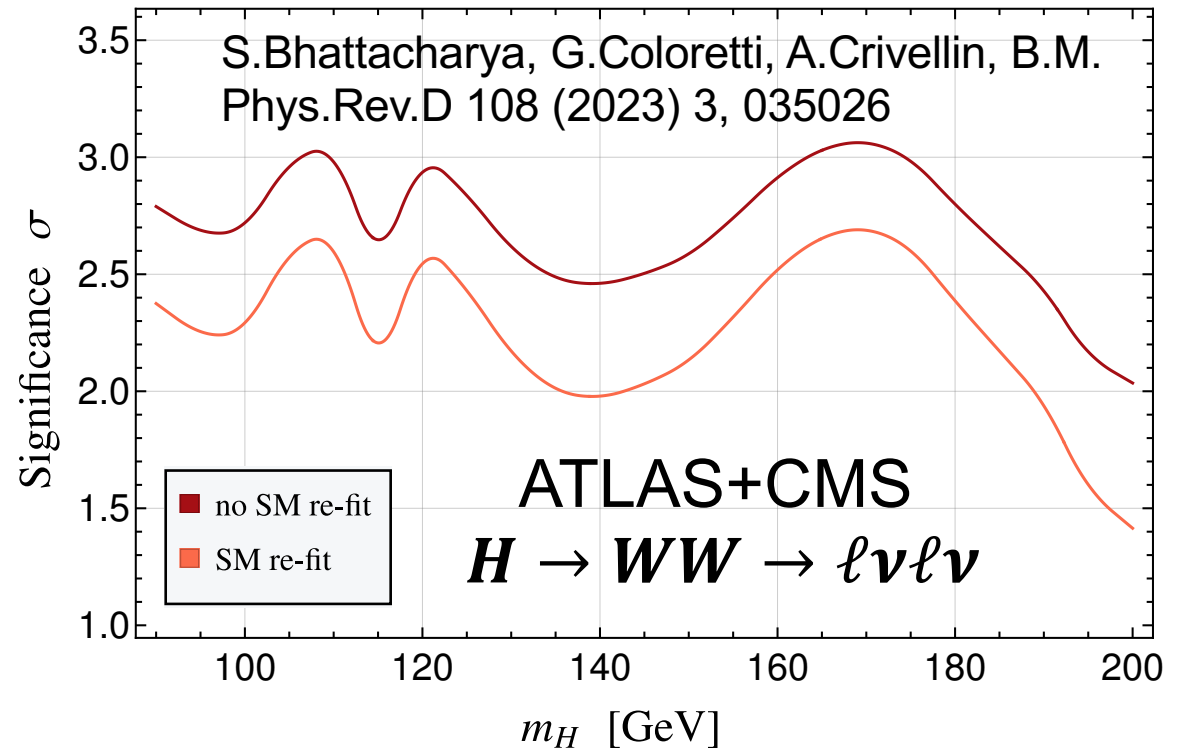
$\gamma\gamma + 2(\tau, \ell)$



Single and double tau are combined assuming $H \rightarrow SS^*$



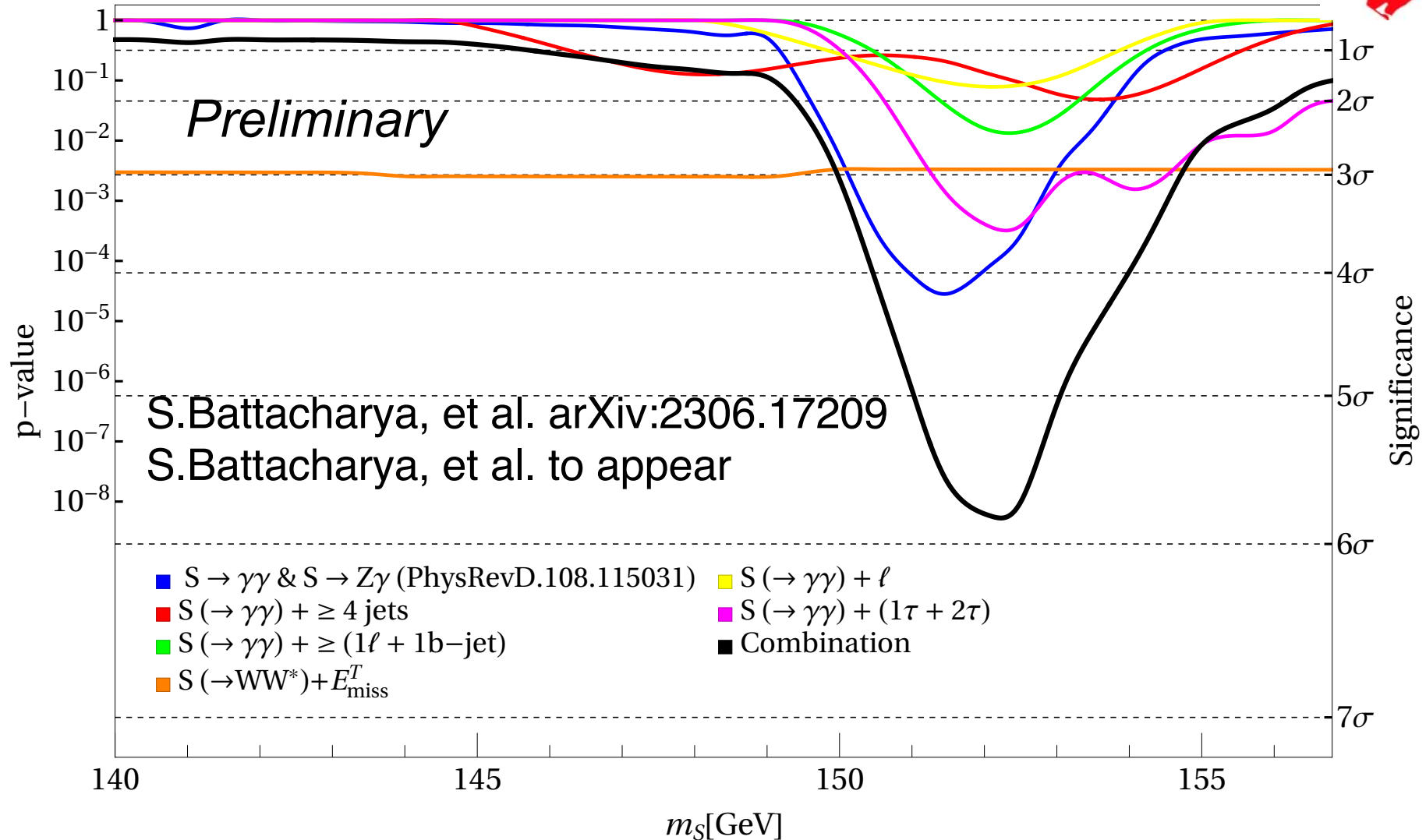
SM Higgs hypothesis alone. alone is having difficulty describing the $l\bar{l} + \text{MET}$ transverse mass spectra, giving room to other Higgs-like signals, including S(151).



Currently, interpreting the broad excess in terms of $H \rightarrow S + \text{MET}$, which appears to be the leading final state in excess described above

Current status of the combination, based on the Fischer method with 6 n.d.o.f yields largest global significance of a narrow structure beyond the SM at the LHC

NEW



Fiducial cross-sections in fb

Preliminary

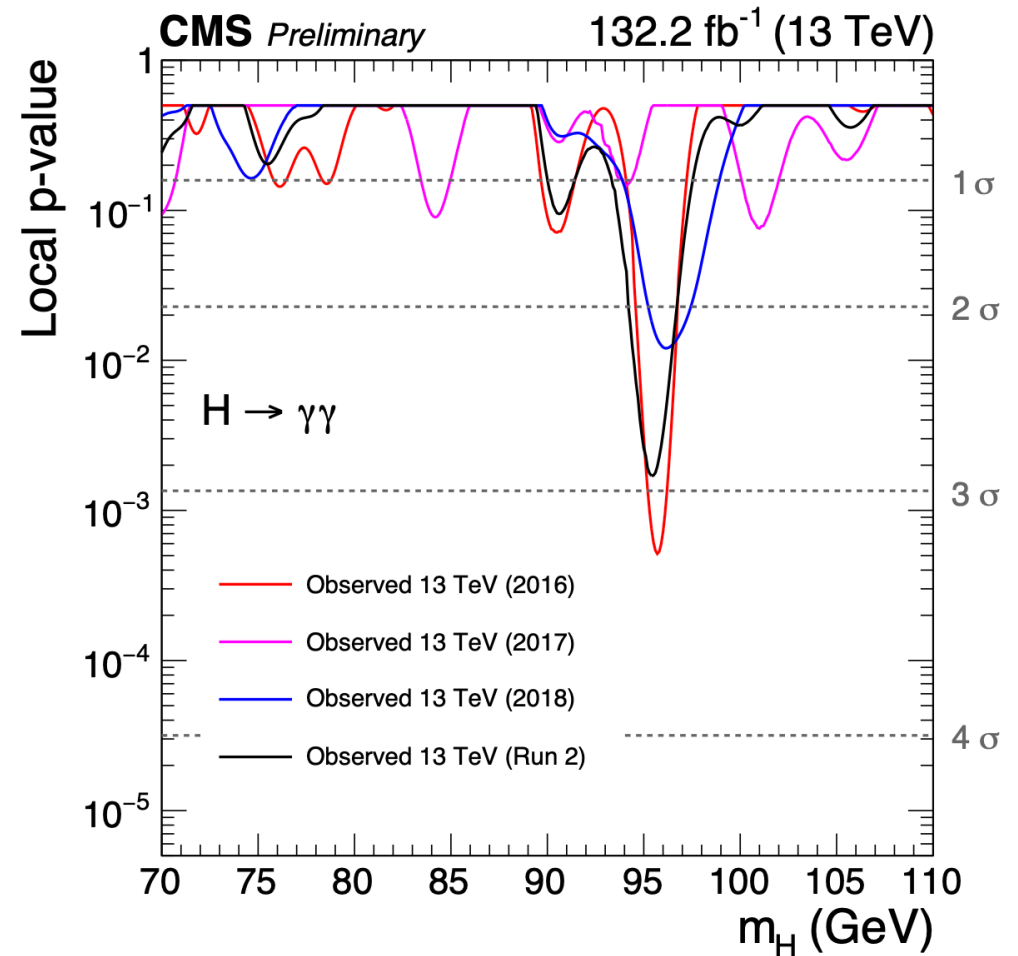
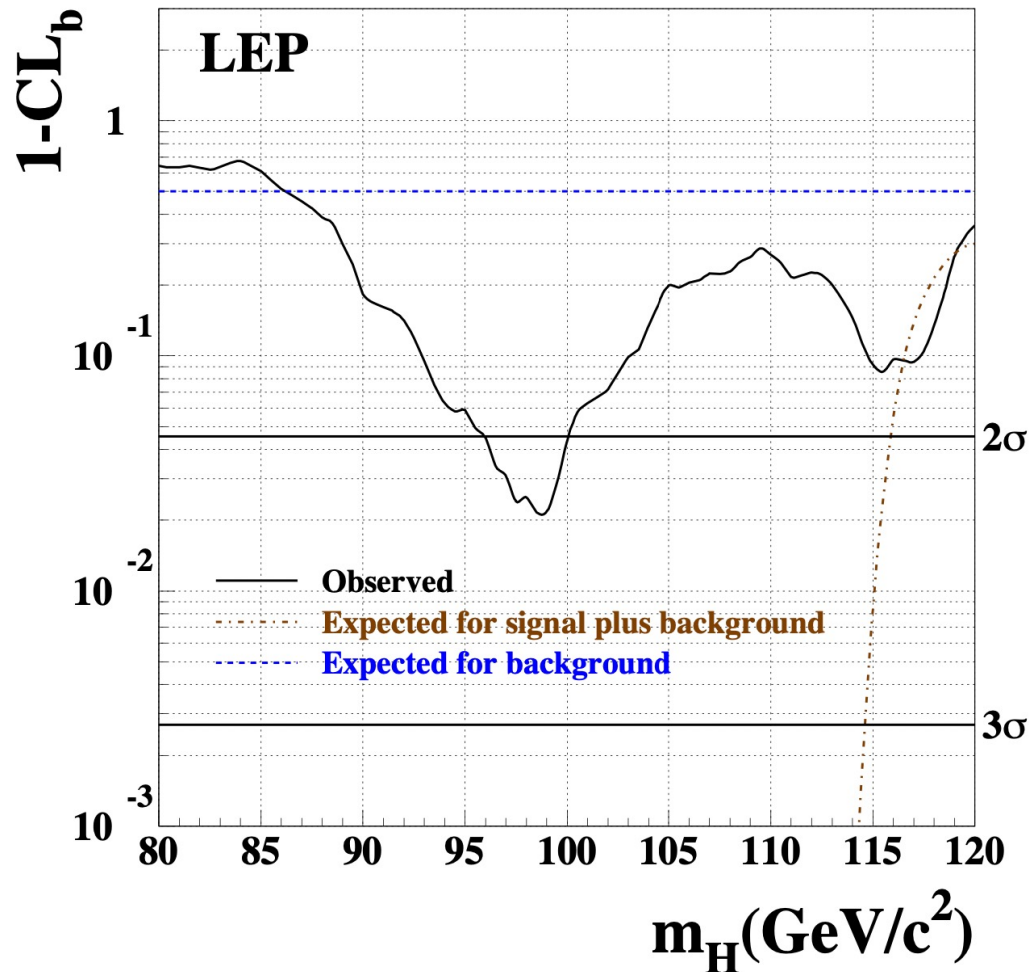
Channel	N_{Sig}	Significance	σ_F in fb
$S(\rightarrow \gamma\gamma) + \tau$	36.04 ± 9.86	3.93	0.54 ± 0.15
$S(\rightarrow \gamma\gamma) + \ell$	10.52 ± 6.22	1.73	0.14 ± 0.08
$S(\rightarrow \gamma\gamma) + \geq 1\ell + 1b\text{-jet}$	13.55 ± 6.16	2.46	0.24 ± 0.11
$S(\rightarrow \gamma\gamma) + \geq 4\text{ jet}$	66.68 ± 35.30	1.69	0.80 ± 0.42
$S(\rightarrow Z(\rightarrow \ell^+\ell^-)\gamma) + jj$	92.43 ± 58.75	1.30	2.16 ± 1.37
$S(\rightarrow Z(\rightarrow \ell^+\ell^-)\gamma) + 1\ell$	4.51 ± 15.48	0.26	0.12 ± 0.41
$S(\rightarrow \gamma\gamma) + b\text{-jet}$	14.70 ± 5.82	2.60	0.23 ± 0.09
$S(\rightarrow \gamma\gamma) + E_{\text{miss}}^T$ (Low)	18.33 ± 7.26	2.48	0.22 ± 0.09
$S(\rightarrow \gamma\gamma) + E_{\text{miss}}^T$ (High)	7.54 ± 3.90	2.35	0.09 ± 0.05
$S(\rightarrow \gamma\gamma) + W, Z$ (CMS)	12.74 ± 14.52	0.78	0.15 ± 0.17
$S(\rightarrow \gamma\gamma) + W, Z$ (ATLAS)	4.69 ± 13.65	0.40	0.06 ± 0.17

The 95 GeV Candidate

Some tantalizing results around 96 GeV from LEP and CMS, not contradicted by ATLAS. Interesting to see what the full Run 2 data set has to say. Further motivates asymmetric searches $H \rightarrow SS'$...

LEP, Phys. Lett. B 565 (2003) 61–75

CMS PAS HIG-20-002



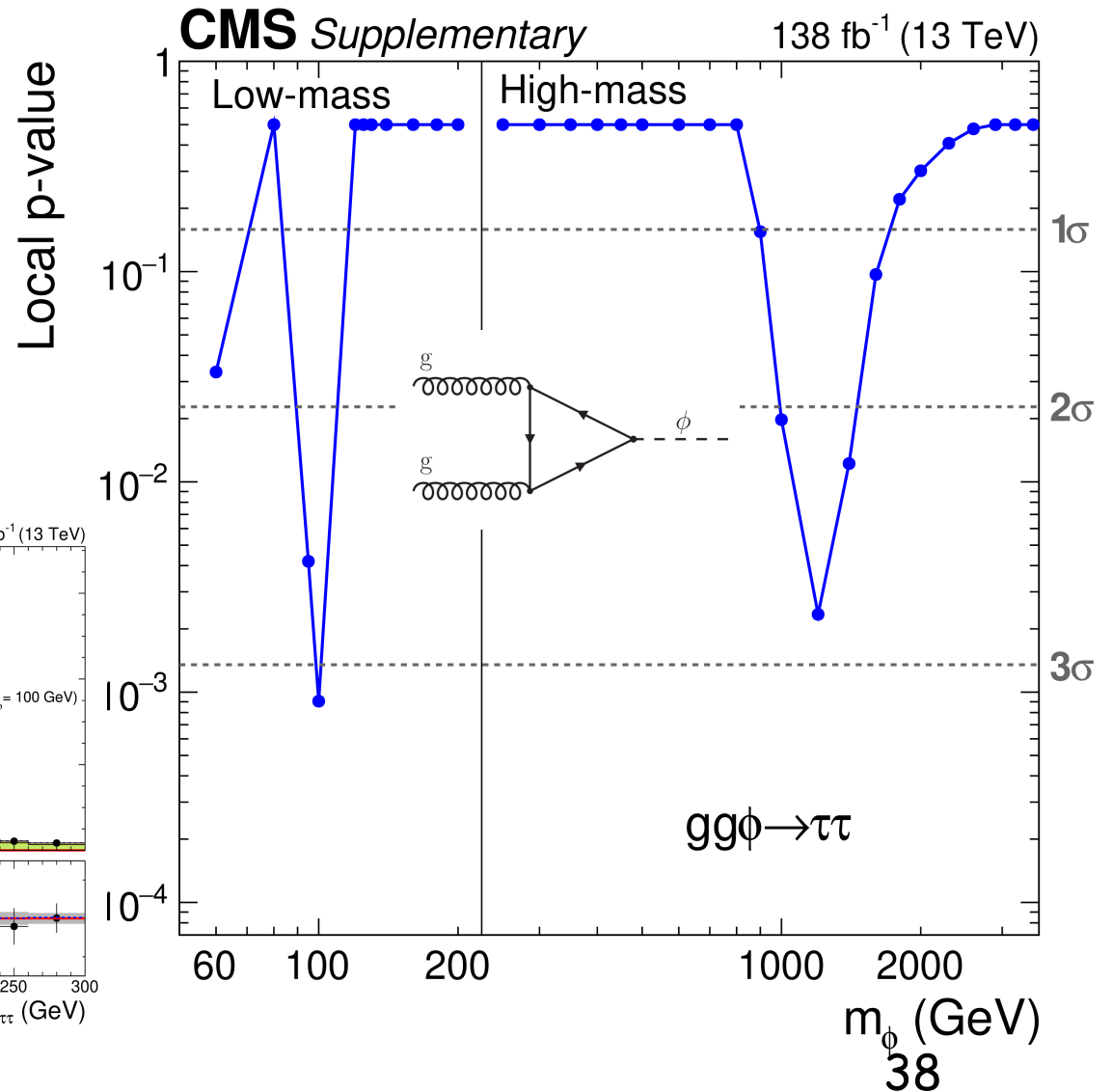
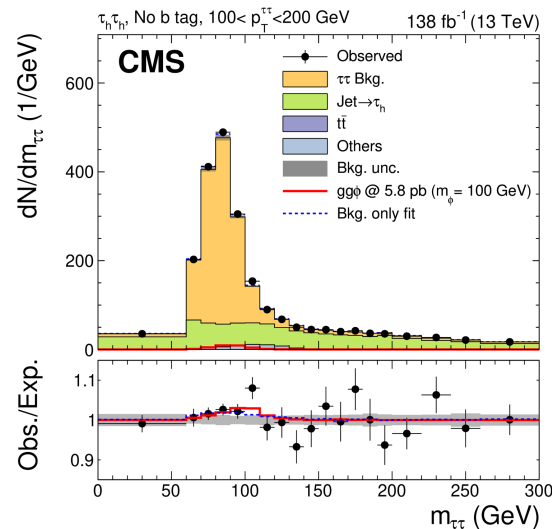
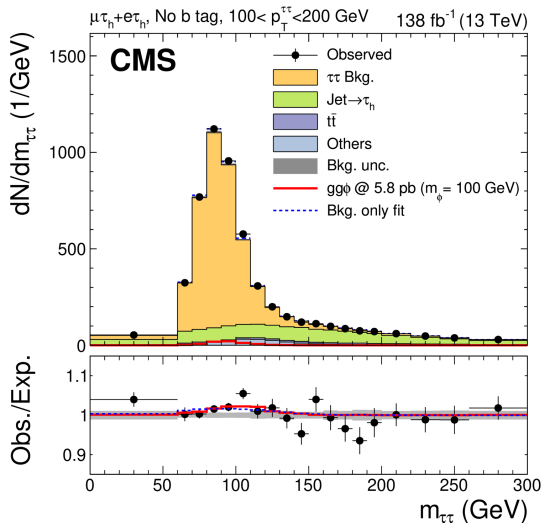
Dedicated search for scalar decaying into tau pairs. CMS observes a local (global) excess of 3.1 (2.7) σ at ~ 100 GeV.

$$H \rightarrow \tau\tau$$

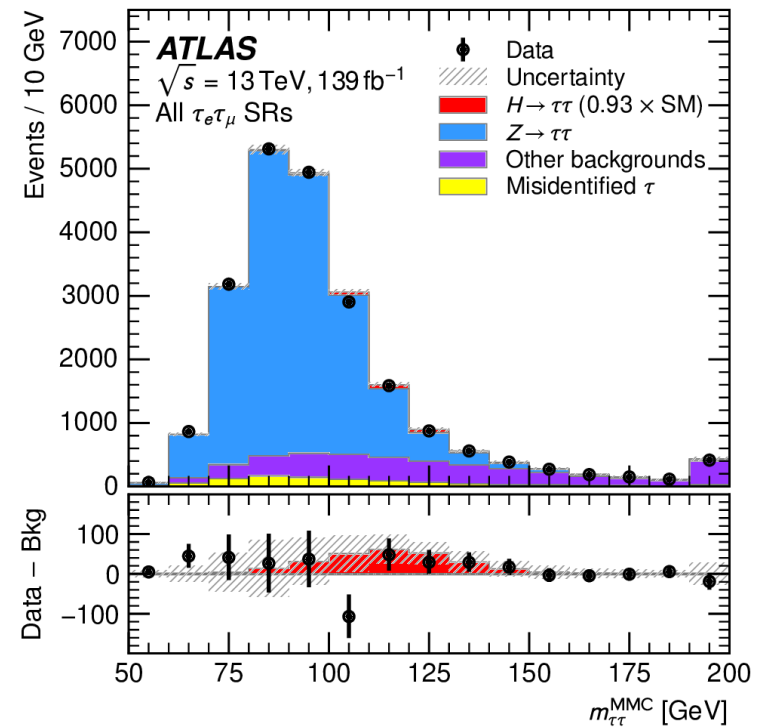
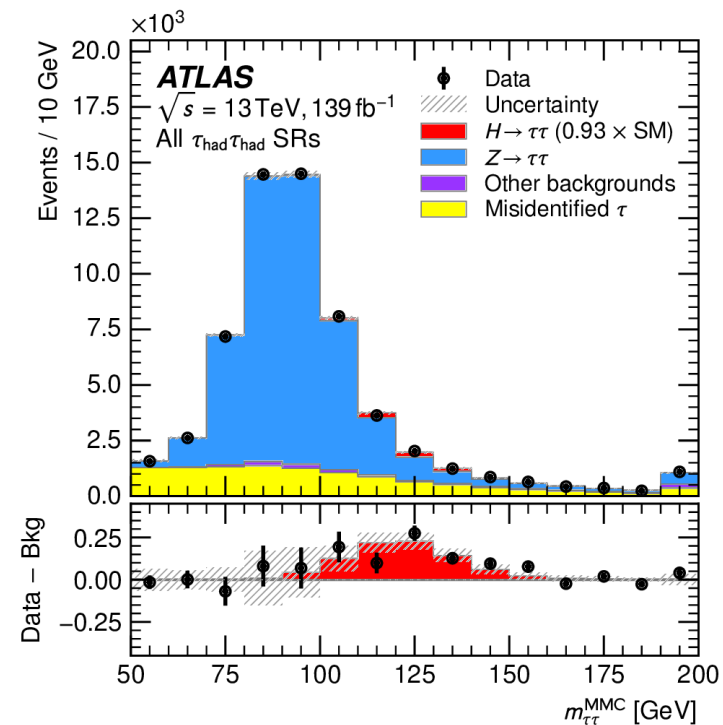
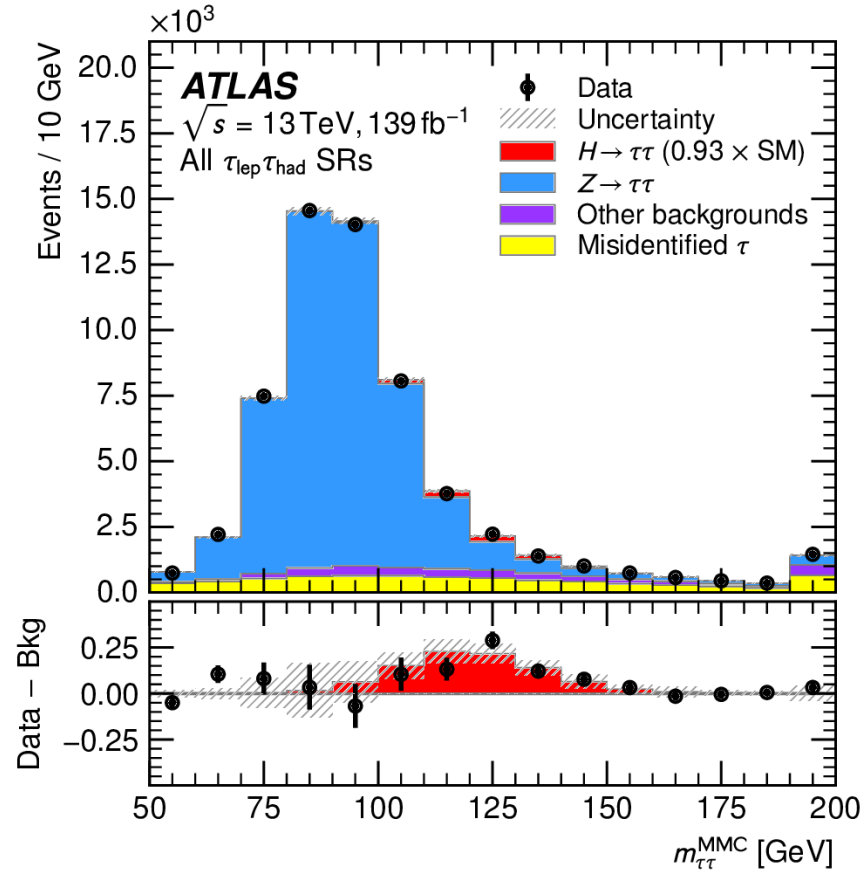
Event classification scheme

	No b-tag			b-tag		
$\tau\tau \rightarrow e\mu$	Low- D_ζ	Medium- D_ζ	High- D_ζ	Low- D_ζ	Medium- D_ζ	High- D_ζ
$\tau\tau \rightarrow e\tau_h$	Loose- m_T		Tight- m_T	Loose- m_T		Tight- m_T
$\tau\tau \rightarrow \mu\tau_h$	Loose- m_T		Tight- m_T	Loose- m_T		Tight- m_T
$\tau\tau \rightarrow \tau_h\tau_h$						
$t\bar{t}(e\mu)$						

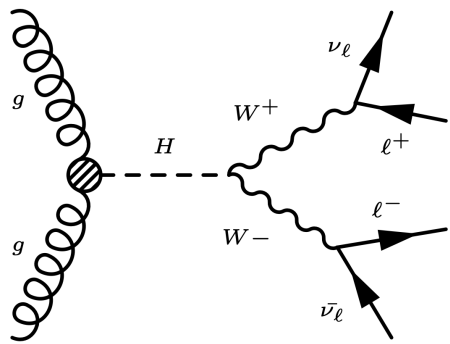
Signal region (SR)
 Control region



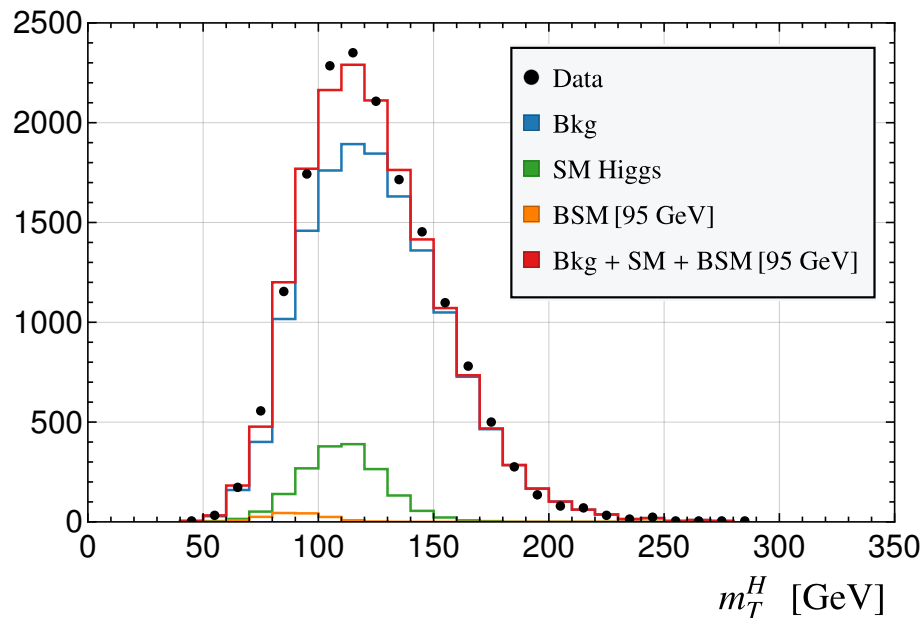
ATLAS, JHEP 08 (2022) 175 $H \rightarrow \tau\tau$



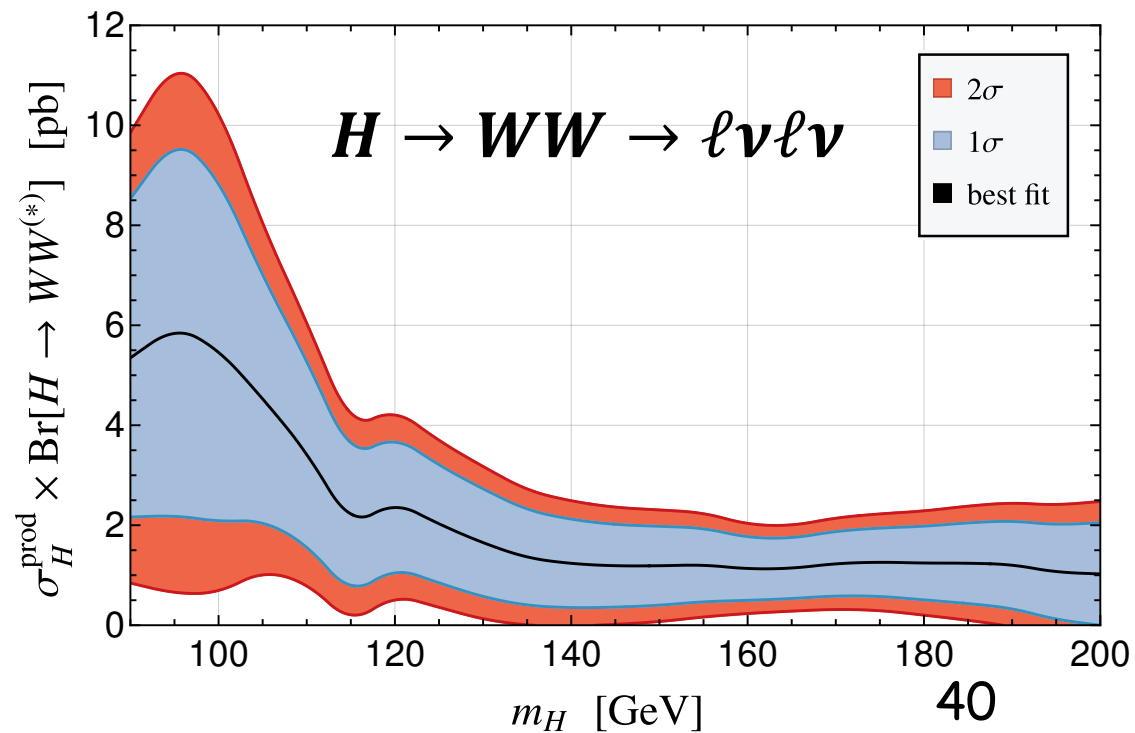
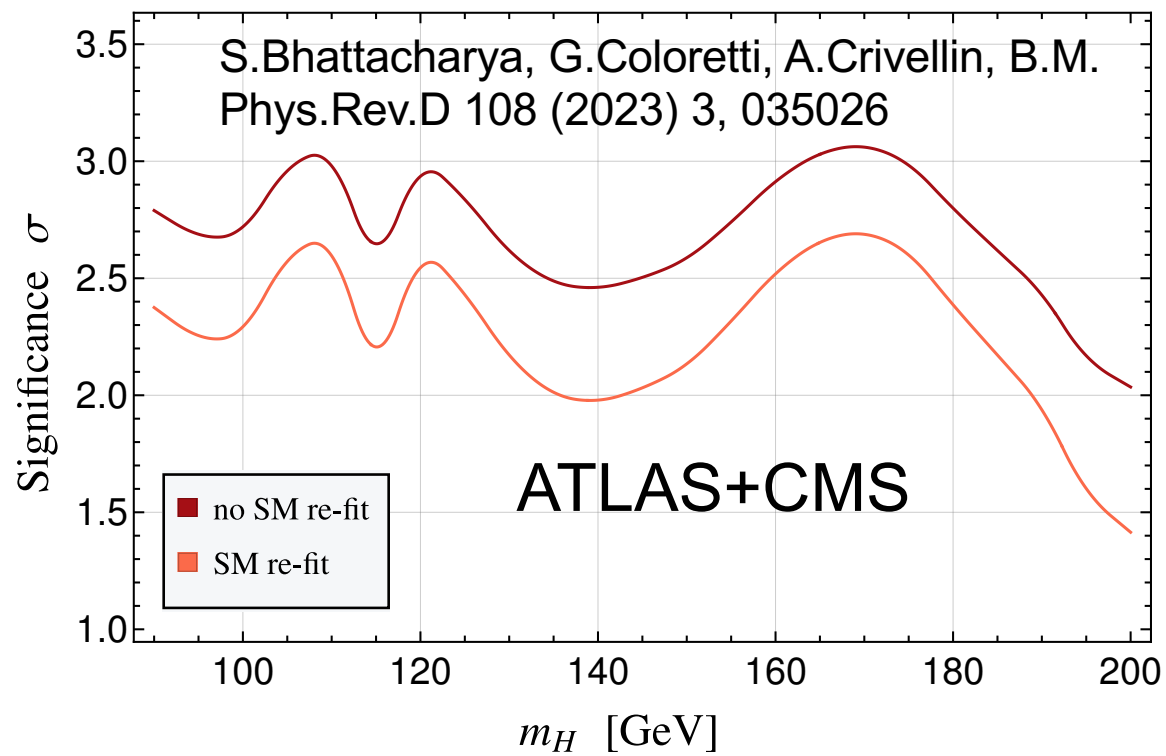
ATLAS has not performed a dedicated search for low mass scalar. That said we do not seem to see a clear excess around 95 GeV in the sideband. Is the CMS excess an upward fluctuation?



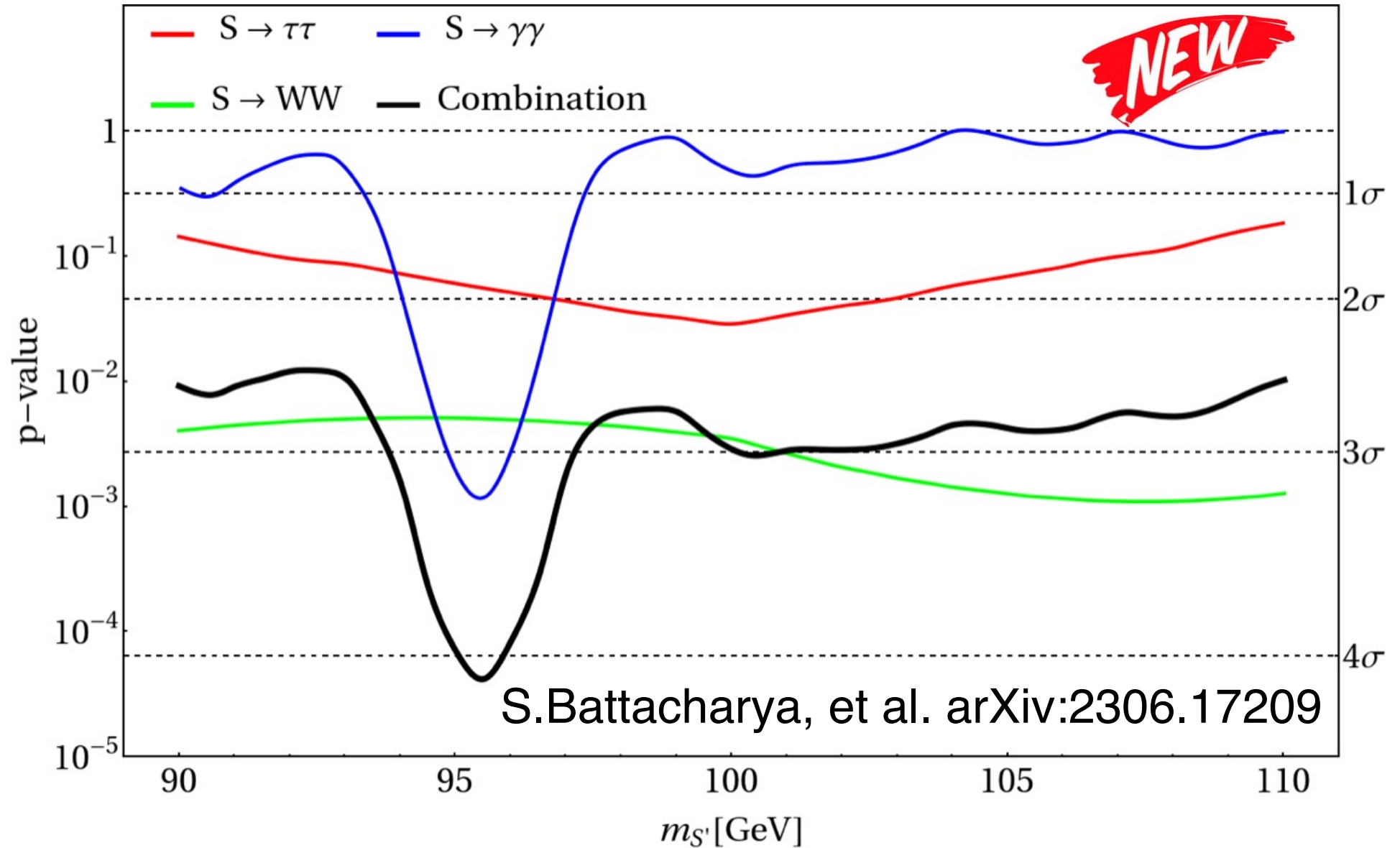
ATLAS



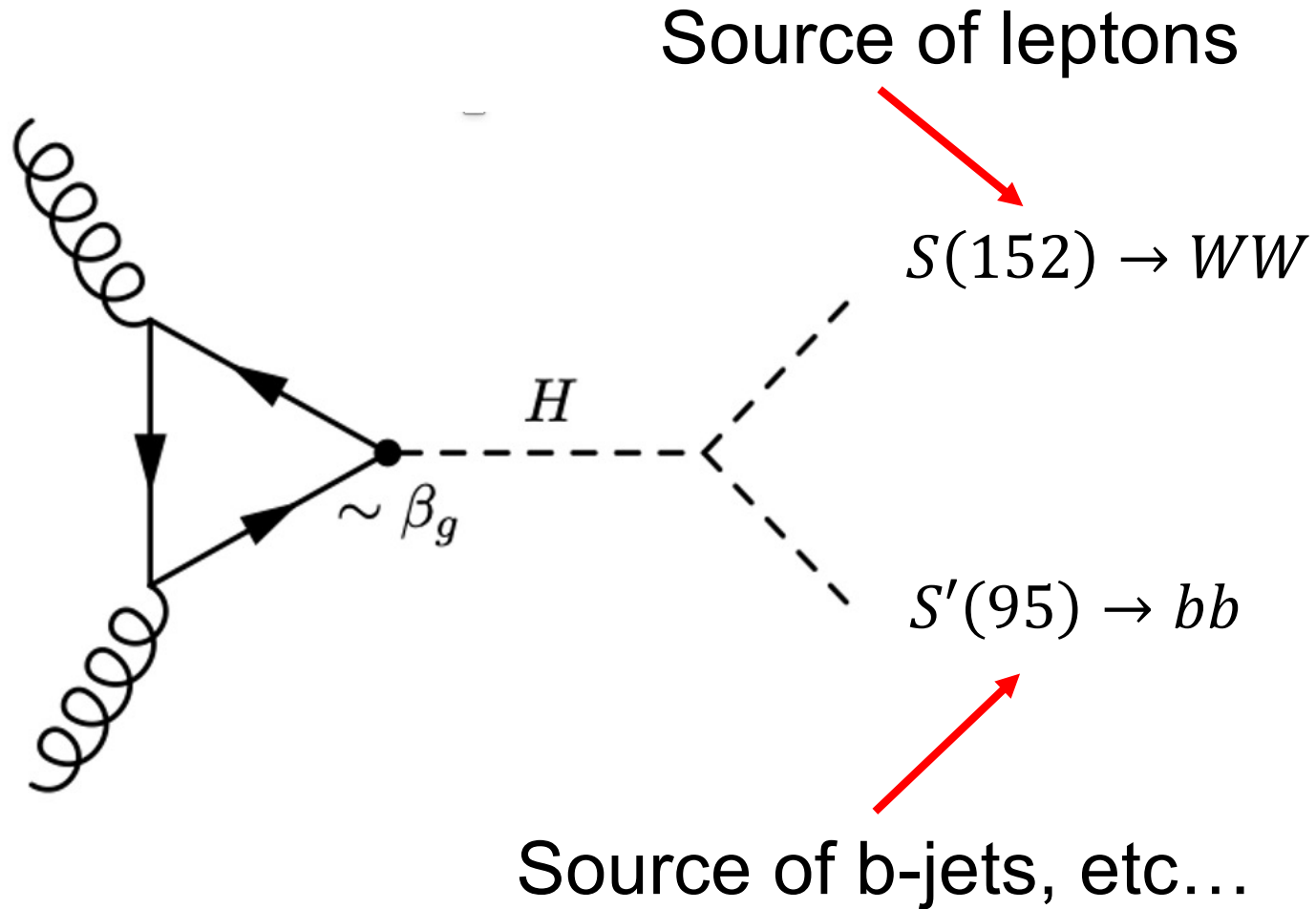
SM Higgs hypothesis alone. alone is having difficulty describing the $ll+\text{MET}$ transverse mass spectra, giving room to other Higgs-like signals. Compatibility with other signals under study.



With recent results reported by the ATLAS experiment the significance of a narrow resonance at 95 GeV has reached 3.8σ global significance.



Potential contributor to multi-lepton anomalies at the LHC



The importance of two and multi-body decays for the (HL)-LHC

- Certain types of two-body decays are unexplored in important regions of the phase-space:

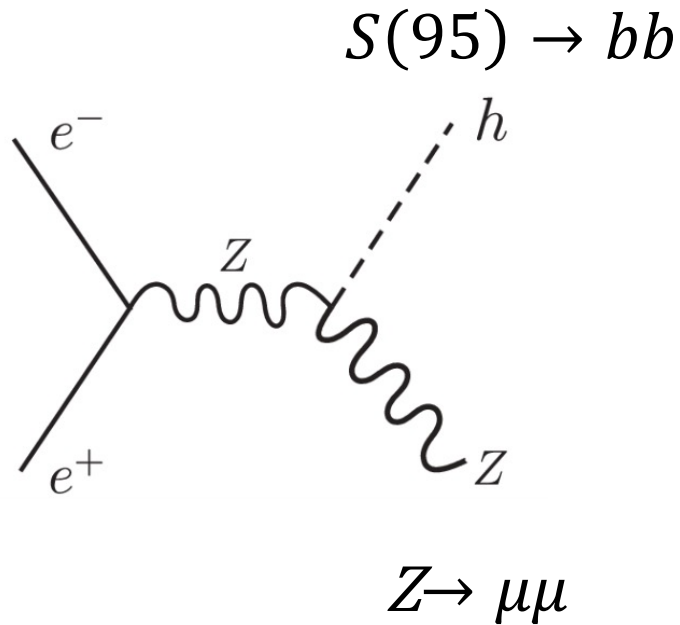
$$A \rightarrow BC \quad A \rightarrow BB^*$$

- Other types of topologies are also unexplored

$$A \rightarrow BB^{(*)} \rightarrow C + X$$

- Machine Learning techniques, such as weak supervision, relevant to minimize model dependence, not used to its fullest potential

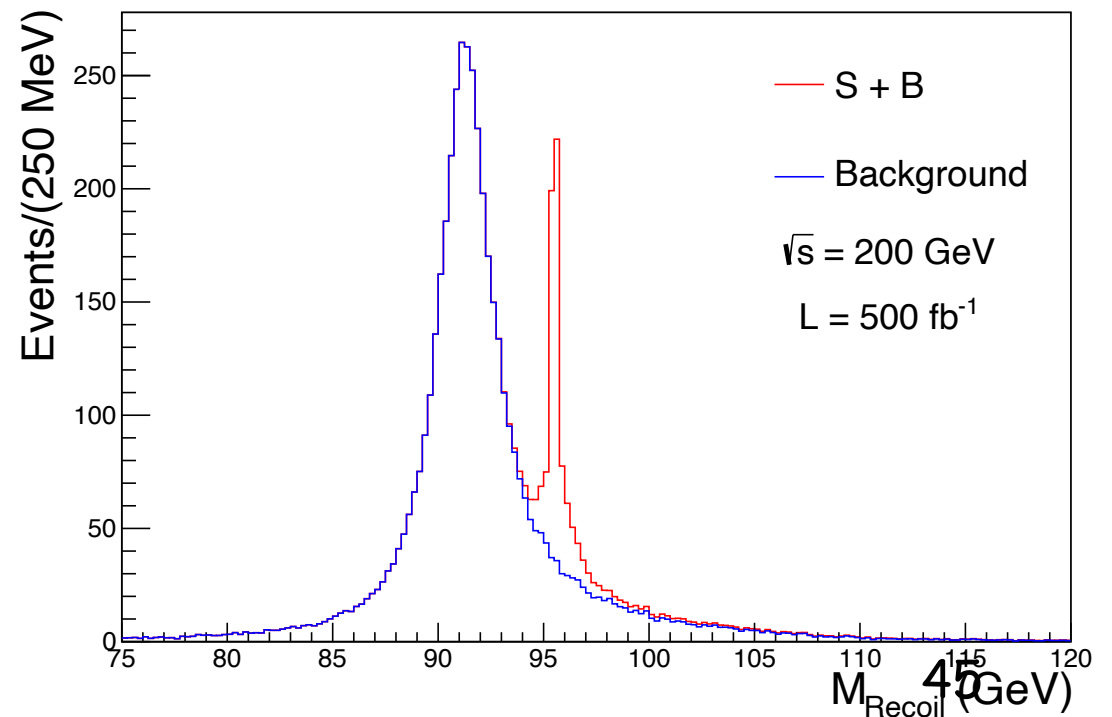
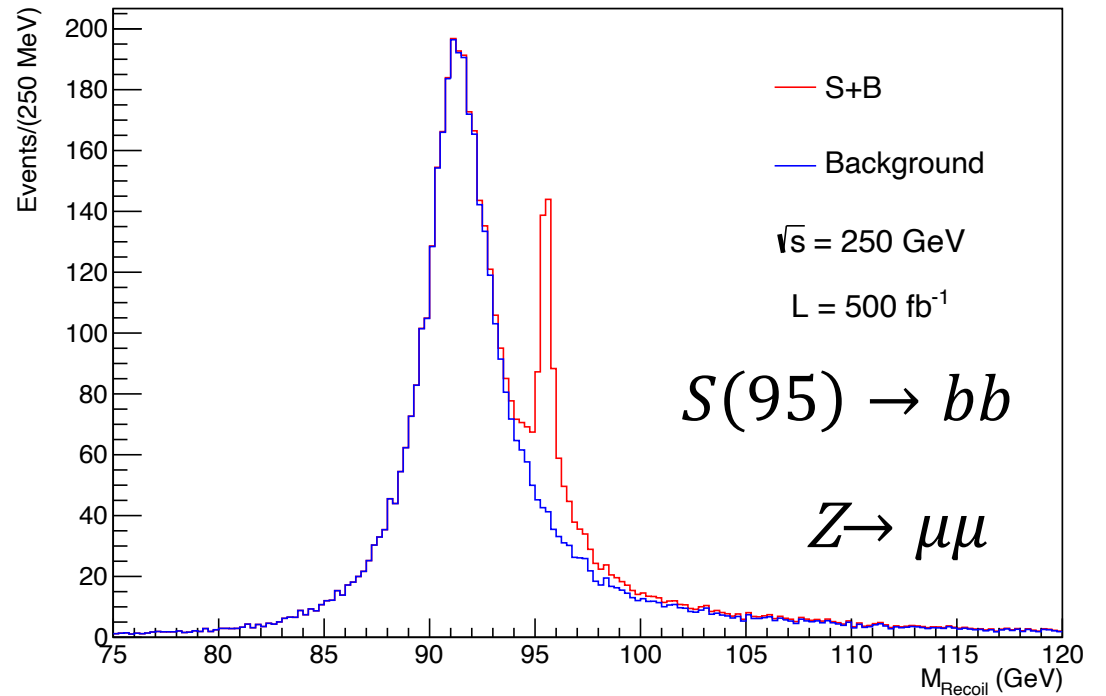
Impact on Future e^+e^- Colliders

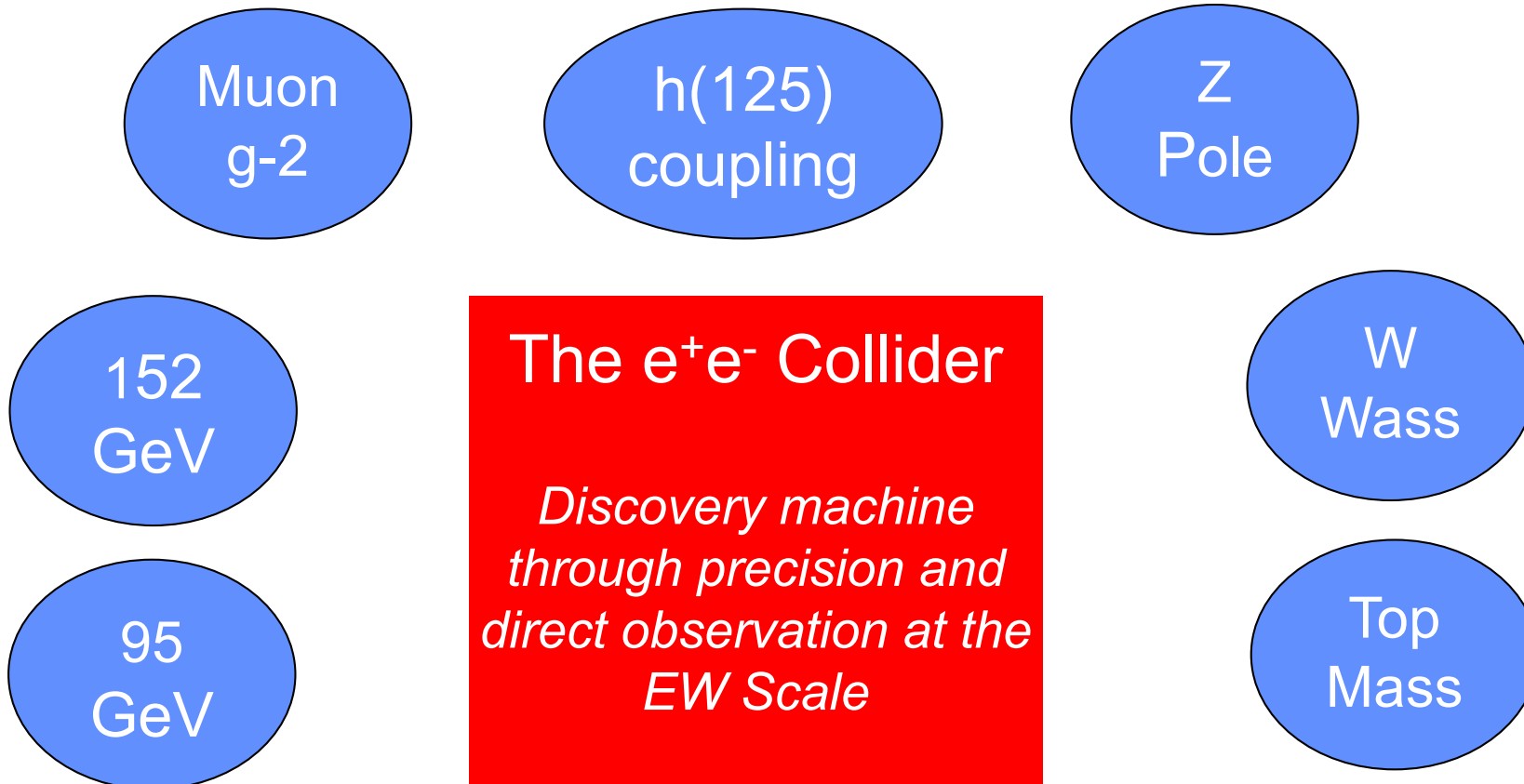


A light Higgs-like scalar like the S(95) candidate would be unequivocally observed in a Higgs factory.

Use superior resolution of Z mass recoil method

Work with Y.Fang, M.Ruan and M.Titov





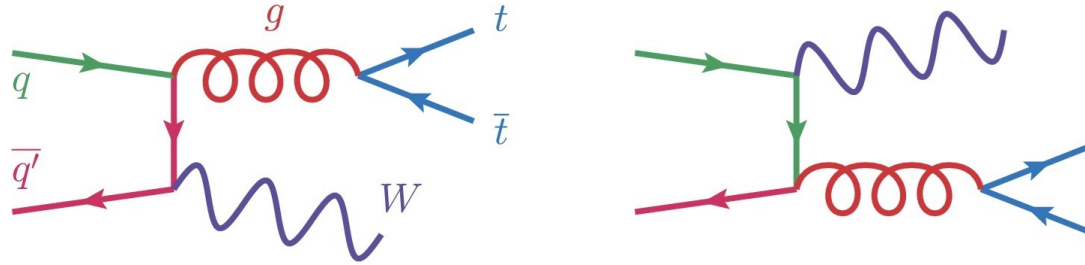
Anomalies in Particle Physics are indicative of unique discovery opportunities at the EW for future e⁺e⁻ accelerators

Outlook and Conclusions

- ❑ **Discrepancies in multi-lepton final states at LHC w.r.t. current MCs are not statistical fluctuations**
 - ❑ **They appear in corners of the phase-space dominated by different processes** ($Wt/tt/4t$, VV , ttV , Vh , WWW)
 - **Excesses are Higgs-like with robust final states**
- ❑ **With these anomalies one predicts a scalar, S , with a mass 150 ± 5 GeV from the decay of a heavier H .**
- ❑ **Analysis of in associated production gives a large ($>5\sigma$) global excess around 152 GeV**
- ❑ **Excesses at 95 GeV have grown, leading to 3.8σ global significance**
 - ❑ **Future e^+e^- collisions to give irrefutable observation**
- ❑ **The discovery potential of BSM at the EW scale at future is the strong suit of future e^+e^- colliders**
 - ❑ **Whether through direct observation or precision**

Additional Slides

The anatomy of inclusive ttW at the LHC



S.Buddenbrock, R.Ruiz and B.M.
Physics Letters B 811
(2020) 135964

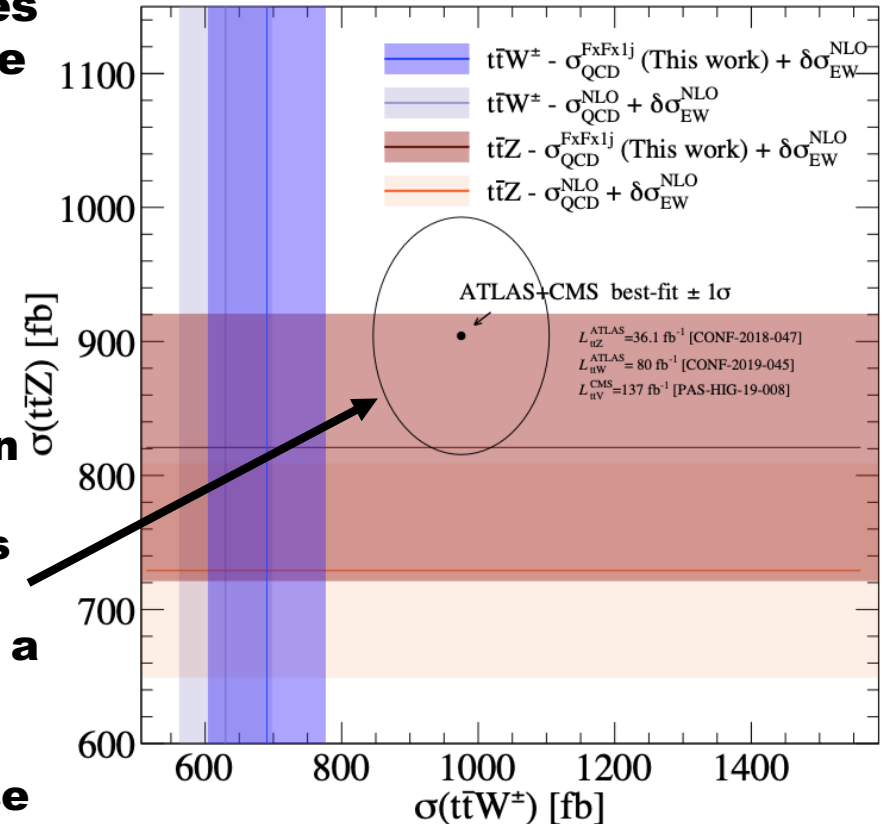
Using fixed order computations at $O(\alpha_s^4\alpha)$ and NLO multi-jet matching yielding similar (10%-14%) corrections to the inclusive rate

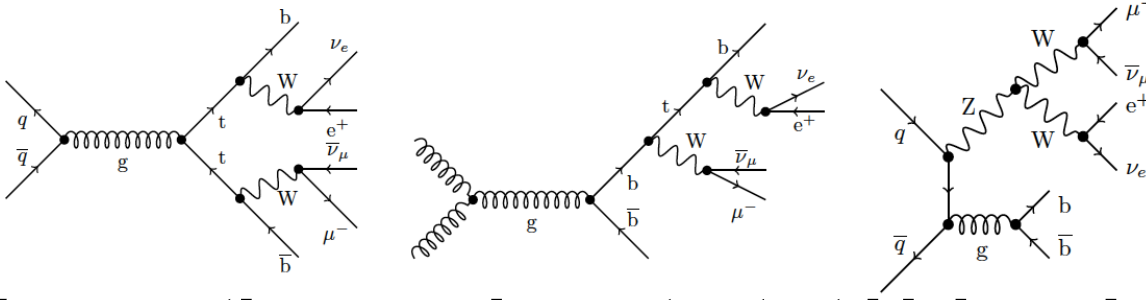
		$ij \rightarrow t\bar{t}W^\pm kl$				
(i, j)	(k, l)	$p_T^{j1 \text{ min}}$	$p_T^{j2 \text{ min}}$	σ [fb]	$\pm\delta_{\mu_f, \mu_r}$	$\pm\delta_{\text{PDF}}$
All	All	75 GeV	75 GeV	34.7 (100%)	+57%	+1.1%
(g, Q)	(g, Q)			23.7 (68%)		
(Q, Q)	(Q, Q)			6.99 (20%)		
(Q, Q)	(g, g)			3.63 (10%)		
(g, g)	(q, \bar{q})			0.437 (1.3%)		
All	All	100 GeV	75 GeV	33.1 (100%)	+57%	+1.0%
(g, Q)	(g, Q)			22.6 (68%)		
(Q, Q)	(Q, Q)			6.78 (20%)		
(Q, Q)	(g, g)			3.28 (9.9%)		
(g, g)	(q, \bar{q})			0.409 (1.2%)		
All	All	100 GeV	100 GeV	21.2 (100%)	+57%	+1.1%
(g, Q)	(g, Q)			14.3 (67%)		
(Q, Q)	(Q, Q)			4.91 (23%)		
(Q, Q)	(g, g)			1.75 (8%)		
(g, g)	(q, \bar{q})			2.58 (1%)		
(g, q_V)	(g, q_V)	75 GeV	75 GeV	20.1 (58%)	+58%	+2.3%
(g, q_V)	(g, q_V)	100 GeV	75 GeV	19.3 (58%)	+58%	+2.3%
(g, q_V)	(g, q_V)	100 GeV	100 GeV	12.2 (58%)	+59%	+2.4%

Table 2: Total cross sections [fb] at $\sqrt{s} = 13$ TeV for the $pp \rightarrow t\bar{t}W^\pm jj$ process at LO, with scale and PDF uncertainties [%], for representative $p_T^{jk \text{ min}}$ with $|\eta^j| < 4.0$. Also shown is the decomposition according to partonic channel, for $q_V \in \{u, d\}$, $q \in \{u, d, c, s\}$, and $Q \in \{q, \bar{q}\}$.

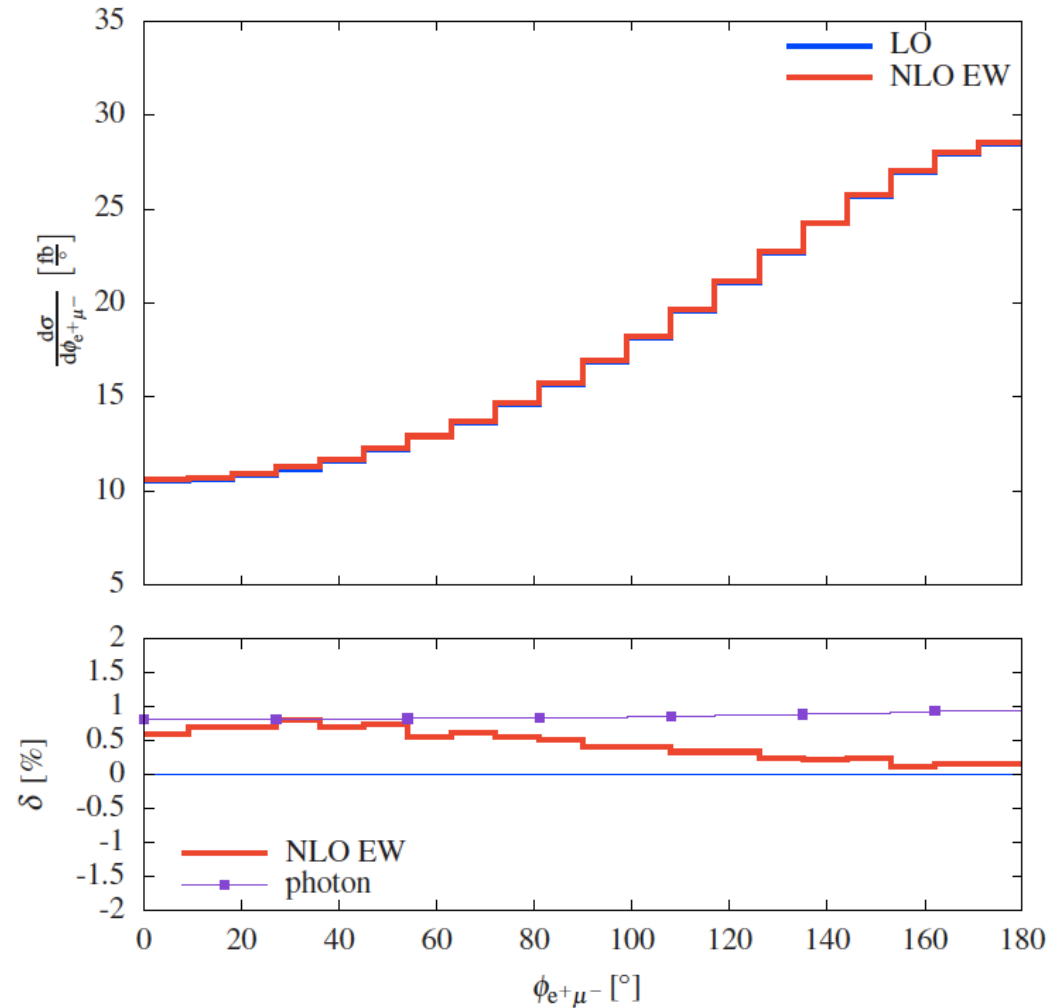
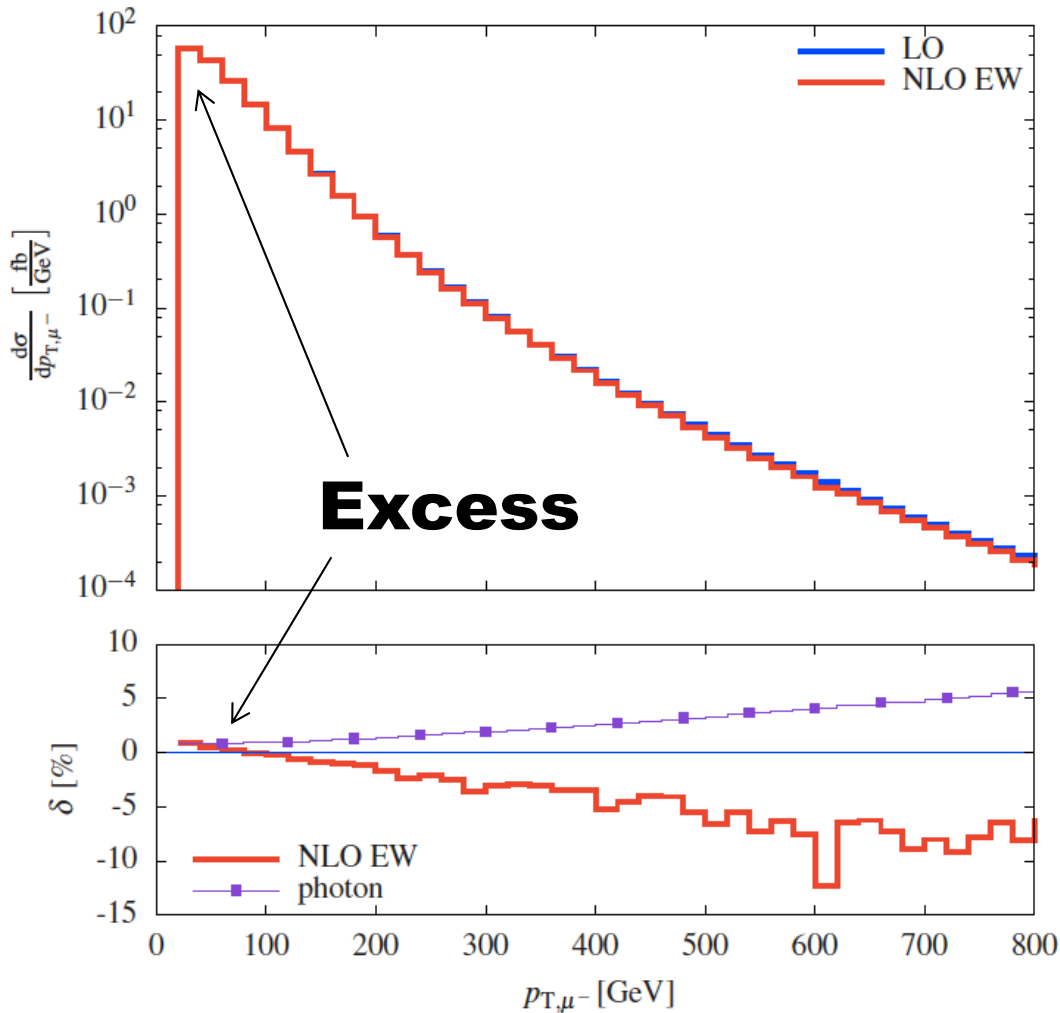
Detailed studies that include the decomposition in partonic channels and differential distributions

Tension between data and predictions does not wane. For this process a complete NNLO computation is needed to reduce theory uncertainty





**EW corrections are important at high p_T due to Sudakov logarithms.
Effect is less than 1% for $m_{ll} < 100$ GeV, where discrepancies are seen.**



The HistFactory method

K. Cranmer, G. Lewis, L. Moneta, A. Shibata, and W. Verkerke, *HistFactory: A tool for creating statistical models for use with RooFit and RooStats*, CERN-OPEN-2012-016.

- **Constructs a likelihood function from template histograms**
- **Allows for a simple implementation of systematic uncertainties that affect normalisation and/or shape**

$$\mathcal{P}(n_{cb}, a_p \mid \phi_p, \alpha_p, \gamma_b) = \prod_{c \in \text{channels}} \prod_{b \in \text{bins}} \text{Pois}(n_{cb} \mid \nu_{cb}) \cdot G(L_0 \mid \lambda, \Delta_L) \cdot \prod_{p \in \mathbb{S} + \Gamma} f_p(a_p \mid \alpha_p)$$

In our case, each “channel” is a different measurement.

The Poisson probability for the “expected” and “observed” number of events per bin.

Functional form of luminosity and its variations (not necessary for us).

Functional form of systematic variation with nuisance parameter α_p .

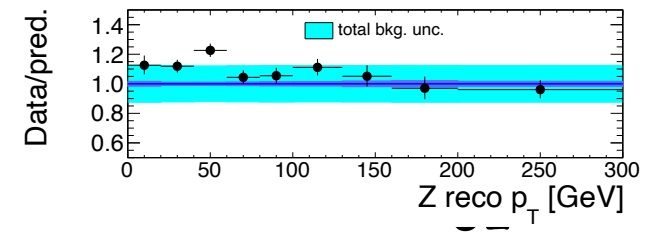
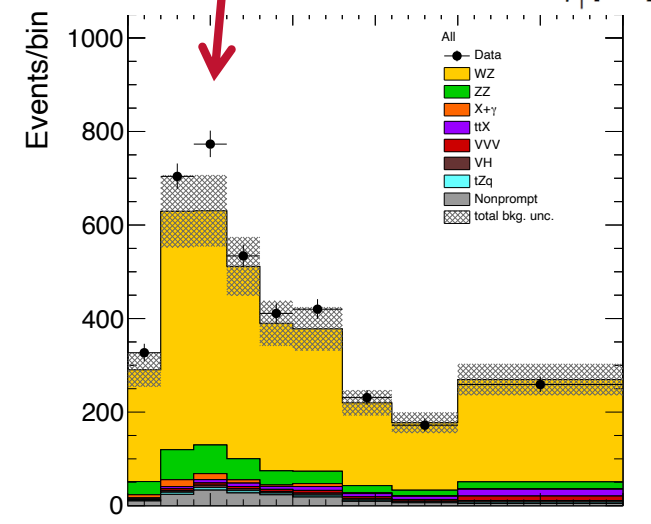
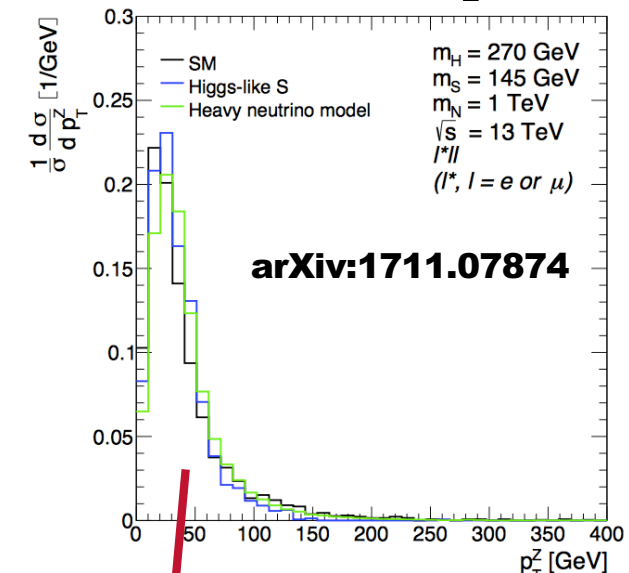
3l with Z→ll (ZW cross-section)

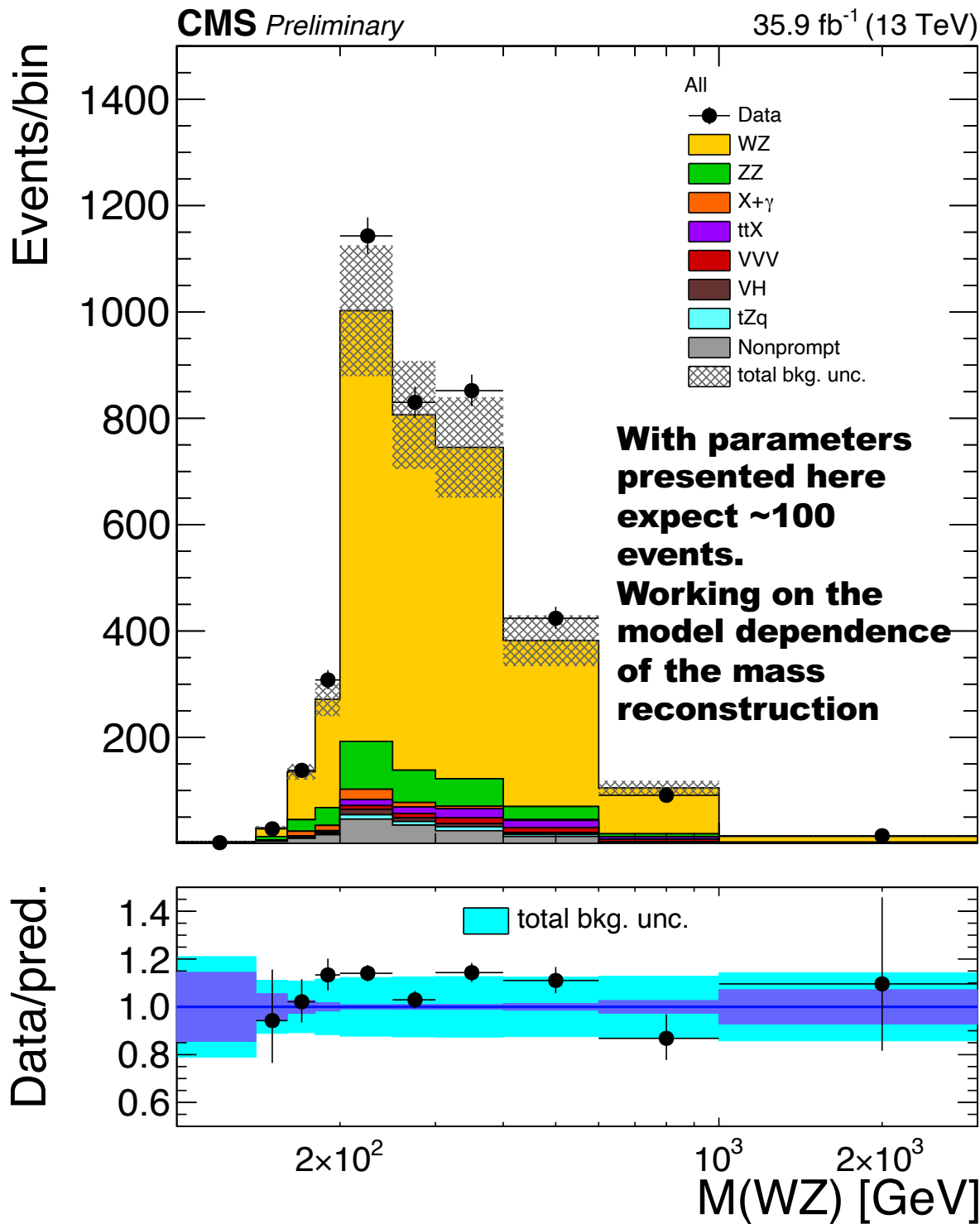
CMS PAS SMP-18-002

Errors in the plot are dominated by the 15% uncertainty on normalization to account NLO/NNLO differences. The uncertainty of the shape is much smaller of order of few %

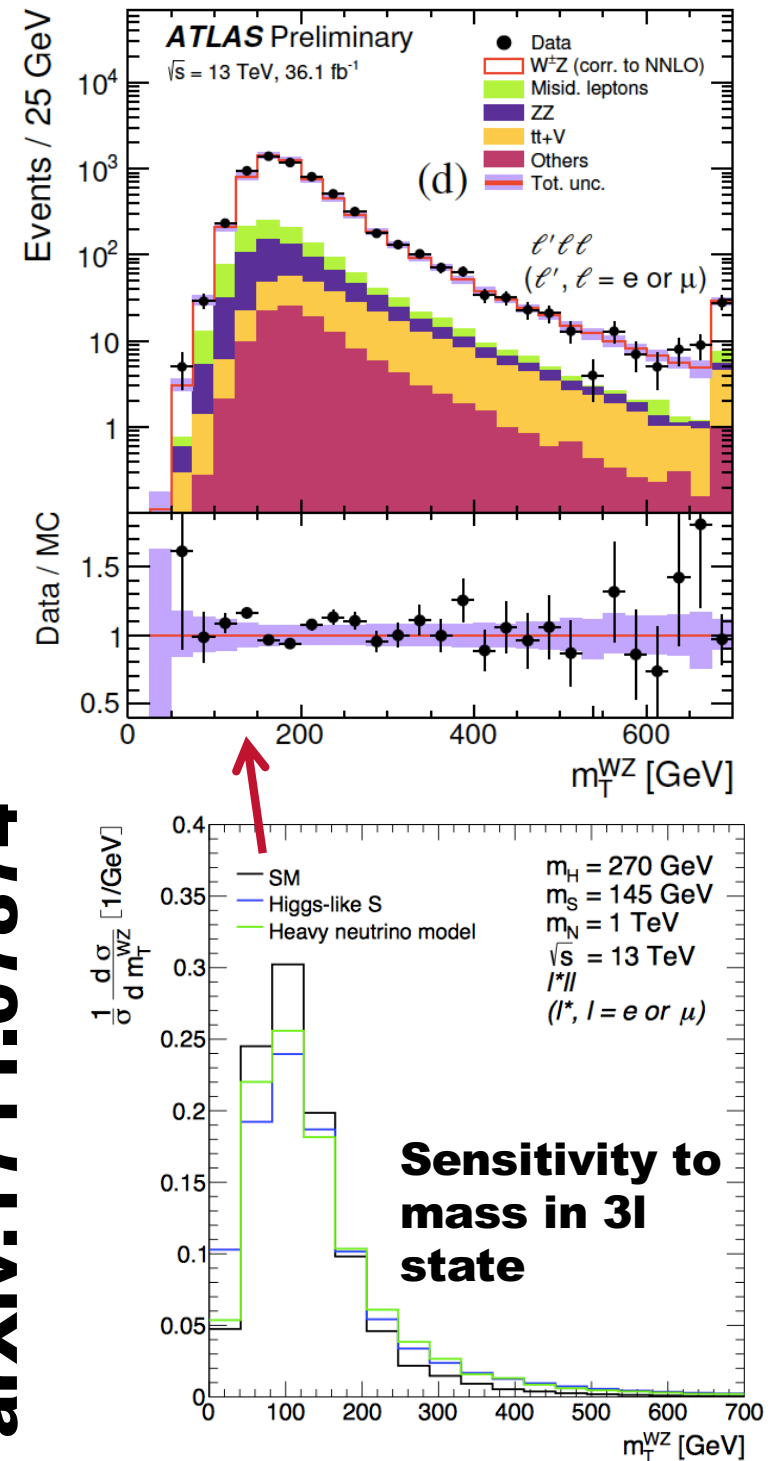
Source	Combined	eee	eeμ	μμe	μμμ
Electron efficiency	1.9	5.9	3.9	1.9	0
Electron scale	0.3	0.9	0.2	0.6	0
Muon efficiency	1.9	0	0.8	1.8	2.6
Muon scale	0.5	0	0.7	0.3	0.9
Trigger efficiency	1.9	2.0	1.9	1.9	1.8
Jet energy scale	0.9	1.6	1.0	1.7	0.8
B-tagging (id.)	2.6	2.7	2.6	2.6	2.4
B-tagging (mis-id.)	0.9	1.0	0.9	1.0	0.7
Pileup	0.8	0.9	0.3	1.3	1.4
ZZ	0.6	0.7	0.4	0.8	0.5
Nonprompt norm.	1.2	2.0	1.2	1.5	1.0
Nonprompt (EWK subs.)	1.0	1.5	1.0	1.3	0.8
VVV norm.	0.5	0.6	0.6	0.6	0.5
VH norm.	0.2	0.2	0.3	0.2	0.2
t \bar{t} V norm.	0.5	0.5	0.5	0.5	0.5
tZq norm.	0.1	0.1	0.1	0.1	0.1
X+γ norm.	0.3	0.8	0	0.7	0
Total systematic	4.7	7.8	5.8	5.7	4.6
Luminosity	2.8	2.9	2.8	2.9	2.8
Statistical	2.1	6.0	4.8	4.1	3.1
Total experimental	6.0	10.8	8.0	7.5	6.3
Theoretical	0.9	0.9	0.9	0.9	0.9

Systematics that will directly affect the shape

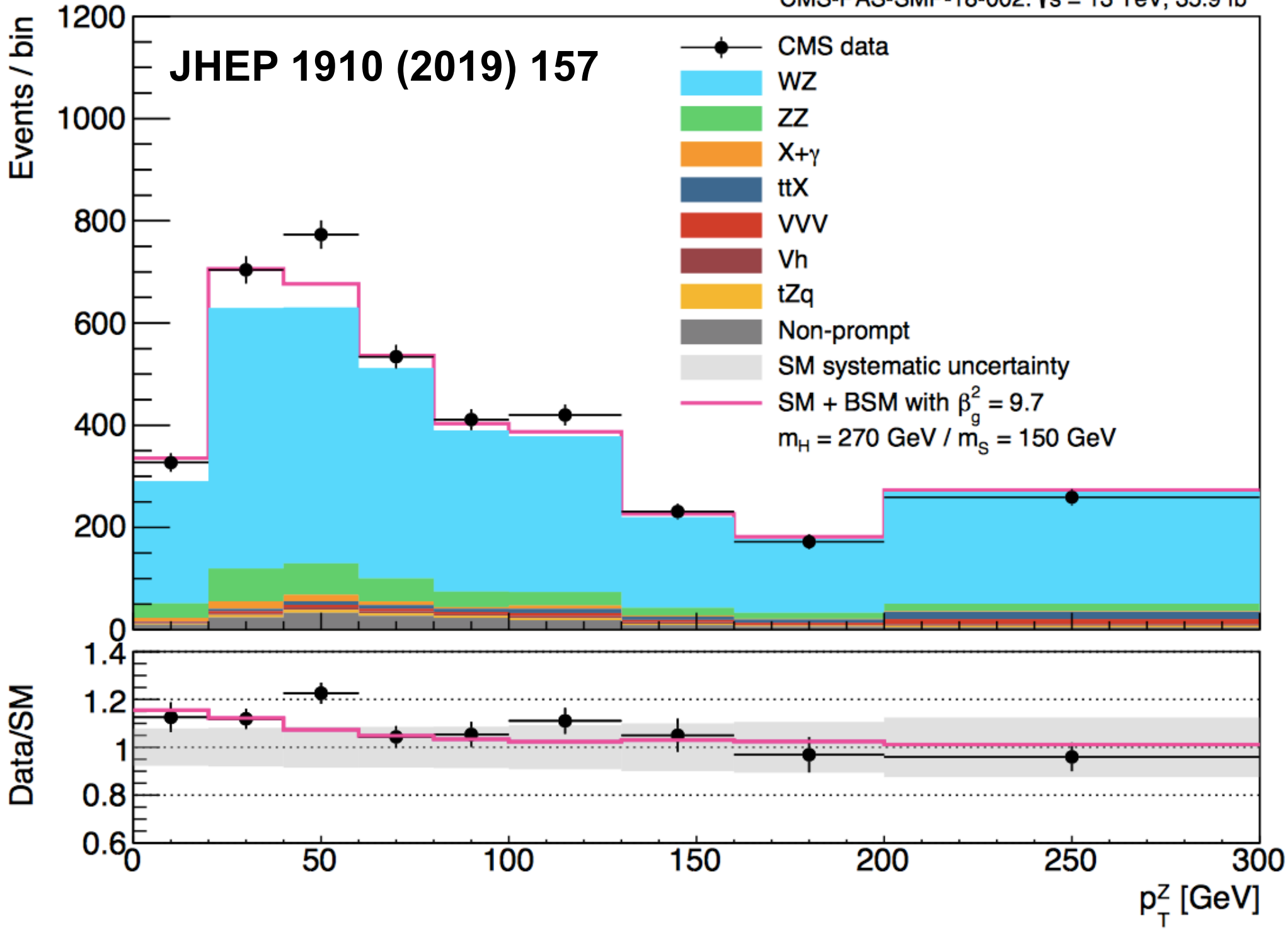




arXiv:1711.07874



JHEP 1910 (2019) 157



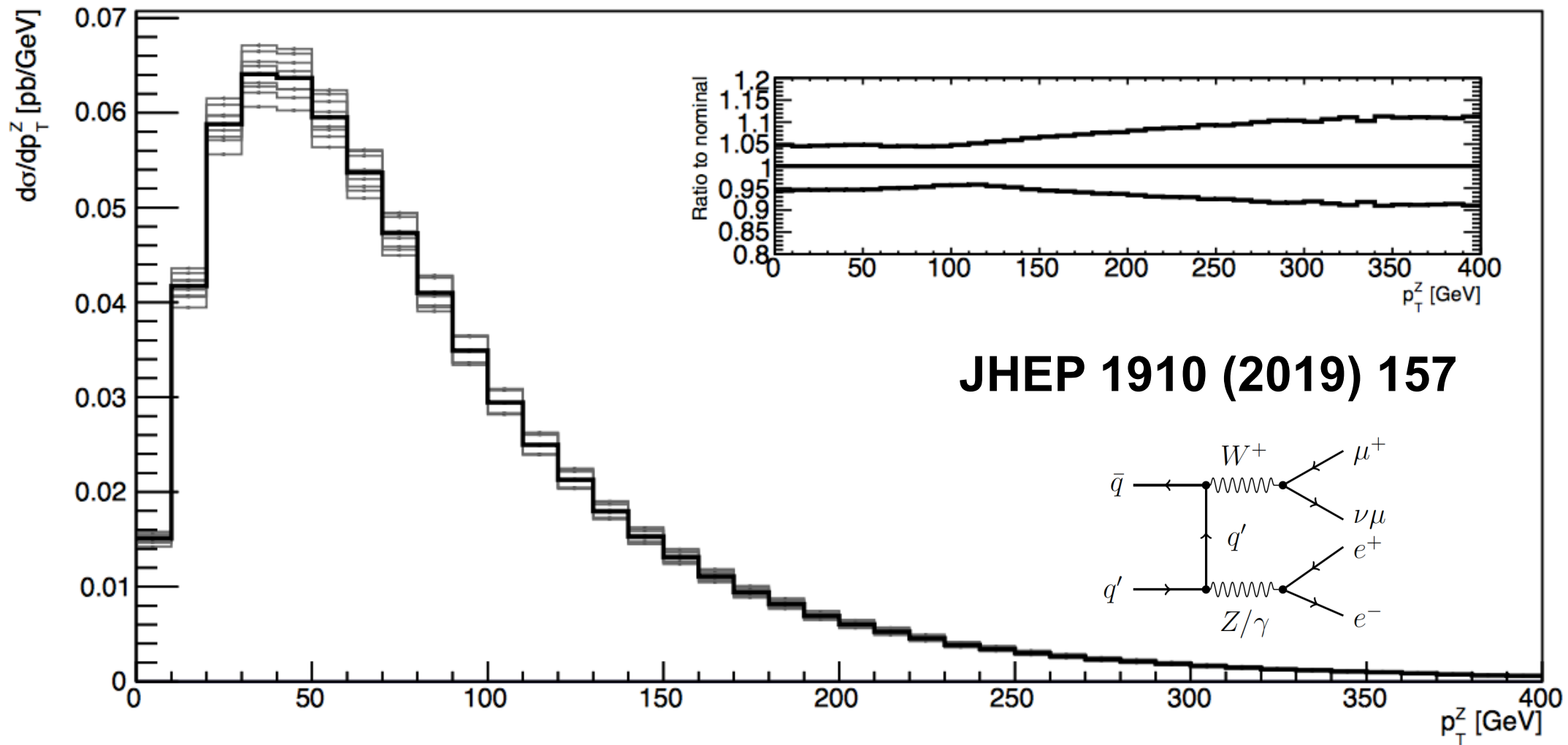


Figure 10: The effects of scale variations in the differential cross section of the SM WZ process as a function of the Z p_T . Here, aMC@NLO and Pythia 8 were used to generate the events. The thick black line represents the spectrum at the nominal scale, and each grey line is a variation of the scale. The insert shows the maximum and minimum relative deviations for all scale variations.

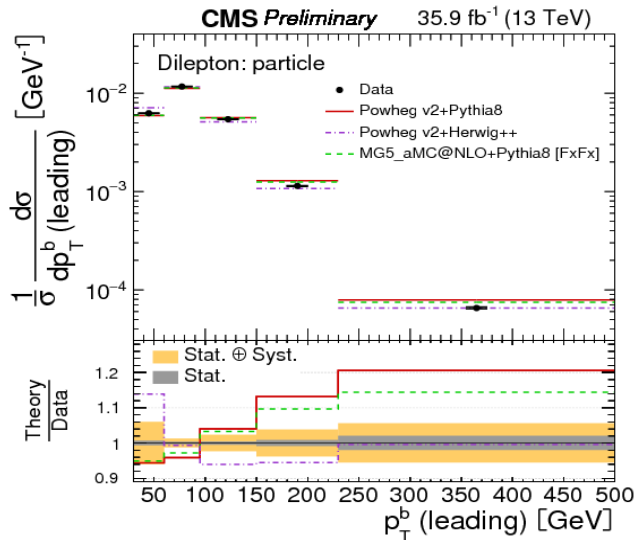
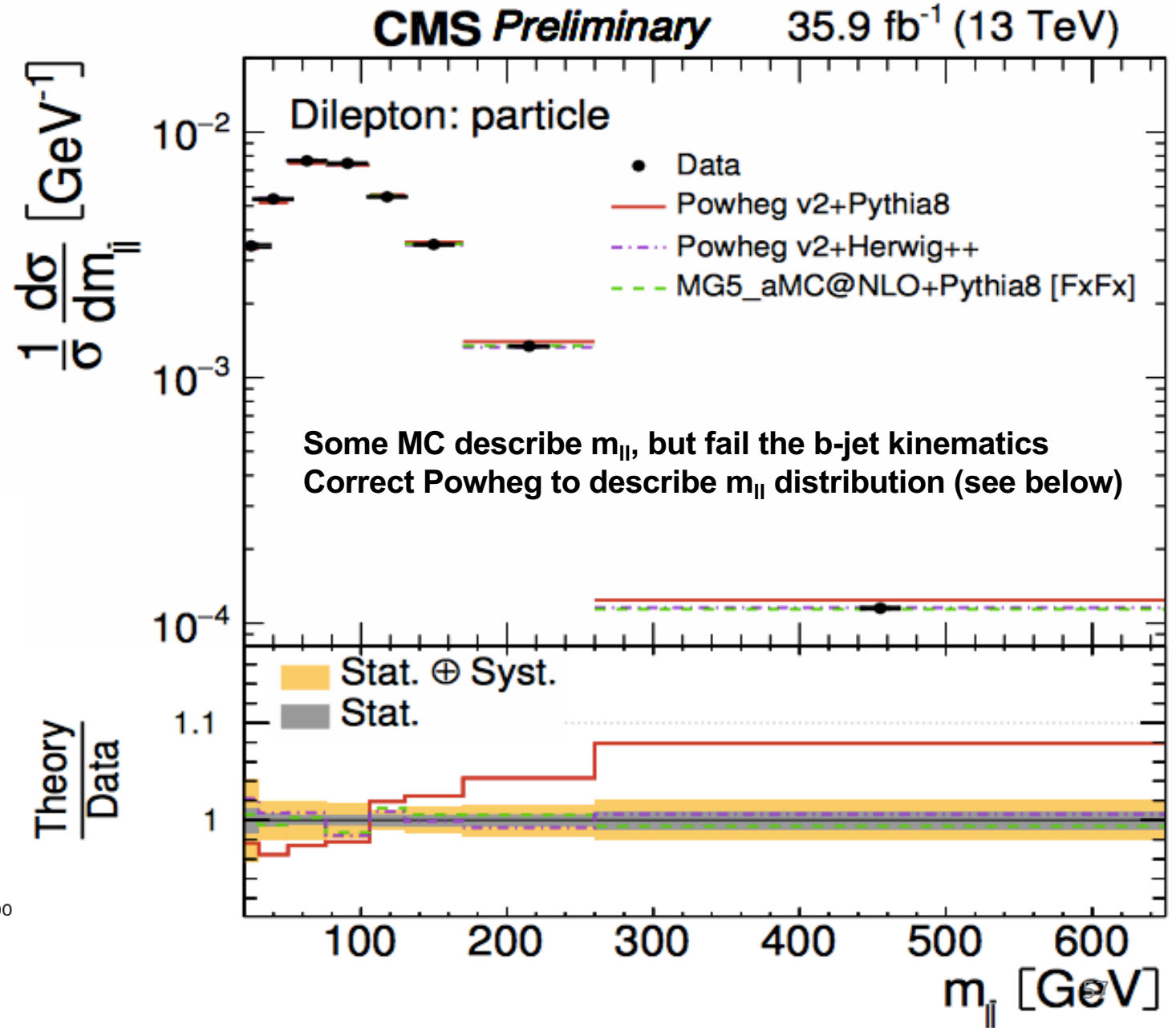
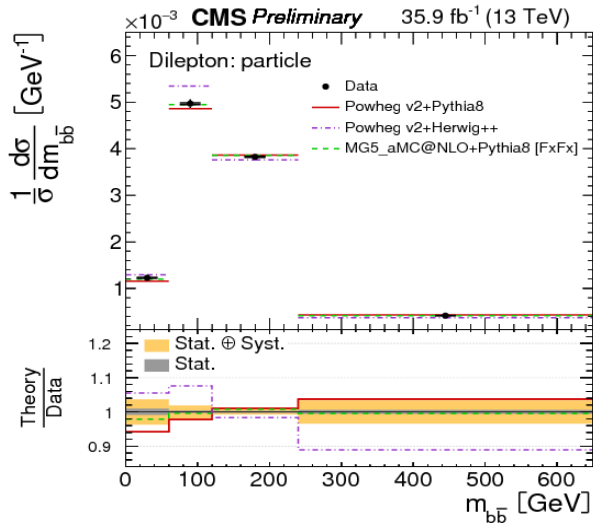
The fitting procedure

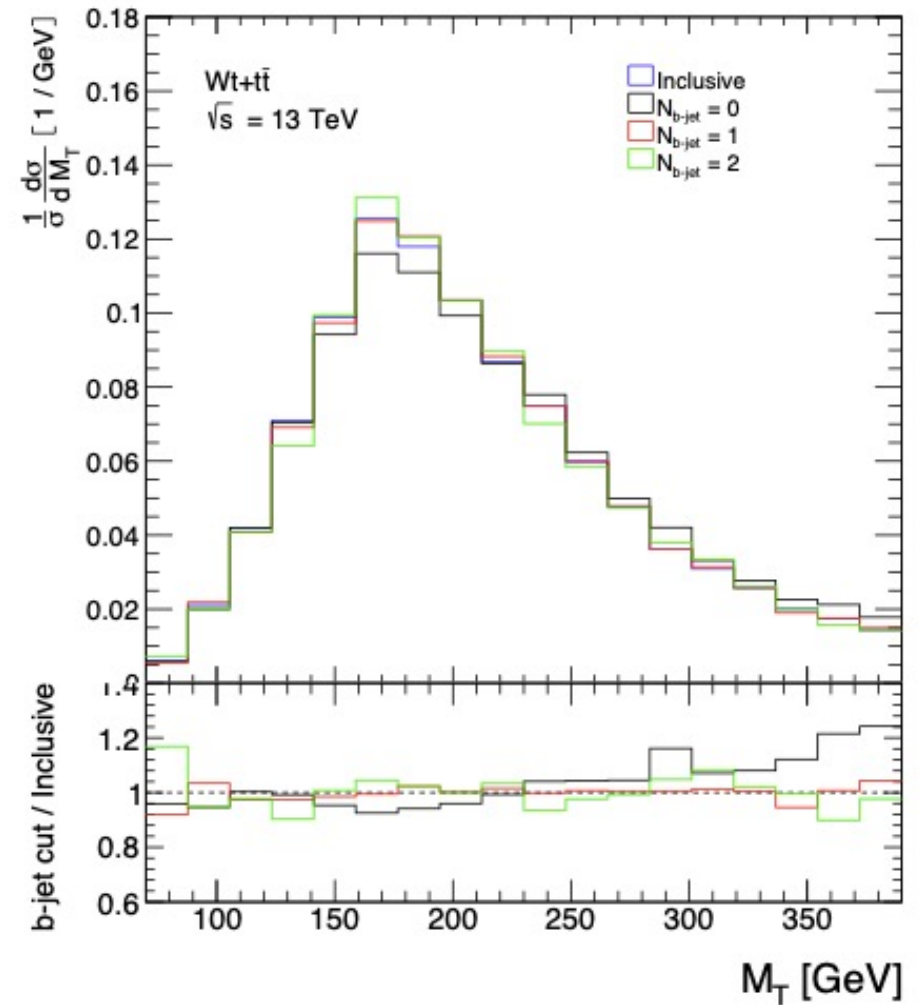
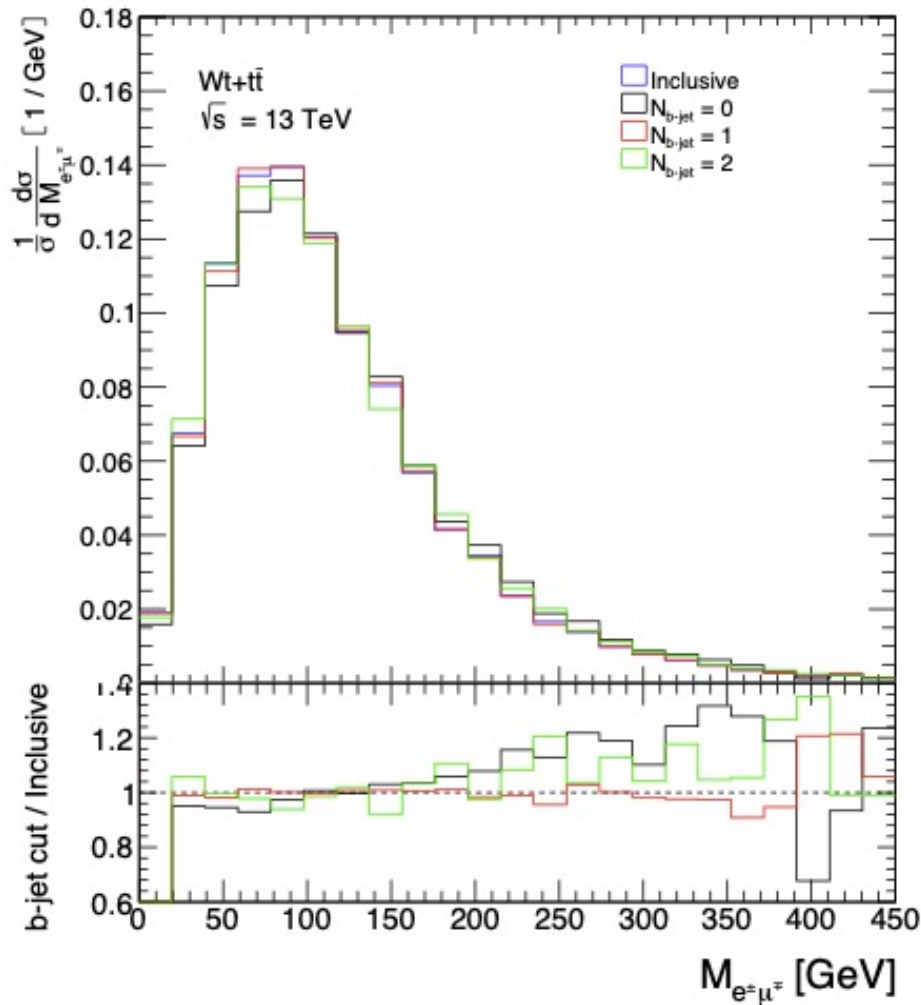
- **The RooStats workspace is made by HistFactory**
- **From the workspace, a profile likelihood ratio is calculated,**

$$\lambda(\beta_g^2) = \frac{L(\beta_g^2 | \hat{\theta})}{L(\hat{\beta}_g^2 | \hat{\theta})} \quad (\text{here } \theta \text{ denotes the nuisance parameters})$$

- **The best-fit value of β_g^2 is then calculated as the minimum of $-2\log(\lambda)$, with an error corresponding to a unit of deviation in this quantity from the best-fit point**
- **The significance is calculated as $\sqrt{-2 \log \lambda(0)}$, since $\beta_g^2 = 0$ corresponds to the SM-only hypothesis**

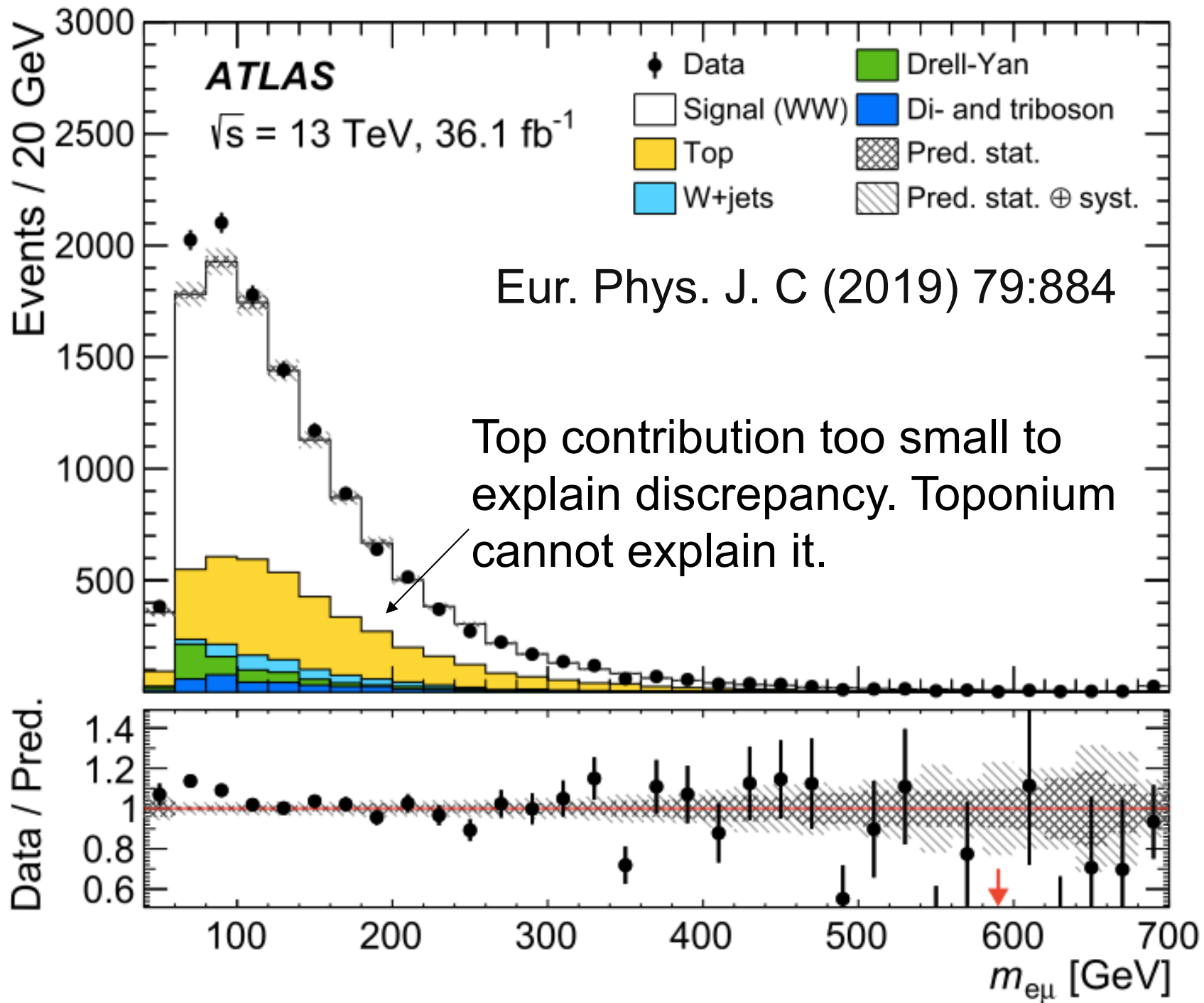
**Event selection with exactly two leptons (e,μ),
m_{ll}>20 GeV and at least 2b-jets**





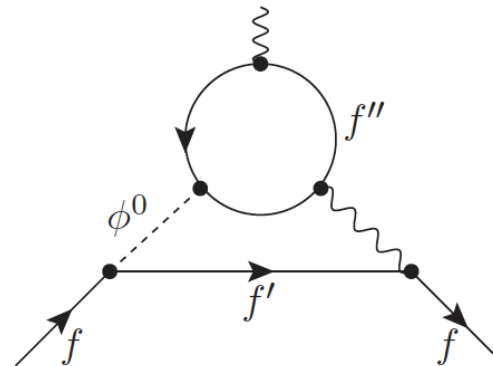
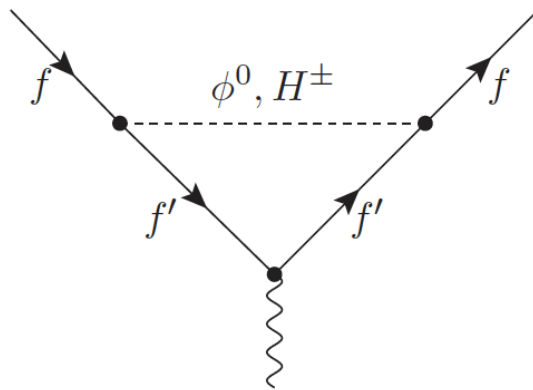
b-jet multiplicity is robust theoretically

Figure 9: Leptonic distributions produced by $t\bar{t}$ and tW processes (see text) as a function of the b -tagged jet multiplicity. The di-lepton invariant mass (left) and the transverse mass of the di-lepton and missing transverse energy system are displayed. Distributions are normalised to unity. The insert shows the ratio of the distributions with exclusive b -tagged jet bins relative to that obtained inclusively.



$$\Delta a_\mu = a_\mu^{\text{Exp}} - a_\mu^{\text{SM}} = 2.87(80) \times 10^{-9}$$

The Muon $g-2$ and the 2HDM+S

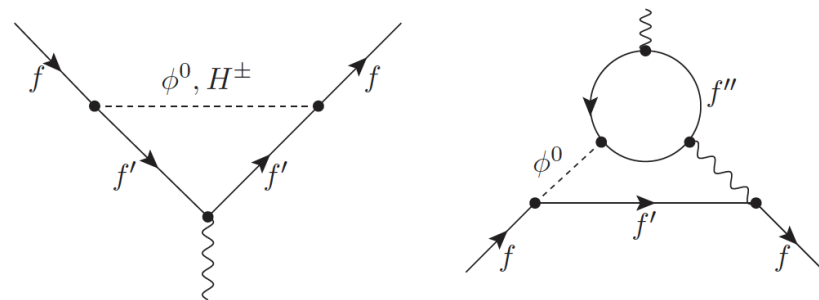


2HDM+S potential with fixed parameters from multi-lepton anomalies at the LHC

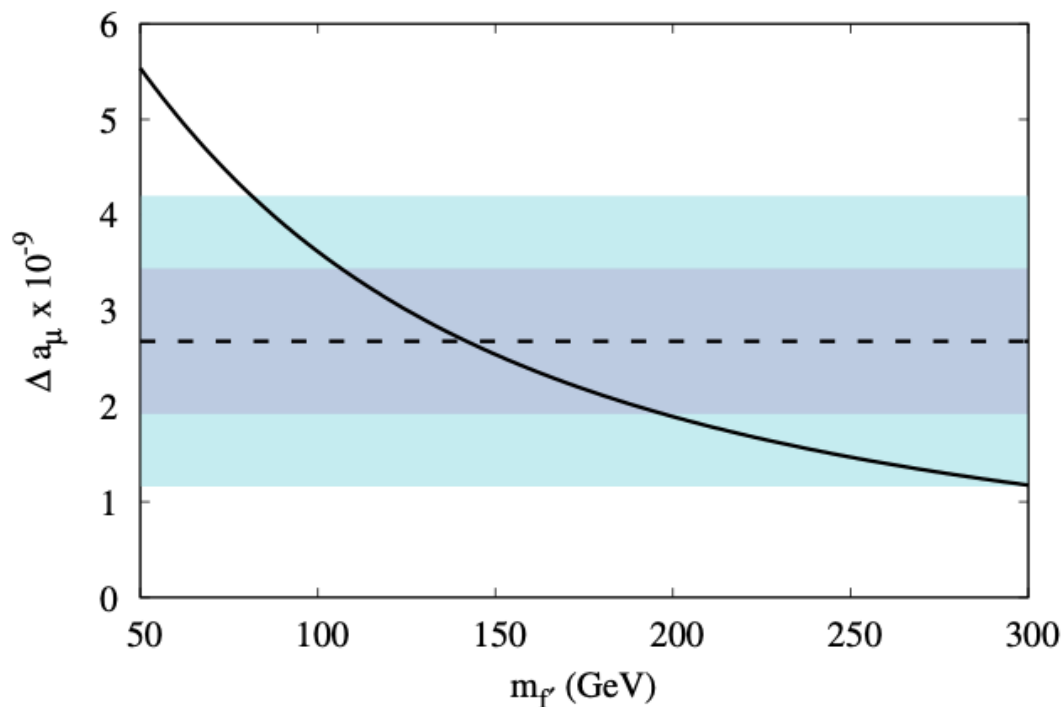
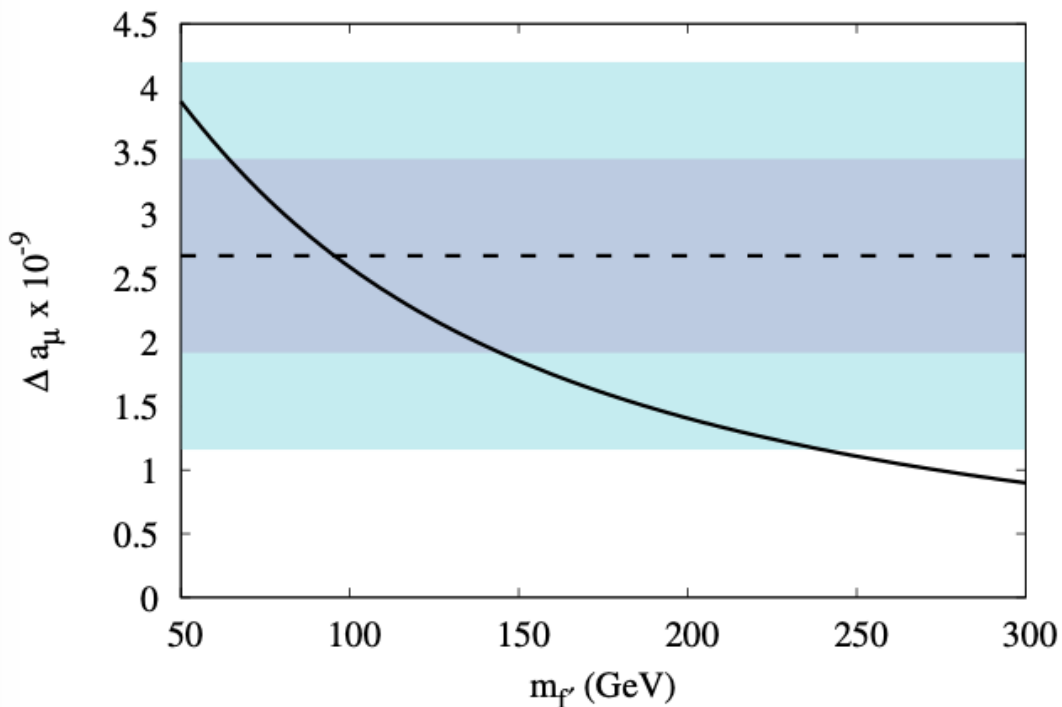
$$\begin{aligned}
 V(\Phi_1, \Phi_2, \Phi_S) &= m_{11}^2 |\Phi_1|^2 + m_{22}^2 |\Phi_2|^2 - m_{12}^2 (\Phi_1^\dagger \Phi_2 + \text{h.c.}) \\
 &+ \frac{\lambda_1}{2} (\Phi_1^\dagger \Phi_1)^2 + \frac{\lambda_2}{2} (\Phi_2^\dagger \Phi_2)^2 + \lambda_3 (\Phi_1^\dagger \Phi_1) (\Phi_2^\dagger \Phi_2) \\
 &+ \lambda_4 (\Phi_1^\dagger \Phi_2) (\Phi_2^\dagger \Phi_1) + \frac{\lambda_5}{2} \left[(\Phi_1^\dagger \Phi_2)^2 + \text{h.c.} \right] \\
 &+ \frac{1}{2} m_S^2 \Phi_S^2 + \frac{\lambda_6}{8} \Phi_S^4 + \frac{\lambda_7}{2} (\Phi_1^\dagger \Phi_1) \Phi_S^2 + \frac{\lambda_8}{2} (\Phi_2^\dagger \Phi_2) \Phi_S^2
 \end{aligned}$$

Consider extra degrees of freedom in the form of SM singlet vector-like fermions

$$\mathcal{L} \supset -y_f^S \bar{l}_R \Phi_S f'_L - \sum_{i=1}^2 y_{f'}^i \bar{L}_l \Phi_i f'_R + \text{h.c.},$$



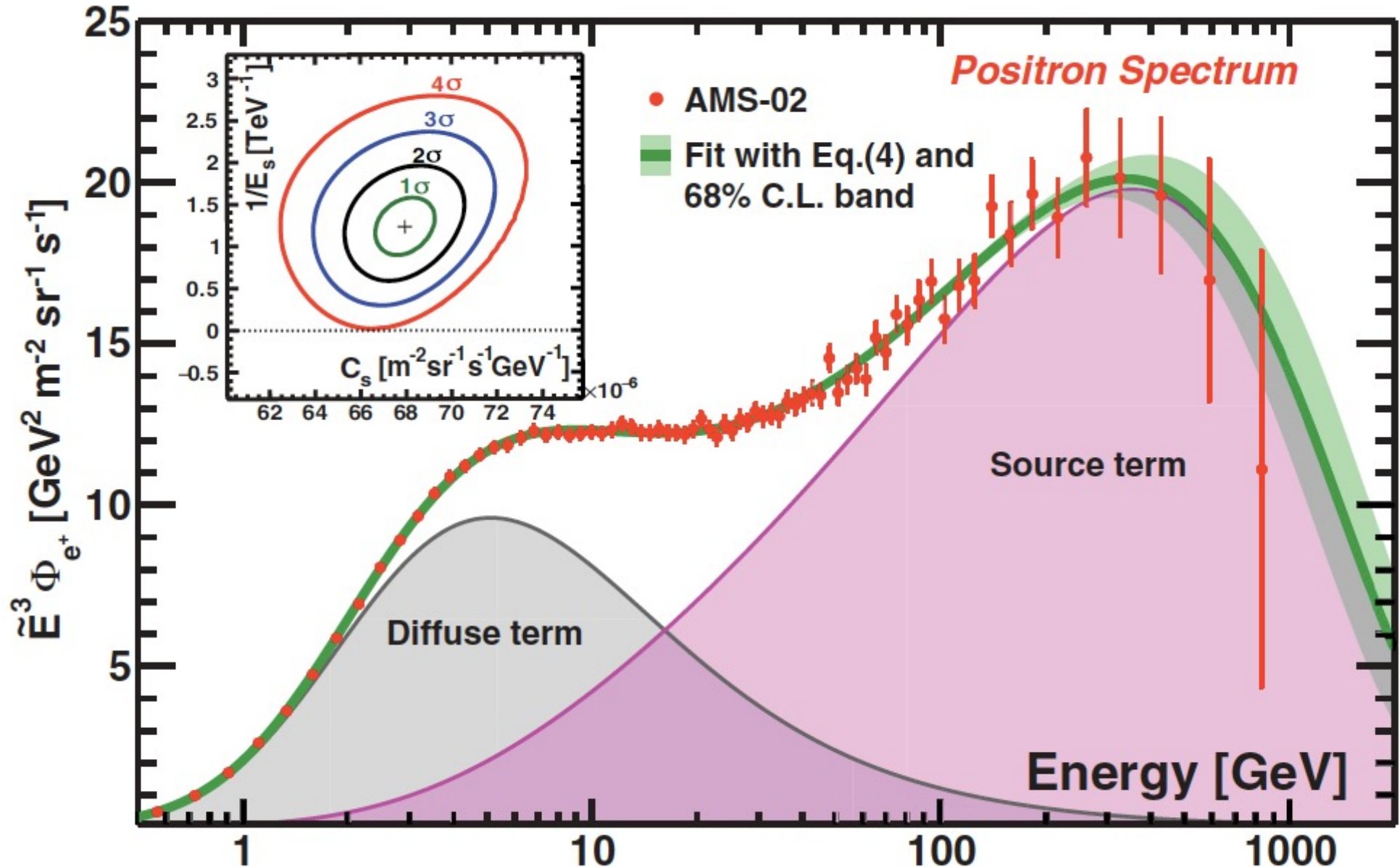
Allowed fermion masses with different choices of Yukawa couplings



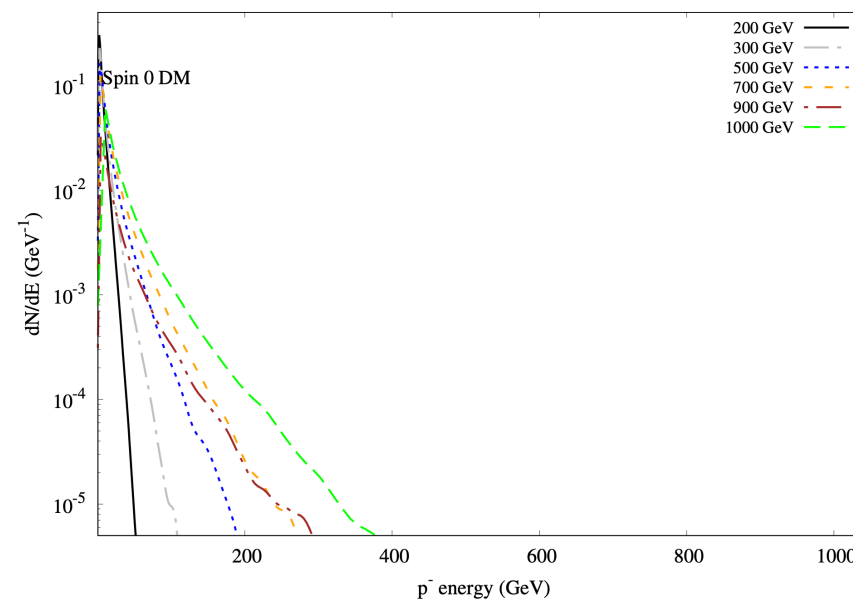
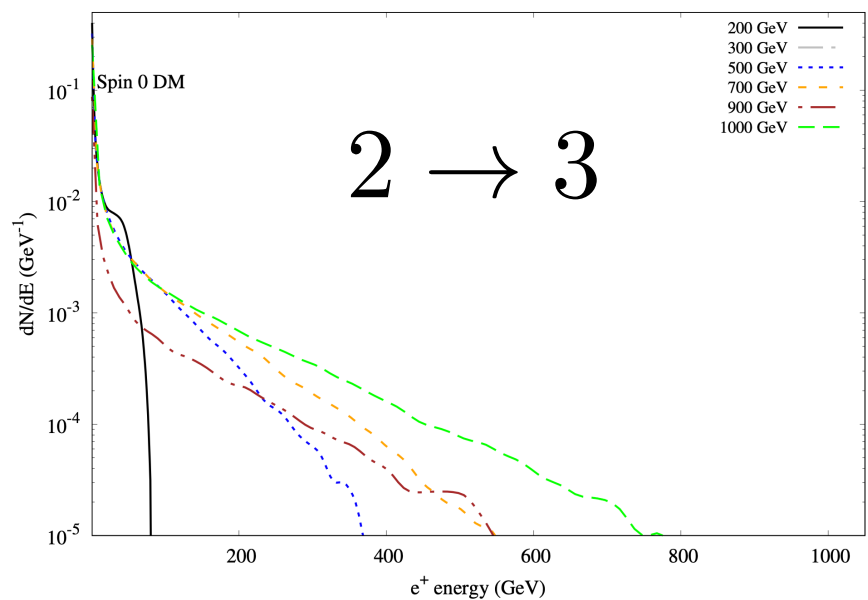
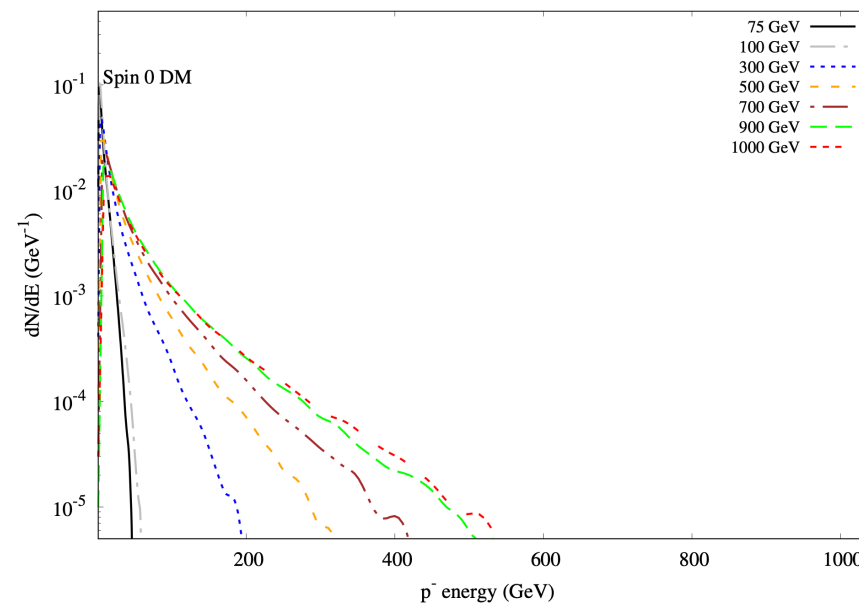
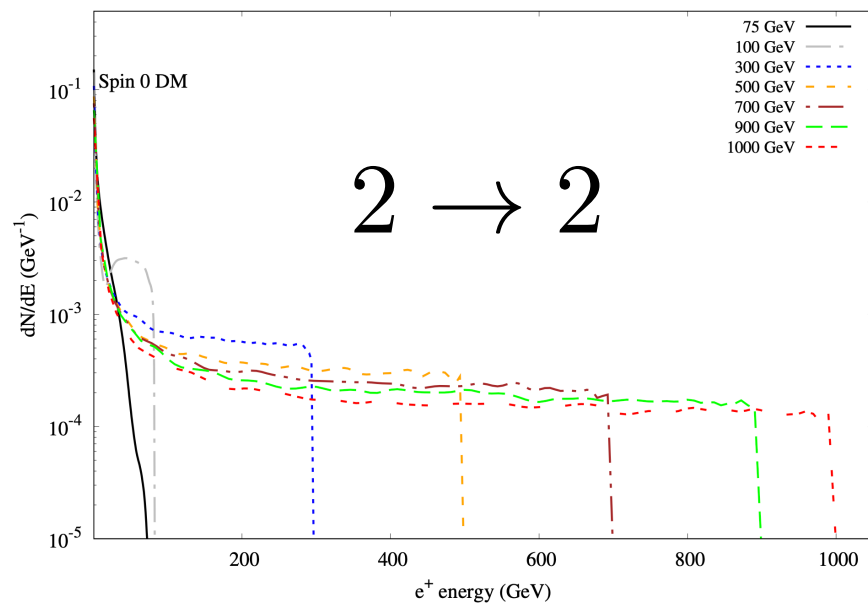
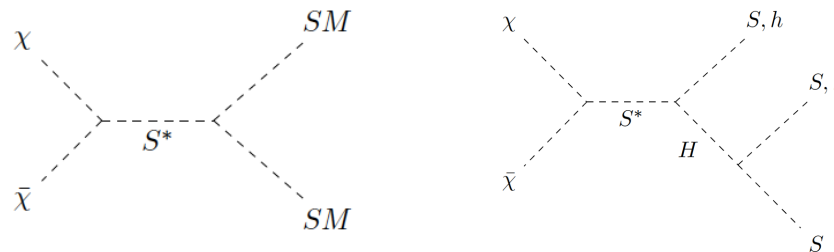
The multi-lepton anomalies and excesses in astrophysics

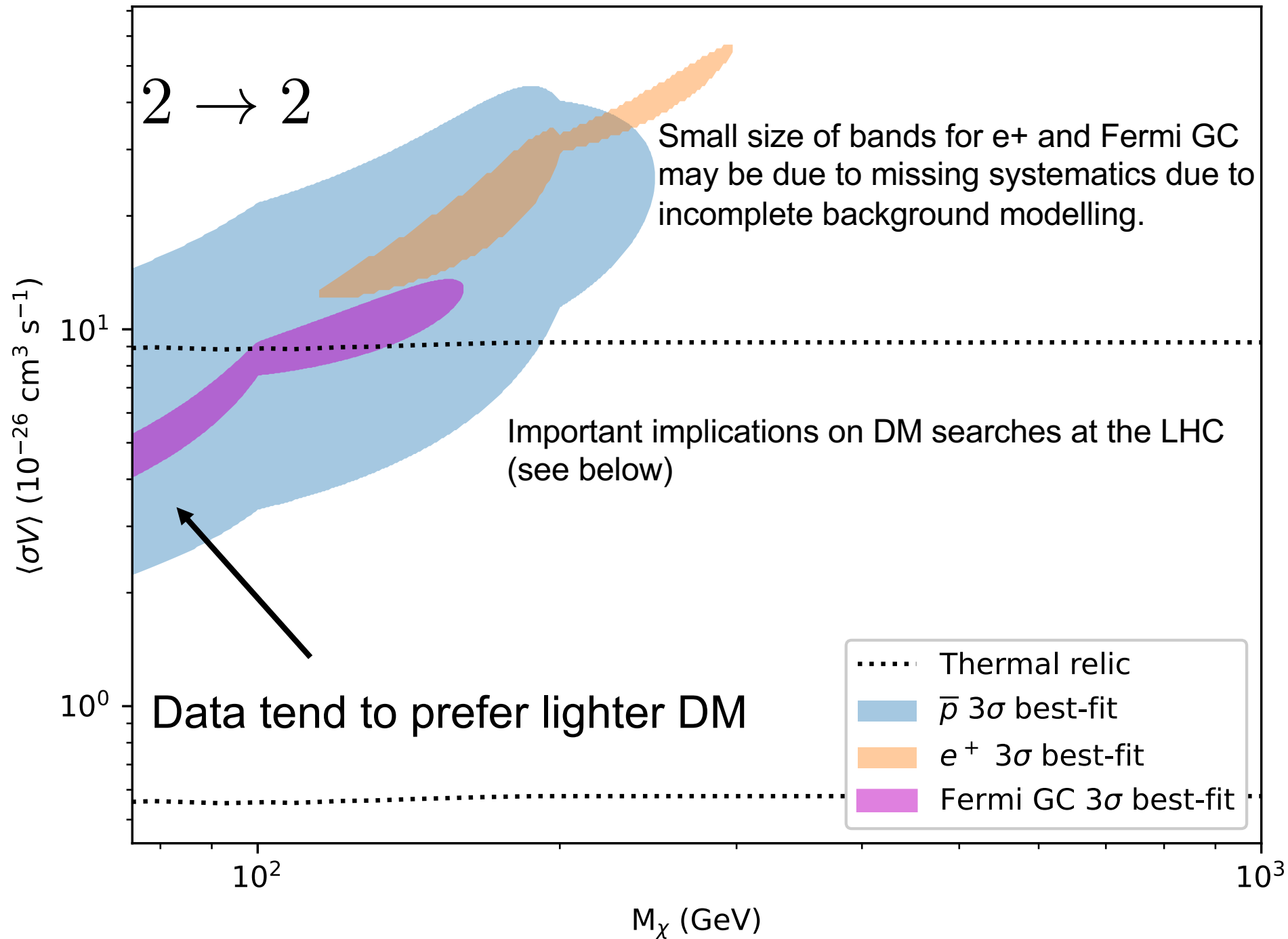


Leptophilic excesses, such as positron rise in PAMELA/AMS02



Dark matter annihilation.
Leptons, photons and protons
from the decays of S .





$2 \rightarrow 2$

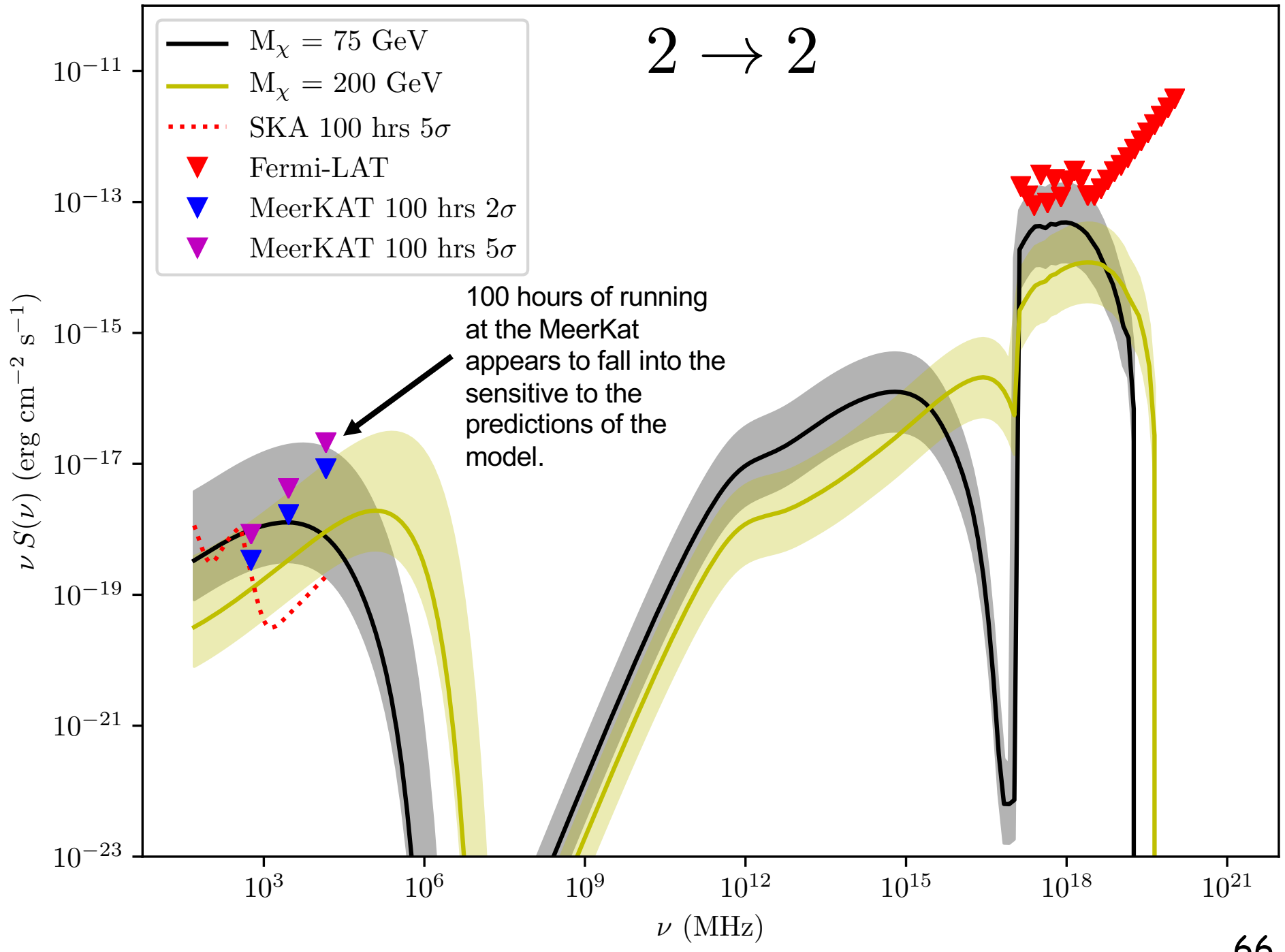


Table 2: Overview of the selection defining the analysis categories.

Category	Number of leptons	Number of jets	Sub-categorization
ggH	2	-	(DF, SF) \times (0 jets, 1 jet, ≥ 2 jets)
VBF	2	≥ 2	(DF, SF)
VH2j	2	≥ 2	(DF, SF)
WHSS	2	≥ 1	(DF, SF) \times (0 jets, 1 jet)
WH3 l	3	0	SF lepton pair with opposite or same sign
ZH3 l	3	≥ 1	(1 jet, 2 jets)
ZH4 l	4	-	(DF, SF)

Table 3: Summary of the selection used in different flavor ggH categories.

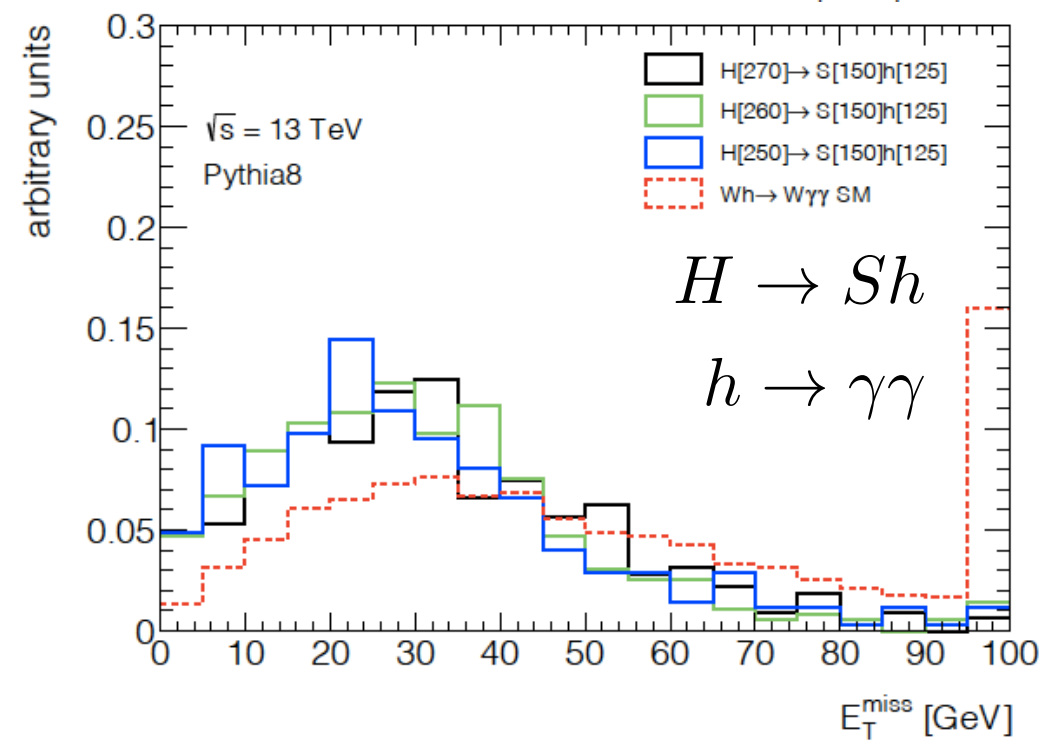
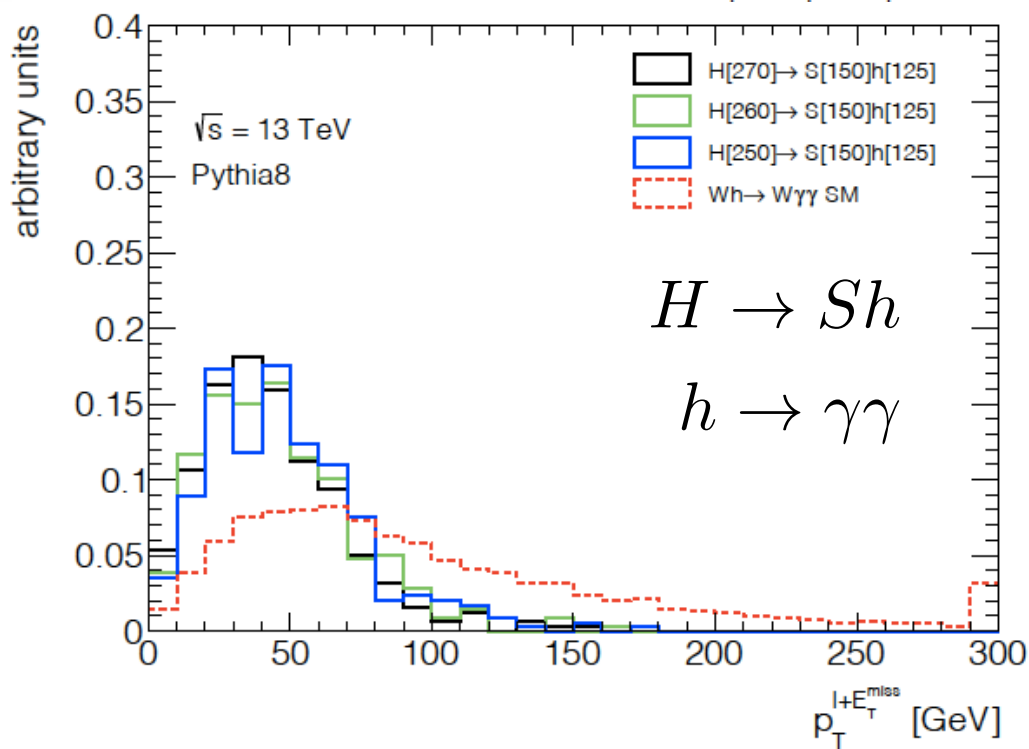
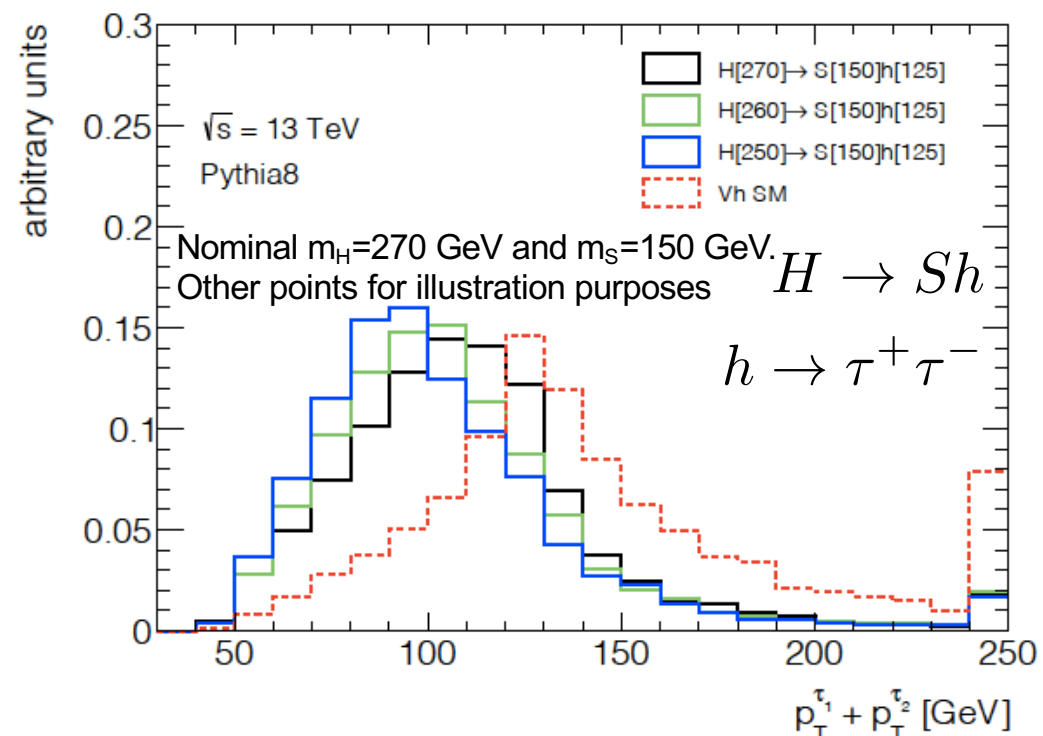
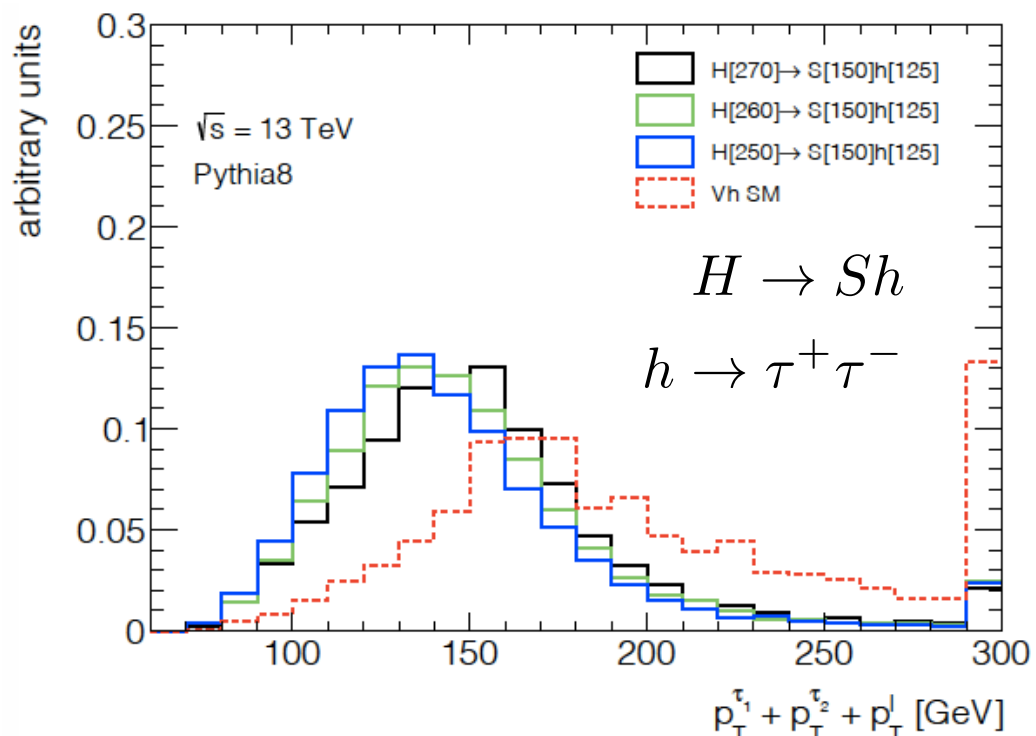
Category	Sub-categories	Selection
Global selection	-	$p_{T1} > 25 \text{ GeV}, p_{T2} > 10 \text{ GeV}$ (2016) or 13 GeV $p_T^{\text{miss}} > 20 \text{ GeV}, p_T^{\ell\ell} > 30 \text{ GeV}, m_{\ell\ell} > 12 \text{ GeV}$ $e\mu$ pair with opposite charge
	$\ell^\pm \ell^\mp, p_{T2} \leq 20 \text{ GeV}$	$m_T^H > 60 \text{ GeV}, m_T(\ell 2, p_T^{\text{miss}}) > 30 \text{ GeV}$ $p_{T2} \leq 20 \text{ GeV}$ No jet with $p_T > 30 \text{ GeV}$ No b-tagged jet with $p_T > 20 \text{ GeV}$
0-jet ggH tagged	Top CR	As SR, no m_T^H requirement, $m_{\ell\ell} > 50 \text{ GeV}$ At least 1 b-tagged jet with $20 \text{ GeV} < p_T < 30 \text{ GeV}$
	$\tau^+ \tau^-$ CR	As SR but with $m_T^H < 60 \text{ GeV}$ $30 \text{ GeV} < m_{\ell\ell} < 80 \text{ GeV}$
	$\ell^\pm \ell^\mp, p_{T2} \leq 20 \text{ GeV}$	$m_T^H > 60 \text{ GeV}, m_T(\ell 2, p_T^{\text{miss}}) > 30 \text{ GeV}$ $p_{T2} \leq 20 \text{ GeV}$ 1 jet with $p_T > 30 \text{ GeV}$ No b-tagged jet with $p_T > 20 \text{ GeV}$
1-jet ggH tagged	Top CR	As SR, no m_T^H requirement, $m_{\ell\ell} > 50 \text{ GeV}$ At least 1 b-tagged jet with $p_T > 30 \text{ GeV}$
	$\tau^+ \tau^-$ CR	As SR but with $m_T^H < 60 \text{ GeV}$ $30 \text{ GeV} < m_{\ell\ell} < 80 \text{ GeV}$
	SR	$m_T^H > 60 \text{ GeV}, m_T(\ell 2, p_T^{\text{miss}}) > 30 \text{ GeV}$ $p_{T2} \leq 20 \text{ GeV}$ At least 2 jets with $p_T > 30 \text{ GeV}$ No b-tagged jet with $p_T > 20 \text{ GeV}$
2-jet ggH tagged	Top CR	$m_{jj} < 65 \text{ GeV}$ or $105 \text{ GeV} < m_{jj} < 120 \text{ GeV}$ As SR, no m_T^H requirement, $m_{\ell\ell} > 50 \text{ GeV}$ At least 1 of the leading jets b-tagged
	$\tau^+ \tau^-$ CR	As SR but with $m_T^H < 60 \text{ GeV}$ $30 \text{ GeV} < m_{\ell\ell} < 80 \text{ GeV}$
	SR	$m_T^H > 60 \text{ GeV}, m_T(\ell 2, p_T^{\text{miss}}) > 30 \text{ GeV}$ $p_{T2} \leq 20 \text{ GeV}$ At least 2 jets with $p_T > 30 \text{ GeV}$ No b-tagged jet with $p_T > 20 \text{ GeV}$

Impact on Higgs Physics

The presence of a BSM signal of the type $H \rightarrow Sh$ would lead to:

- ❑ The presence of extra leptons in association with h . Affects the Wh measurement (Eur.Phys.J.C 81 (2021) 365)**
- ❑ Distortion of Higgs p_T and rapidity (under study)**

No tuning of model parameters performed. Look at fixed corners of the phase-space fixed with parameters of 2017.



Survey of LHC results on Vh (V=W,Z) production (Eur.Phys.J.C 81 (2021) 365)

The BSM (H→Sh) signal appears at low p_{Th} and the SM signal is prevalent at larger p_{Th} (no tuning of parameters)

Include those results from ATLAS and CMS where no requirements on p_{Th} (or correlated observables) is not done or used in an MVA.

Those results where the final state is treated more “inclusively” display elevated signal strengths for Wh production:

$$\mu(Wh) = 2.41 \pm 0.37$$

This represents a 3.8σ deviation from the SM value of 1. BSM signal normalization less than expected from multilepton excesses assuming $Br(H\rightarrow Sh)=100\%$. Indicates that $Br(H\rightarrow SS) > Br(H\rightarrow Sh)$

Higgs decay	Ref.	Experiment	\sqrt{s}, \mathcal{L} TeV, fb ⁻¹	Final state	Category	μ	Used in combination	Comments
WW	[66]	ATLAS	7, 4.5 8, 20.3	2 ℓ	DFOS 2j	$2.2^{+2.0}_{-1.9}$	✓	2ℓ combination: $\mu = 3.7^{+1.9}_{-1.3}$ $m_{\ell_0\ell_2}$ used as input BDT discriminating variable
					SS 1j	$8.4^{+4.3}_{-3.8}$	✓	
					SS 2j	$7.6^{+6.0}_{-5.4}$	✓	
				3 ℓ	1SFOS	$-2.9^{+2.7}_{-2.1}$	x	
					0SFOS	$1.7^{+1.9}_{-1.4}$	✓	
					1SFOS 0SFOS	$2.3^{+1.2}_{-1.0}$	✓	
WW	[67]	ATLAS	13, 36.1	3 ℓ	1SFOS 0SFOS	$2.3^{+1.2}_{-1.0}$	✓	1SFOS channel uses $m_{\ell_0\ell_2}$ in the BDT but excess driven by 0SFOS
	[68]	CMS	7, 4.9 8, 19.4	2 ℓ	DFOS 2j	$0.39^{+1.97}_{-1.87}$	✓	Discrepancy at low $m_{\ell\ell}$
				3 ℓ	0+1SFOS	$0.56^{+1.27}_{-0.95}$	✓	
	[69]	CMS	13, 35.9	2 ℓ	DFOS 2j	$3.92^{+1.32}_{-1.17}$	✓	Discrepancy at low $m_{\ell\ell}$
				3 ℓ	0+1SFOS	$2.23^{+1.76}_{-1.53}$	✓	
	$\tau\tau$	[70]	ATLAS	8, 20.3	1 ℓ	$\ell + \tau_h \tau_h$	1.8 ± 3.1	✓
2 ℓ					$e^{\pm}\mu^{\pm} + \tau_h$	1.3 ± 2.8	✓	
[71]		CMS	7, 4.9 8, 19.7	1 ℓ	$\ell + \tau_h \tau_h$	-0.33 ± 1.02	x	
				2 ℓ	$e^{\pm}\mu^{\pm} + \tau_h$	-0.33 ± 1.02	x	
[72]		CMS	13, 35.9	1 ℓ	$\ell + \tau_h \tau_h$	$3.39^{+1.68}_{-1.54}$	✓	
				2 ℓ	$e^{\pm}\mu^{\pm} + \tau_h$	$3.39^{+1.68}_{-1.54}$	✓	
$\tau\tau$	[73]	ATLAS	7, 5.4 8, 20.3	$\ell\nu$	One-lepton	1.0 ± 1.6	x	$E_T^{miss} > 70 - 100$ GeV
				$\ell\nu, \nu\nu$	E_T^{miss}	1.0 ± 1.6	x	$p_T^{\tau\gamma} > 70$ GeV
				jj	Hadronic	1.0 ± 1.6	x	Split E_T^{miss} at 45 GeV
	[74]	CMS	7, 5.1 8, 19.7	$\ell\nu$	One-lepton	$-0.16^{+1.16}_{-0.79}$	x	$E_T^{miss} > 70$ GeV
				$\ell\nu, \nu\nu$	E_T^{miss}	$-0.16^{+1.16}_{-0.79}$	x	$p_T^{\tau\gamma} > 13m_{\tau\gamma}/12$
				jj	Hadronic	$-0.16^{+1.16}_{-0.79}$	x	
[75]	ATLAS	13, 139	$\ell\nu$	One-lepton	$2.41^{+0.71}_{-0.70}$	✓	$p_T^{\ell+E_T^{miss}} < 150$ GeV	
			$\ell\nu, \nu\nu$	E_T^{miss}	$2.64^{+1.16}_{-0.99}$	x	$p_T^{\ell+E_T^{miss}} > 150$ GeV	
			jj	Hadronic	$2.64^{+1.16}_{-0.99}$	x	$E_T^{miss} > 75$ GeV	
[76]	CMS	13, 35.6	$\ell\nu$	One-lepton	$0.76^{+0.95}_{-0.83}$	x	$60 < m_{jj} < 120$ GeV	
			$\ell\nu, \nu\nu$	E_T^{miss}	$0.76^{+0.95}_{-0.83}$	x	$m_{jj} \in [0, 60] \cup [120, 350]$ GeV	
			jj	Hadronic	$3.16^{+1.84}_{-1.72}$	✓		
[77]	CMS	13, 137	$\ell\nu$	One-lepton	$3.0^{+1.5}_{-1.3}$	x	Superseded by full Run 2 result	
			$\ell\nu, \nu\nu$	E_T^{miss}	$3.0^{+1.5}_{-1.3}$	x	$E_T^{miss} > 85$ GeV	
			jj	Hadronic	$5.1^{+2.5}_{-2.3}$	✓	$p_T^{\tau\gamma}/m_{\tau\gamma}$ not used	
[78]	ATLAS	13, 139	$\ell\nu$	One-lepton	$1.31^{+1.42}_{-1.12}$	✓	$p_T^{\nu} < 75$ GeV	
			$\ell\nu, \nu\nu$	E_T^{miss}	$1.31^{+1.42}_{-1.12}$	x	$p_T^{\tau\gamma}/m_{\tau\gamma}$ used in BDT	
			jj	Hadronic	$0.89^{+0.89}_{-0.91}$	x		
ZZ	[79]	CMS	13, 137.1	$\ell\ell\ell + \ell\nu$	Lep-enriched	$1.44^{+1.17}_{-0.93}$	x	Number of jets used in MVA
				$\ell\ell\ell + q\bar{q}$	2j	$1.44^{+1.17}_{-0.93}$	x	m_{jj} used in MVA
				$\ell\ell\ell + \ell\nu$	Lep-low p_T^{Δ}	$3.21^{+2.49}_{-1.85}$	✓	$p_T^{\Delta} < 150$ GeV
[79]	CMS	13, 137.1	$\ell\ell\ell + \ell\nu$	Lep-high p_T^{Δ}	$0.00^{+1.57}_{-0.60}$	x	$p_T^{\Delta} > 150$ GeV	
			$\ell\ell\ell + q\bar{q}$	2j	$0.57^{+1.20}_{-0.57}$	x	$60 < m_{jj} < 120$ GeV	

CMS *Preliminary*

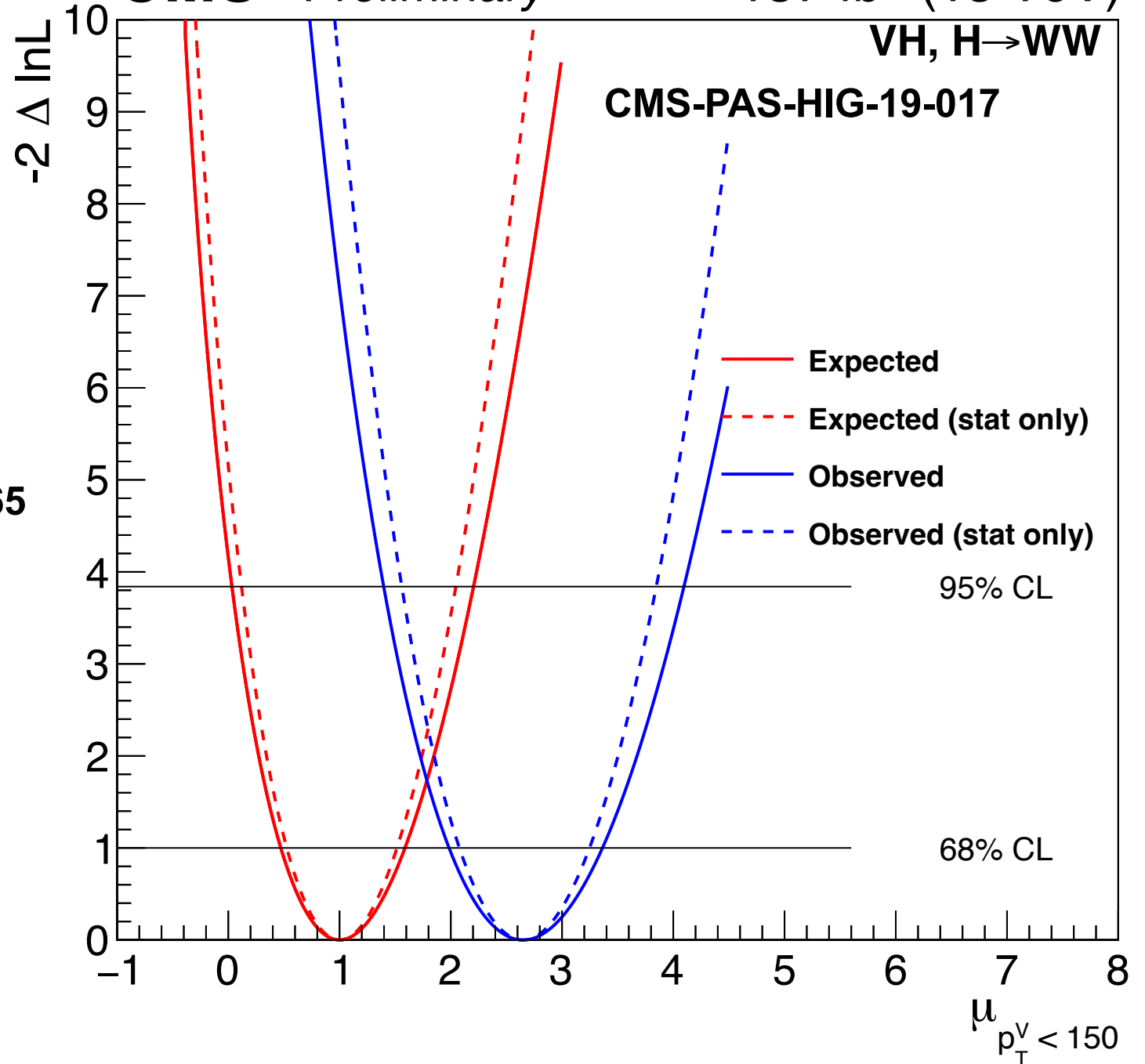
137 fb⁻¹ (13 TeV)

VH, H→WW

CMS-PAS-HIG-19-017

New results from CMS in the measurement of Vh, h→WW add to the anomalies reported in Eur.Phys.J.C 81 (2021) 365

Deviation from the SM becomes stronger with p_T^V<150 GeV

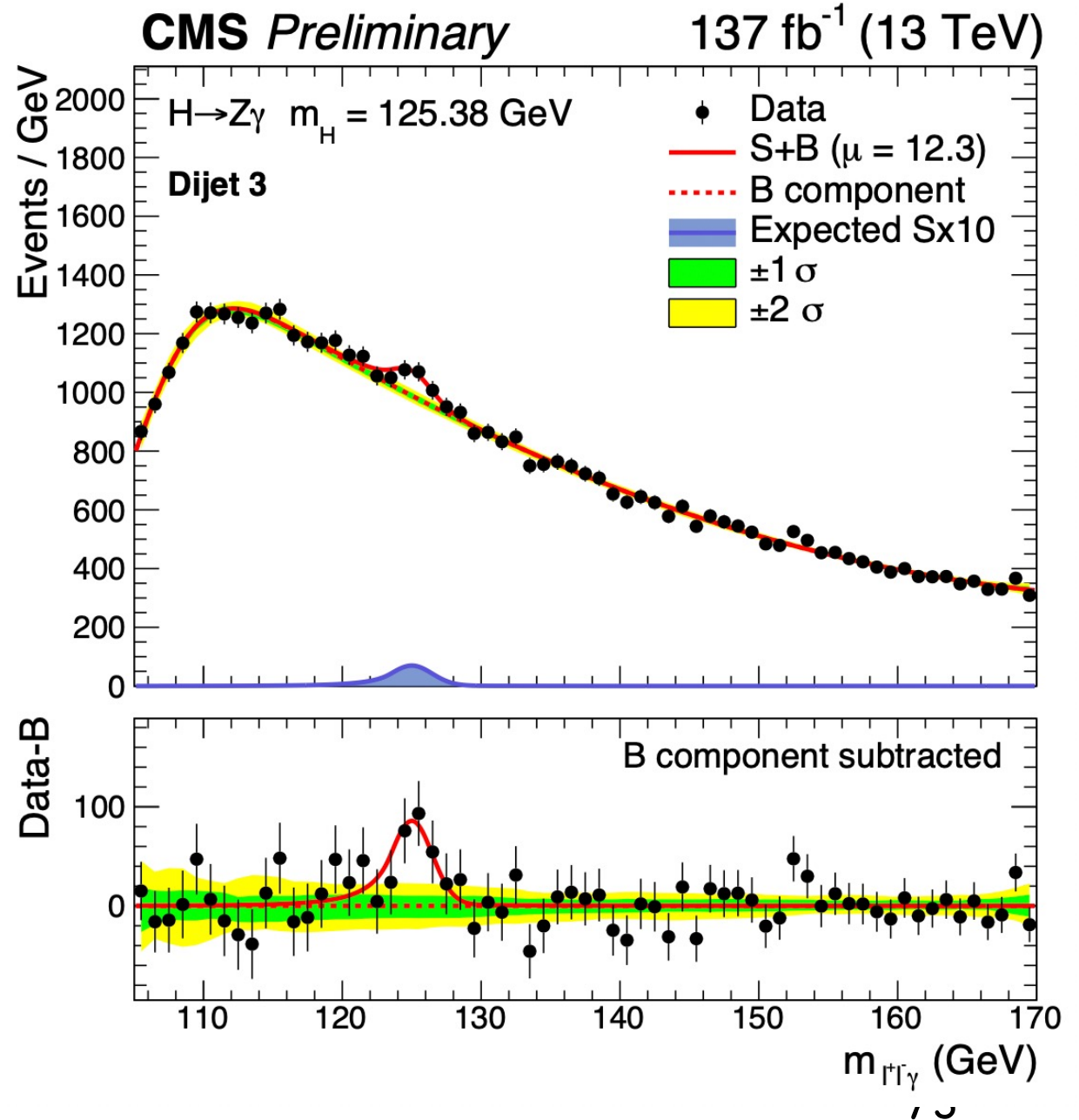


CMS Physics Analysis Summary

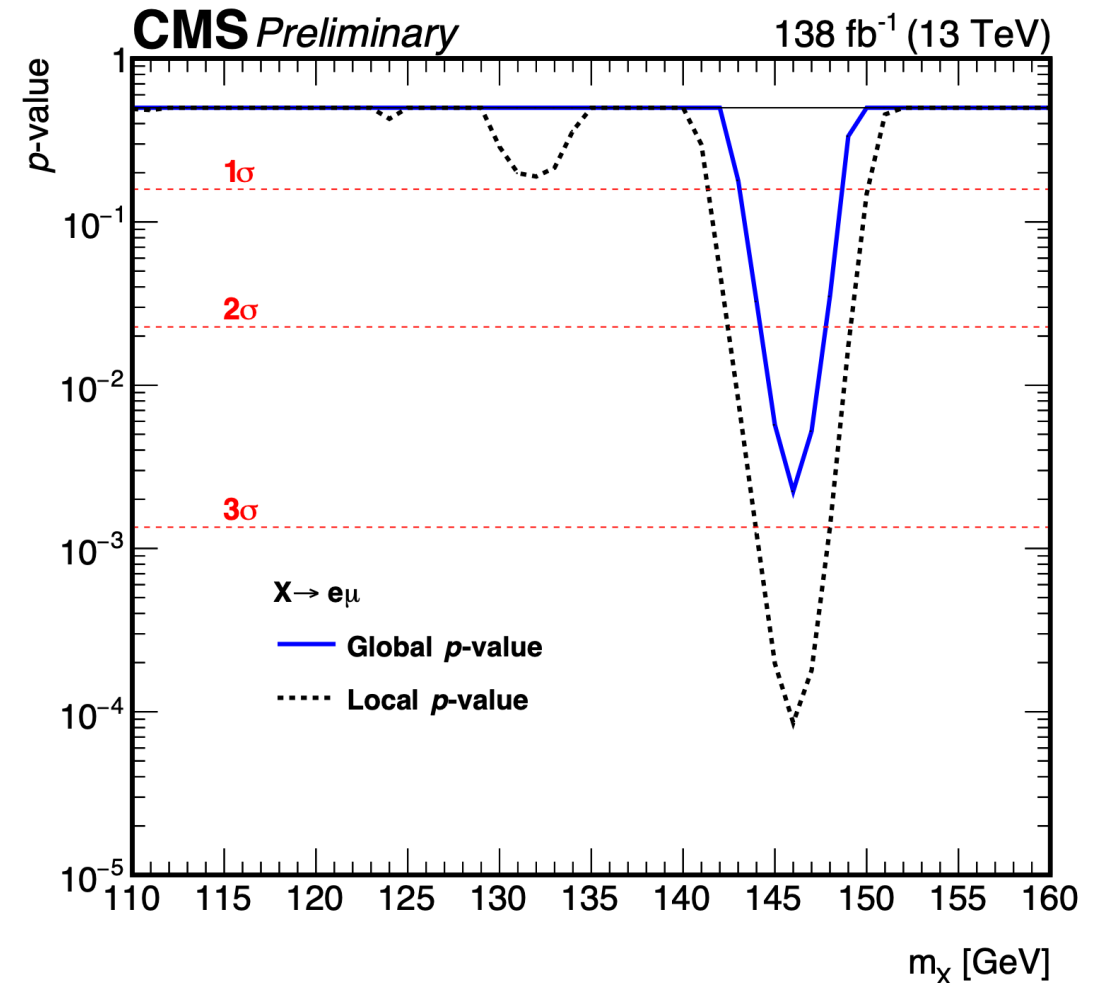
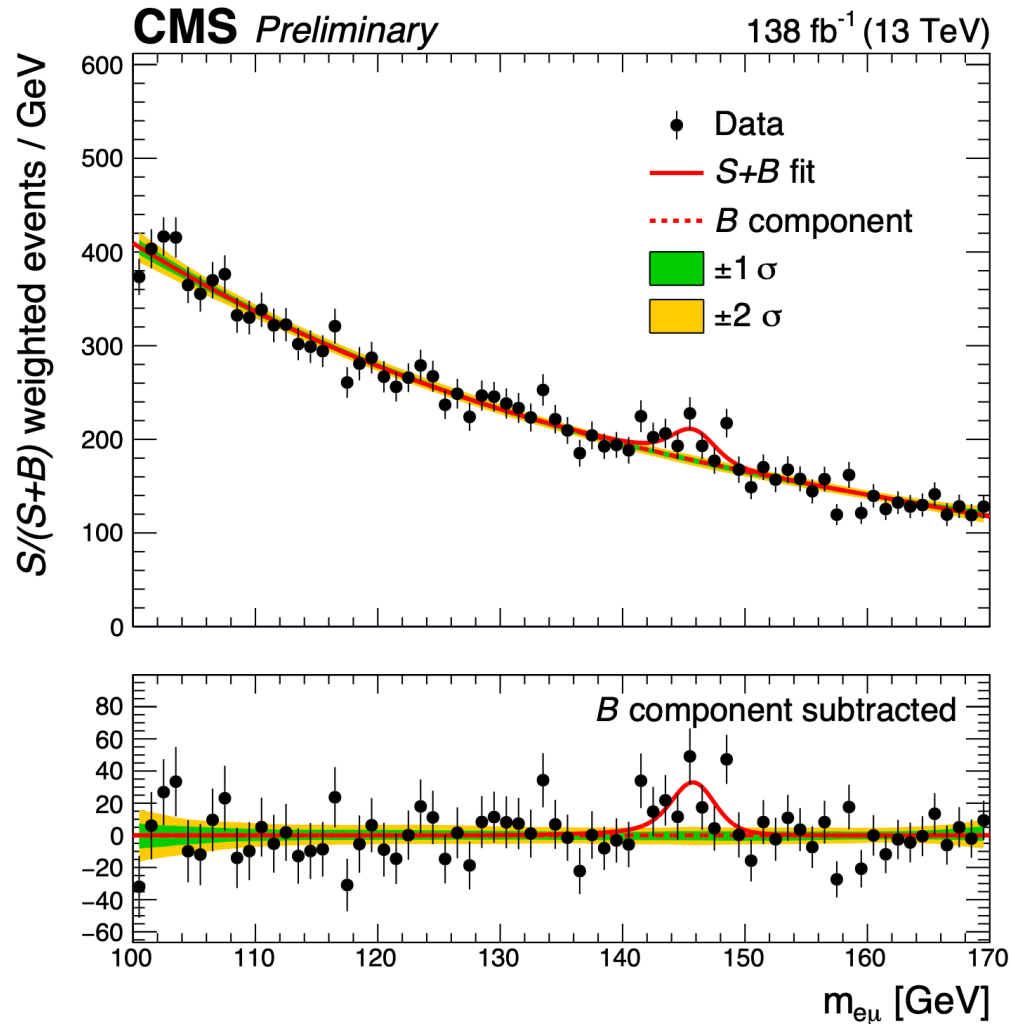
Search for the Higgs boson decay to $Z\gamma$ in proton-proton collisions at $\sqrt{s} = 13$ TeV

The CMS Collaboration

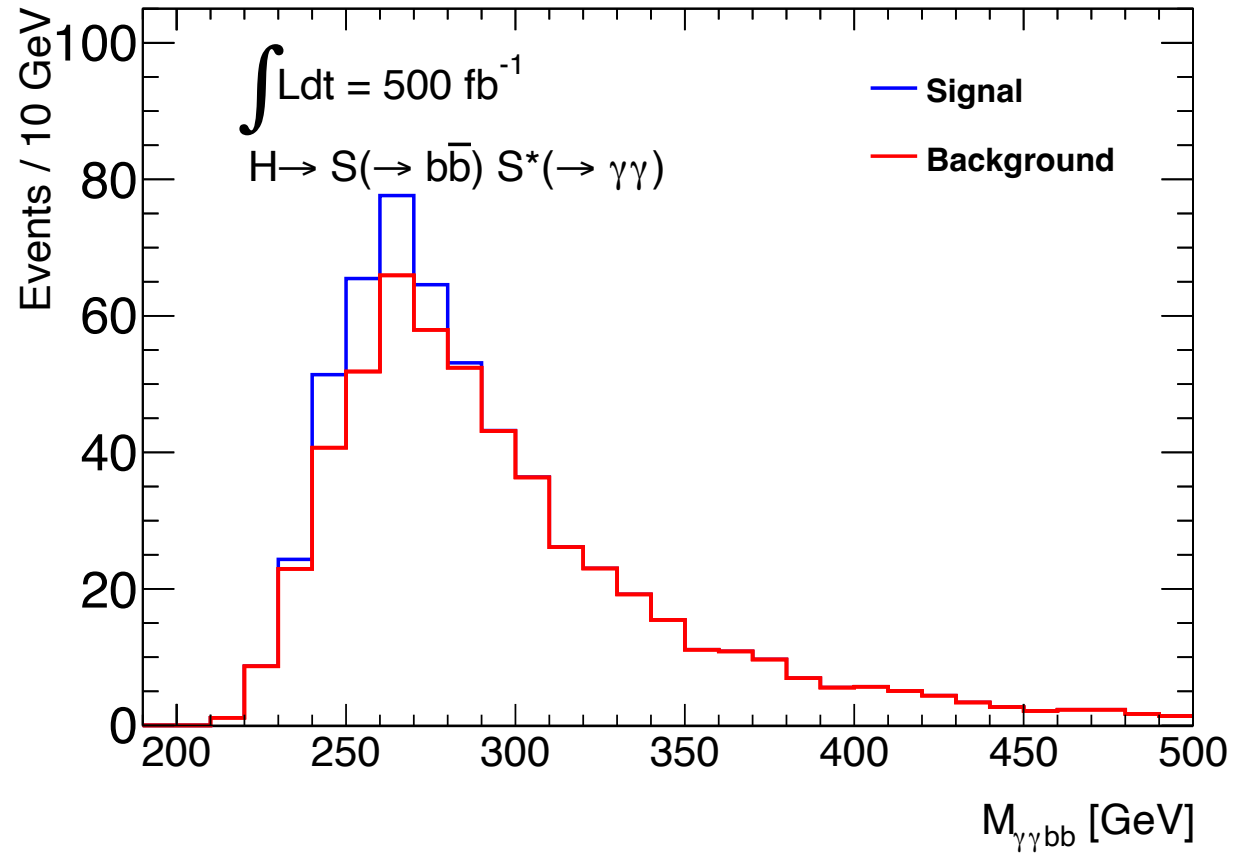
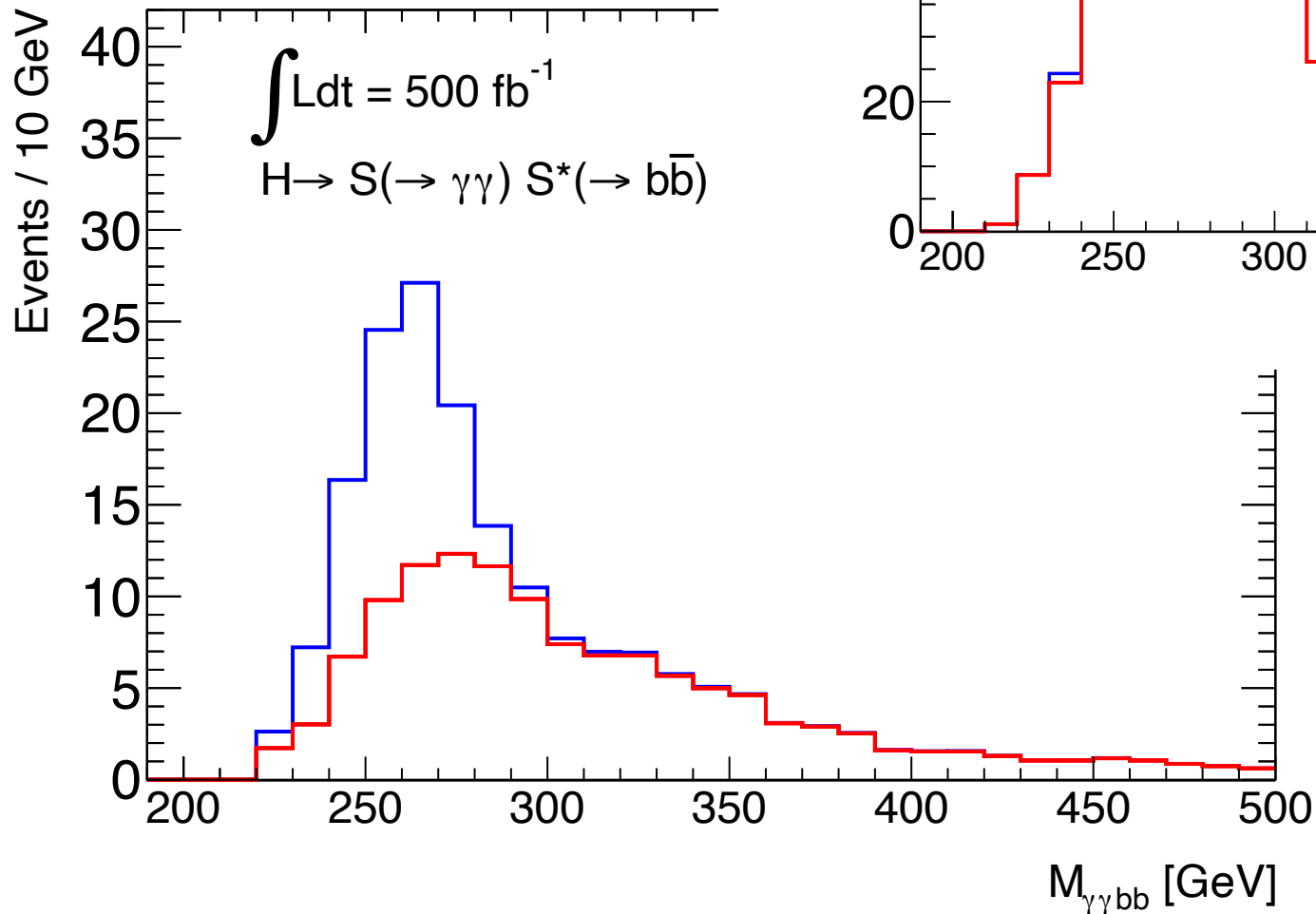
CMS observes what appears to be an upward fluctuation of the $h \rightarrow Z\gamma$ in the di-jet bin optimized for the measurement of Wh production. The Signal strength deviates from unity by 3.2σ .



Search for the lepton flavor violating decay of a Higgs boson in the $e\mu$ final state in proton-proton collisions at $\sqrt{s} = 13$ TeV



Abovementioned excess further motivates searches for bosons in asymmetric $\gamma\gamma b\bar{b}$ configurations not performed before at the LHC



Expect more than 7σ significance for one experiment with the Run 2 + Run 3 data sets.

Unveiling Hidden Physics at the LHC

Oliver Fischer^{†,1}, Bruce Mellado^{†,2,3},
 Stefan Antusch⁴, Emanuele Bagnaschi⁵, Shankha Banerjee⁶, Geoff Beck²,
 Benedetta Belfatto^{7,8}, Matthew Bellis⁹, Zurab Berezhiani^{10,11}, Monika
 Blanke^{12,13}, Bernat Capdevila^{14,15}, Kingman Cheung¹⁶, Andreas
 Crivellin^{5,6,17}, Nishita Desai¹⁸, Bhupal Dev¹⁹, Rohini Godbole²⁰, Tao Han²¹,
 Philip Harris^{22, 23}, Martin Hoferichter²⁴, Matthew Kirk^{25,26}, Suchita
 Kulkarni²⁷, Clemens Lange²⁸, Kati Lassila-Perini²⁹, Zhen Liu³⁰, Farvah
 Mahmoudi^{6,31}, Claudio Andrea Manzari^{5,17}, David Marzocca³², Biswarup
 Mukhopadhyaya³³, Antonio Pich³⁴, Xifeng Ruan², Luc Schnell^{35, 36}, Jesse
 Thaler^{22, 23}, and Susanne Westhoff³⁷

¹*Department of Mathematical Sciences, University of Liverpool, Liverpool, L69 7ZL, UK*

²*School of Physics and Institute for Collider Particle Physics, University of the Witwatersrand, Johannesburg, Wits 2050, South Africa.*

³*iThemba LABS, National Research Foundation, PO Box 722, Somerset West 7129, South Africa.*

⁴*Department of Physics, University of Basel, Klingelbergstr. 82, CH-4056 Basel, Switzerland*

⁵*Paul Scherrer Institut, CH-5232 Villigen PSI, Switzerland*

⁶*CERN Theory Division, CH-1211 Geneva 23, Switzerland*

⁷*Dipartimento di Fisica "E. Fermi", Università di Pisa, Largo Bruno Pontecorvo 3, I-56127 Pisa, Italy*

⁸*INFN Sezione di Pisa, Largo Bruno Pontecorvo 3, I-56127 Pisa, Italy*

⁹*Siena College, 515 Loudon Road, Loudonville, NY 12211-1462, United States*

¹⁰*Dipartimento di Fisica e Chimica, Università di L'Aquila, 67100 Coppito, L'Aquila, Italy*

¹¹*INFN, Laboratori Nazionali del Gran Sasso, 67100 Assergi, L'Aquila, Italy*

¹²*Institute for Astroparticle Physics (IAP), Karlsruhe Institute of Technology, Hermann-von-Helmholtz-Platz 1, D-76344 Eggenstein-Leopoldshafen, Germany*

¹³*Institute for Theoretical Particle Physics (TTP), Karlsruhe Institute of Technology, Engesserstrasse 7, D-76128 Karlsruhe, Germany*